HARDEN, PETER MICHAEL

A STRUCTURAL AND SPECTROSCOPIC INVESTIGATION OF SOME TIN- AND TITANIA- BASED PIGMENTS

MSc UP 1995

A structural and spectroscopic investigation of some tin- and titania- based pigments

by

Peter Michael Harden

Presented in part fulfilment of the requirements for the degree

Master of Science
Chemistry

in the Faculty of Science

University of Pretoria

Pretoria

SEPTEMBER 1995

ACKNOWLEDGEMENTS

I would like to express my sincere gratitude to the following people, departments, companies and institutions for their support throughout my studies.

- My supervisor Professor Anton M. Heyns (Head of the Chemistry Department, University of Pretoria) for his guidance and encouragement throughout this project. His energy is truly inspirational.

- My parents and family for their unconditional support in this venture. A special thanks to my father in his capacity as a ceramist, for useful discussions, for taking care of some of my more customised calcining requirements and for help in testing pigments from time to time.

- My friends for all their support.

- The rest of the research group; Dr Danita De Waal, Mrs Linda Prinsloo and fellow students Gerard Pretorius and Anton van Dyk.

- Sabine Veryn (XRD) of the Department of Geology.
  André Botha (SEM) of the Department of Electron microscopy.
  Leonora Wydeman of the Academic Information Services.

- Chris Greyling and various other people of the R&D department at Iscor Refractories (formerly Cullinan Refractories) for allowing me access to their expensive high temperature ovens.

- Various people at the CSIR (MATEK) for valuable discussions and access to their literature.

Peter Michael Harden
BSc(HONS) University of Natal, Pietermaritzburg

SUMMARY

A structural and spectroscopic investigation of some tin- and titania- based pigments

by

Peter Michael Harden

Presented for the degree MSc (Chemistry)

Supervisor
Professor Anton M. Heyns
Department of Chemistry
University of Pretoria

Two types of pigments suitable for colouring ceramic materials were investigated structurally and spectroscopically. The two types of pigments investigated were firstly yttrium/tin ($Y_2Sn_2O_7$) and yttrium/titanium ($Y_2Ti_2O_7$) pyrochlores doped with calcium and vanadium, and secondly, malayaite ($CaSnSiO_5$ - and related compounds) doped with chromium and cobalt.

The synthesis techniques of the two types of pigments were investigated and optimised based on a two-fold approach; the physical and asthetic properties of the pigments and the economic implication of the synthesis techniques.

The structures of the host materials of both pigment types were investigated using the following sophisticated techniques. Scanning electron microscopy, X-ray powder diffraction, Raman spectroscopy, infrared spectroscopy and electronic spectroscopy.

The chemical state of the dopants and their structure in relation to their host materials were investigated spectroscopically using Raman spectroscopy, infrared spectroscopy, and electronic spectroscopy.

OPSOMMING

ń Strukturele en spectroskopiese ondersoek van sommige tin- en titaangebaseerde pigmente

deur

Peter Michael Harden

Voorgele vir die grade MSc (Chemie)

Promotor
Professor Anton M. Heyns
Departement Chemie
Universiteit van Pretoria

Twee soorte pigmente, wat gebruik kan word om keramiese materiale mee te kleur, is spektroskopies en struktureel ondersoek. Die soorte pigmente wat ondersoek is, is eerstens yttrium/tin ($Y_2Sn_2O_7$) en yttrium/titaan ($Y_2Ti_2O_7$) pirochloorverbindings, wat doteer is met kalsium en vanadium, en dan tweedens maleiët ('malayaite') ($CaSnSiO_5$ - en verwante verbindings) wat doteer is met chroom en kobalt.

Die sintesetegnieke van die twee pigmente is ondersoek en optimiseer met ħ tweedeelige benadering; die fisiese en estetiese eienskappe van die pigmente en die ekonomiese implikasie van die sintese-tegnieke.

Die strukture van die gasheermateriale van beide soorte is ondersoek deur die volgende gesofistikeerde tegnieke te gebruik; skanderende elektronmikroskopie, X-straal poeierdiffraksie, Raman spektroskopie, infrarooispektroskopie en elektroniese spektroskopie.

Die chemiese toestand van die doteermiddels en hulle strukture met betrekking tot die gasheermaterial is spektroskopies ondersoek deur Raman-infrarooi- en elektroniese spektroskopie te gebruik.

CONTENTS

CHAPTER 1

Introduction

1.1 HISTORICAL BACKGROUND

It is likely that prehistoric caveman's first artificially produced article was a pot formed of clay that was made firm by burning, and that it was used for retaining food and water for storage and general use. The manufacture of ceramic products spelt the beginning of man's tireless quest to free himself from his total dependance on natural materials. As far as it has been established, this important event took place in the seventh millennium BC in Iraq [1]. Indeed, the art of making pottery by forming and burning clay is the oldest technology of mankind. Proof of this assertion are the discoveries of burned clay fragments dating back to the early Neolithic Age [2]. The colour of these fragments varied from reddish through brown to greyish depending on the clay impurities and was at the beginning accidental rather than intentional. Man, however, soon learned to utilise the differently coloured raw materials to achieve decorating effects and strikingly beautiful pottery resulted from his efforts.

Since pottery is one of the oldest human activities, it is not surprising that the deliberate colouring of pottery is so as well. Due to the high stability of inorganic pigments, their use can be traced back over millennia. In prehistoric times, inorganic pigments, both coloured and uncoloured, were obtained from naturally occurring minerals [3]. Synthetic pigments were the next step, and Noll et al. have shown that pigments were already being made synthetically in the city and river cultures of antiquity [1]. Some examples of the development of ceramic pigments are described below [4].

Early pottery found in Egypt, Asia Minor, Crete, and Greece exhibit progressively refined application techniques and ornamentation details. At

this time the potters started using the naturally occurring earth pigments such as ochre, sienna, umber, and black magnetite to colour the clay body of their ware and to use coloured dip-coats for glassing. The effect of firing atmosphere was also recognised and effectively used to achieve desired shades.

The oldest Greek vases used a black ceramic decoration on a red body. Since then (500B.C) this changed to a red-coloured decoration on a glossy black ceramic base.

The Romans, successors of the cultural achievements of the Greeks, carried this technology further and produced beautiful red-coloured ceramics (so called "Terra Sigillata"). The secret of this manufacture has just recently been unveiled.

The art of glazing (a technique of colouring only the surface of a ceramic article rather that colouring the clay from which it is made) is also almost as old as that of pottery. Beads adorning some Egyptian mummies were found coated with a blue coloured glaze and pieces of glass dating back more than 5000 years have also been discovered. The ancient Egyptians preferred the blue colour because of their reverence for the sky. The mineral azurite was extensively used as a colouring agent to obtain the pharaohnic blue and the turquoise shades that decorated their temples and monuments. Since there was only a limited amount of azurite available, they soon learned to imitate nature and produce a synthetic crystalline compound even more useful than its natural counterpart. A chunk of such a blue disk dating back some 4000years was excavated from a tomb in Luxor, Egypt in 1965. Two

Egyptian physicists dispelled the mystery of the chemical nature of this crystalline matter and proved it to be the calcination product of copper oxide (1 mole), calcium oxide (1 mole), and silica (4 moles) that was ground and mixed with some egg yolk and gum.

Since the beginning of the 18th century, ceramic pigments have become the object of scientific studies to the point were today research makes use of the latest techniques in solid state physics and chemistry to try to understand the very sophisticated properties of these ceramic pigments. In the last eighty years or so, based on our ideas of technically and aesthetically important properties, it has become possible to synthesis pigments with properties superior to their natural counterparts. In addition, the volume of production of these synthetic pigments have been increased dramatically while maintaining the pigment properties or improving them. The range of ceramic pigments available for industrial application has also been increased by the addition of new ceramic pigments. The ideal situation for ceramic pigment synthesis would be to have an understanding of ceramic pigments that would enable one to design a ceramic pigment for a specific application, taking into account the aesthetic, technical, economic and of coarse the all important ecological aspects of ceramic pigment synthesis, and consequently to synthesis the ceramic pigment, cost effectively, on an industrial scale.

1.2 CERAMIC PIGMENTS

There are a number of ways to obtain colour in a ceramic material [2]. They are listed below.

1. Ceramic materials containing transition metal ions will often be coloured, particularly if they are vitreous. Although this method is

used to make coloured glass, it is rarely used in other products because adequate tinting strength and purity of colour cannot be obtained in this way.

2. A second method used to obtain colour in a ceramic is to induce the precipitation of a crystalline phase in a glassy matrix during processing. Certain oxides such as zirconium dioxide and titanium dioxide dissolve to the extent of several weight percent in a vitreous material at high temperature. When the temperature is reduced, the solubility is also reduced and precipitation occurs. This method is widely used for opacification; the production of opaque white colour in a vitreous matrix. For oxide colours other than white, this method lacks the necessary control for reproducible results and, therefore, is seldom used.

3. The most common method of obtaining colour in a ceramic material is to disperse in that material a coloured crystalline phase which is insoluble in the matrix. This crystalline phase, or *pigment*, imparts its colour to the matrix.

Pigments imply *colour*. The range of the electromagnetic spectrum in which we are interested, ranges from around 400nm to around 700nm; that is from violet through blue, green, yellow, and all the other colours of the rainbow, to red. Pigments are a sub-group of colorants.

There can be no new colours..... but colorants are a different matter.

Colorants have certain physical and chemical characteristics which vary in degree and quality from one to another [5]. These characteristics are summarised in table 1.1 below.

Table 1.1 Physical and chemical characteristics of colorants.

Principal Optical Properties	Secondary Properties
Colour (hue) (chroma)	Heat fastness
Tinting strength (saturation)	Light fastness
Opacity	Chemical Resistance
Refractive index	Dispersibility

Colorants can be divided into two categories.

I DYES : colorants that are coloured and *transparent*.

II PIGMENTS : colorants that are coloured or uncoloured and *opaque*.

The Dry Colour Manufacturers Association (DCMA) of America has prepared the following, legally accepted definition of a pigment [6]. Essentially, a pigment is a coloured, black, white, or fluorescent particulate organic or inorganic solid which is usually insoluble in, and essentially physically and chemically unaffected by, the vehicle or substrate into which it is incorporated. A pigment will alter appearance by selective absorption and/or by scattering of light. The pigment is usually dispersed in a vehicle or substrate for application as, for example, in the manufacture of paints, plastics, or other polymeric materials and inks. The pigment will retain its own unique crystalline or particulate structure throughout the incorporation process.

Pigments may further be divided into two categories.

I ORGANIC II INORGANIC

The colorants that we are dealing with are *pigments* that are *inorganic*. A host lattice is doped with a small amount of a metal element (most commonly a transition metal element) that is responsible for imparting colour on the host lattice. The host lattice is formed at high temperatures and so is in a very stable chemical state. It is therefore not surprising that more often than not, the host lattice takes on the structure of a naturally occurring mineral (or minerals) that by the nature of their being, are stable. These colorants are not only suitable for the colouring of ceramics, but also paints, resins, plastics etc. They are not used extensively in these areas though since, because of their high stability, they are expensive to produce and so, for applications where a less stable colorant will suffice, the cheaper alternative is preferred. Hence the name *ceramic pigments*.

1.3 CERAMIC PIGMENT PROPERTIES

When a photon enters a pigmented film, one of three events may occur:

1. It may be absorbed by a pigment particle.
2. It may be scattered by a pigment particle.
3. It may simply pass through the film (the binder being assumed to be non-absorbent).

The important physical-optical properties of pigments are therefore their light-absorption and light-scattering properties [7]. If absorption is very small compared with scattering, the pigment is white. If absorption is much higher than scattering over the entire visible region, the pigment is black. In a coloured pigment, absorption (and usually scattering) are selective (ie. dependant on wave length).

The key feature of ceramic pigments, over and above the all important

colour, is that they should be thermally stable, and many good pigments are useless to the ceramic industry because they are not sufficiently stable. They must also be of good saturation, since more often than not, they are mixed with opaque white materials or other materials of high refractive index. Saturation cannot be improved upon and so is vital in the basic colorant. It also determines the amount of pigment which must be used to achieve a particular colour and there are usually good reasons why this should be as little as possible, not least of all freedom of formulation and the all important cost factor.

Other properties special to ceramic pigments include good chemical resistance to acids and alkalis and low solubility in glass. Ceramic pigments are subjected to the very harsh and corrosive conditions resulting during the vitrification of the fluid vitrifiable medium. It is important to note that the ceramic pigment is only one of a number of components present during processing. Others may include the glaze or body, opacifiers, various additives and application media. Conversely of course, any glass, glaze, body, opacifier etc. used should be as transparent, stable and as unaggressive as possible to reduce to a minimum the effect on the pigment.

There are limitations on all existing ceramic pigments. An example of this is the unhappy relationship between chromium-containing pigments and zinc-containing glasses. Another example is the positive features of the zircon colorants recommended for use under all glasses and whose only serious limitation is lack of strength or saturation.

There have always been conflicting demands on the colour suppliers and in

the foreseeable future there will be many more. The potters and transfer makers will be asking for stronger, brighter, cleaner colorants. They will be seeking consistency at lower cost to enhance profitability. They will be seeking intermixability because this will minimise stock holdings and reduce the skill and training necessary to achieve a flexible product range. All this will be sought against a background of a need for colorants which are safer to produce and use, safer for the environment, and safer for the consumer. In addition, the colours must be presented in 'inks' or 'paints' which are stable, easy to apply, safe to the user, and tolerant of any process conditions or application technique which may be employed. To achieve this more needs to be learned of the properties of ceramic pigments.

All of the above properties of ceramic pigments (and the properties of all colorants for that matter) are related to the 'molecular' structure of the pigment. There are four basic principles which determine the structures of inorganic solid state materials [2].

1. The principle component of free energy of an ionic solid material at room temperature is its lattice energy which is determined almost totally by the nearest-neighbour cation-anion distance.
2. The coordination polyhedra of the anions about each cation in ionic solid phases are determined almost unequivocally by the radius ratio of cations to anions.
3. The structures that can be built from any combination of cations and anions are subject to the rules for electrostatic neutrality. This means that in a stable ionic structure the valence of each anion, with changed sign, is exactly or nearly equal to the sum of the strengths of the electrostatic bonds to it from adjacent cations.

4. The coordination of a cation must increase as the charge of the anion decreases, and decreases as the field strength increases.

The host lattice formed at high temperatures will most certainly conform rigorously to all of these principles. They are invariably very stable. The introduction of the dopant must also conform to these principles since the pigment also needs to be stable. They do not conform as rigorously though, since their chemical and physical properties will be different and consequently, they place strain on their immediate environment. Conversely, strain is also placed on the dopant by the host lattice. It is this interaction that results in the colour of the ceramic pigment. Clearly the microscopic structure of these pigments are all important.

1.4 A STRUCTURAL AND SPECTROSCOPIC INVESTIGATION OF SOME TIN- AND TITANIA- BASED PIGMENTS

The chemistry of ceramic pigments synthesis is more often than not very complicated and not well understood. People in the business like to refer to ceramic pigment synthesis as 'black magic'. To a large extent ceramic pigment synthesis takes place on an empirical basis. Often little is known about the chemical properties of the pigments and their properties are optimised by trial and error. The vast number of elements that make up the host lattice, and the vast number of elements that are used as dopants, and the vast number of compounds that might be useful as mineralisers, and the very diverse conditions of synthesis make it an enormous if not impossible task to synthesis new pigments or optimise pigment synthesis on an empirical basis. What is needed for more efficient ceramic pigment synthesis and the development of new ceramic pigments is a better understanding of

of these pigments.

The purpose of this study was two-fold. Firstly, to investigate and consequently optimise the techniques and conditions of synthesis of two types of pigments; two pyrochlores (chapter 2), and malayaite and titanite (chapter 3). Optimisation was carried out on a two-fold approach; the physical and aesthetic properties of the pigments and the economic implications of the synthesis technique. Secondly, to investigate their complex structural properties spectroscopically. The following techniques were employed to this end.

1. Scanning Electron Microscopy (SEM)
2. X-Ray Powder Diffraction (XRD)
3. Raman Spectroscopy
4. Infrared Spectroscopy (IR spectroscopy)
5. Ultraviolet-Visible Spectroscopy (UV-VIS spectroscopy)

CHAPTER 2

The Pyrochlore Compounds

2.1 INTRODUCTION

Pyrochlore compounds have the general chemical formula $A_2B_2O_7$. The properties of various pyrochlore compounds have been widely studied. These studies include a vibrational study of various pyrochlore compounds [8;9;10] and the publication of the crystal structures and cell parameters of a large number of pyrochlores [11]. Various rare earth tin containing pyrochlore compounds (rare earth stannates) have also been synthesised [12], and their properties studied. These include the XRD data studies [13] and ^{119}Sn MAS NMR studies [14].

This study focuses on two rare earth pyrochlores (the host lattices), and the effect that doping with vanadium and calcium has on the properties of the respective pyrochlores. The chemical state of the dopants are also investigated. The chemical formulas of the two pyrochlores investigated are

I $Y_2Sn_2O_7$ (yttrium tin pyrochlore)

II $Y_2Ti_2O_7$ (yttrium titanium pyrochlore)

Studies involving the yttrium tin pyrochlore include X-Ray diffraction data [13], structure refinement [11;15] and ^{119}Sn MAS NMR [14]. Synthesis techniques for vanadium doped $Y_2Sn_2O_7$ and $Y_2Ti_2O_7$ have also been reported by Fujiyoshi et al.[16]. These vanadium doped pyrochlores are synthesised at high temperatures ($\pm$1300°C). The doping of the two pyrochlores is reported to produce strong, brightly coloured yellow powders that are stable at high temperatures. It is these properties that make these two pyrochlores candidates for ceramic pigments. Initial samples were prepared in a similar way to that reported by Fujiyoshi et.al.

2.2 EXPERIMENTAL

2.2.1 SYNTHESIS OF $Y_2Sn_2O_7$ AND $Y_2Ti_2O_7$ DOPED WITH CALCIUM AND WITH VANADIUM - THE FIRST REACTION MIXTURES

Stoichiometric quantities of yttrium and tin, in the form of Y_2O_3 (yttrium oxide) and SnO_2 (tin oxide; the mineral cassiterite), were intimately wet mixed with calcium and vanadium as dopants, in the form of $CaCO_3$ (calcium carbonate) and NH_4VO_3 (ammonium metavanadate). The reaction mixture was then dried and dry mixed with a mortar and pestle, and then calcined. The reaction mixture was heated from room temperature to 1300°C. The temperature was held at 1300°C for six hours. The oven was then turned off and the reaction mixture was allowed to cool to room temperature inside the oven. The resultant product was ground with a mortar and pestle and water leached (washed in boiling water) to remove any water soluble matter that might have been produced by the calcination process.

The titanite reaction mixtures were prepared in exactly the same way except that titanium, in the form of TiO_2 (titanium dioxide; the mineral anatase), was substituted for tin oxide.

A number of reactions with varying concentrations of dopant were carried out. The details of these reaction mixtures are summarised in table 2.1 A ($Y_2Sn_2O_7$) and table 2.1 B ($Y_2Ti_2O_7$) below.

Table 2.1 A The first reaction mixtures of $Y_2Sn_2O_7$.

Reaction number	* Y	:	Sn	dopant $\%NH_4VO_3$	dopant $\%CaCO_3$
1	1		1	0	0
2	1		1	1	1
3	1		1	2	2
4	1		1	4	4

* Ratio of Y to Sn; and atom percent of dopants used.
(Atom percent of total number of atoms of Y and Sn before calcining.)

Table 2.1 B The first reaction mixtures of $Y_2Ti_2O_7$.

Reaction number	* Y	:	Ti	dopant $\%NH_4VO_3$	dopant $\%CaCO_3$
1	1		1	0	0
2	1		1	1	1
3	1		1	2	2
4	1		1	4	4

* Ratio of Y to Ti; and atom percent of dopants used.
(Atom percent of total number of atoms of Y and Ti before calcining.)

2.2.2 SYNTHESIS OF UNDOPED $Y_2Sn_2O_7$ AND $Y_2Ti_2O_7$ - THE SECOND REACTION MIXTURES

These reaction mixtures were synthesised based on the results of the first reaction mixtures. None of these reaction mixtures were doped with calcium or vanadium. The method of synthesis, calcination temperatures and calcination times were the same as those of the first reaction mixtures but the ratio of yttrium to tin, and yttrium to titanium respectively, were not one

to one, but were varied. The details of the second reaction mixtures are summarised in table 2.2 A ($Y_2Sn_2O_7$) and table 2.2 B ($Y_2Ti_2O_7$) below.

Table 2.2 A The second reaction mixtures of $Y_2Sn_2O_7$.

Reaction number	* Y	:	Sn
1	2		1
2	3		1
3	4		1

* Ratio of Y to Sn.

Table 2.2 B The second reaction mixtures of $Y_2Ti_2O_7$.

Reaction number	* Y	:	Ti
1	2		1
2	3		1
3	4		1

* Ratio of Y to Ti.

2.2.3 SYNTHESIS OF $Y_2Sn_2O_7$ AND $Y_2Ti_2O_7$ DOPED WITH CALCIUM AND WITH VANADIUM - THE THIRD REACTION MIXTURES

These reaction mixtures were synthesised based on the results of the first and second reaction mixtures. The method of synthesis, calcination temperatures and calcination times were the same as those of the first and second reaction mixtures. The ratio of yttrium to tin, and yttrium to titanium

respectively, were varied, and these reaction mixtures were all doped with the same amount of dopant. The details of the second reaction mixtures are summarised in table 2.3 A ($Y_2Sn_2O_7$) and table 2.3 B ($Y_2Ti_2O_7$) below.

Table 2.3 A The third reaction mixtures of $Y_2Sn_2O_7$.

Reaction number	* Y	:	Sn	dopant $\%NH_4VO_3$	dopant $\%CaCO_3$
1	1		1	4	4
2	2		1	4	4
3	3		1	4	4
4	4		1	4	4

* Ratio of Y to Sn; and atom percent of dopants used.
(Atom percent of Sn and one part Y atoms before calcining.)

Table 2.3 B The third reaction mixtures of $Y_2Ti_2O_7$.

Reaction number	* Y	:	Ti	dopant NH_4VO_3	dopant $CaCO_3$
1	1		1	4	4
2	2		1	4	4
3	3		1	4	4
4	4		1	4	4

* Ratio of Y to Sn; and atom percent of dopants used.
(Atom percent of Sn and one part Y atoms before calcining.)

2.2.4 SYNTHESIS OF $Y_2Sn_2O_7$ DOPED WITH CALCIUM AND VANADIUM - THE FOURTH REACTION MIXTURES

Stoichiometric quantities of yttrium and tin, in the form of Y_2O_3 and SnO_2,

were intimately wet mixed with one atom percent of calcium and of vanadium as dopants respectively, in the form of $CaCO_3$ and NH_4VO_3. The reaction was then dried and dry mixed with a mortar and pestle. This is exactly the same synthesis technique used for the first, second and third reaction mixtures above. The product was then tightly packed into a tall and narrow crucible, and then calcined. The reaction mixture was heated from room temperature to 1450°C. The temperature was held constant for two hours after which the reaction mixture was allowed to cool to room temperature inside the oven. The reaction product was easily broke down into a soft powder in the water leaching process.

2.2.5 SYNTHESIS OF $Y_2Sn_2O_7$ AND $Y_2Ti_2O_7$ DOPED WITH CALCIUM AND WITH VANADIUM - THE FIFTH REACTION MIXTURES

Stoichiometric quantities of yttrium and tin, in the form of Y_2O_3 (yttrium oxide) and SnO_2 (tin oxide; the mineral cassiterite), were weighed out. The yttrium oxide was then dissolved in the minimum amount of hot HCl (hydrochloric acid). To this solution, was added the tin. This solution was then made basic by the addition of NH_4OH (ammonium hydroxide) in order to precipitate the yttrium out of the solution. Small amounts of calcium and vanadium, in the form of $CaCO_3$ and NH_4VO_3, were then added to the mixture as dopants. The mixture was then intimately wet mixed and then heated to dryness. The resulting powder was then dry mixed with a mortar and pestle, and calcined. The reaction mixture was heated from room temperature to 1150°C. The temperature was held constant for six hours after which the reaction mixtures were allowed to cool to room temperature inside the oven. The resultant products were water leached to produce soft powders.

The titanite reaction mixtures were prepared in exactly the same way except that titanium, in the form of TiO_2 (titanium dioxide; the mineral anatase), was substituted for tin oxide. The details of the fifth reaction mixtures are summarised in table 2.4 A ($Y_2Sn_2O_7$) and table 2.4 B ($Y_2Ti_2O_7$) below.

Table 2.4 A The fifth reaction mixtures of $Y_2Sn_2O_7$.

Reaction number	Y	:	Sn	dopant $\%NH_4VO_3$	dopant $\%CaCO_3$
1	1		1	-	-
2	1		1	2	2
3	1		1	4	4

* Ratio of Y to Sn; and atom percent of dopants used.
(Atom percent of total number of atoms of Y and Sn before calcining.)

Table 2.4 B The fifth reaction mixtures of $Y_2Ti_2O_7$.

Reaction number	Y	:	Ti	dopant $\%NH_4VO_3$	dopant $\%CaCO_3$
1	1		1	-	-
2	1		1	2	2
3	1		1	4	4

* Ratio of Y to Ti; and atom percent of dopants used.
(Atom percent of total number of atoms of Y and Ti before calcining.)

2.3 RESULTS AND DISCUSSION

2.3.1 THE FIRST REACTION MIXTURES

The details of these reaction mixtures are summarised in table 2.1 A ($Y_2Sn_2O_7$), and table 2.1 B ($Y_2Ti_2O_7$) above. Reaction numbers 1 of each of

the respective pyrochlores were undoped and, as expected, both were white in colour. Reaction numbers 2 and 3 and 4 of the respective pyrochlores were doped with 1, 2, and 4 atom percent of calcium and vanadium respectively. The colours of the reaction mixtures containing 1 and 2 atom percent of dopants were pale yellow and indistinguishable from one another in both cases. The colour did not seem to be a function of the amount of dopants added to the reaction mixtures before calcination. The colours of the reaction mixtures containing 4 atom percent of dopants in both cases were more intense than the reaction mixtures doped with less calcium and vanadium, especially in the case of the yttrium titanium pyrochlore. The physical properties of all of the reaction products were very similar. The reaction mixtures were all in the form of soft lumps that were easily broken down to soft, relatively fine powders in the water leaching process that followed calcination. This is a favourable property of a ceramic pigment since particle size is very important. The pigment needs to be fine to have an optimum colouring effect (not so fine that it cannot be seen though). Therefore the pigments are milled (ground) after calcining. The finer the pigment, the less milling required, the cheaper the pigment.

SEM analysis was done on the reaction products of the first reaction mixtures. The results are summarised in table 2.5 A ($Y_2Sn_2O_7$) and table 2.5 B ($Y_2Ti_2O_7$) below. The SEM analysis technique is discussed in appendix III. The technique was found to be accurate only to within about 5 atom percent up or down. The dopants are present in quantities between 1 and 4 atom percent. While the reaction mixtures were tested for the presence of the dopants, these results are omitted since as expected, they are grossly inaccurate and not at all reproducible.

Table 2.5 A SEM analysis results for $Y_2Sn_2O_7$ products of the first reaction mixtures.

Reaction number	Atom %	
	Y	Sn
1	20.19	79.81
2	26.21	73.79
3	29.88	70.12
4	26.63	73.37

Table 2.5 B SEM analysis results for $Y_2Ti_2O_7$ products of the first reaction mixtures.

Reaction number	Atom %	
	Y	Ti
1	30.59	69.41
2	42.40	57.60
3	37.25	62.75
4	27.56	72.44

Loss of dopants to the vapour phase is not desirable for a number of reasons. Firstly it is not environmentally friendly. Secondly, since the intensity of the colour is generally a function of, and proportional to the amount of dopant present, loss of dopant results in a lower colour intensity, so that more dopant is required to achieve the desired colour intensity. Generally transition metal dopants are very expensive and so the less one uses the better. The SEM analysis technique cannot tell us if any of the

dopants are being lost to the vapour phase in the calcining process. The fact that the undoped reaction mixtures are white is however a good indication that these reaction mixtures have not been contaminated and consequently that the dopants are not volatile at these temperatures. In addition, the Raman spectra of these reaction mixtures show conclusively that the undoped reaction mixtures are not contaminated. The spectrum of a doped tin pyrochlore has two vanadium bands at around 755 and 806 cm^{-1}. These bands are not seen in the spectrum of the undoped tin pyrochlore. (See figures 2.3 and 2.4 - appendix I). Similarly, the spectrum of a doped titanium pyrochlore has two vanadium bands at around 752 and 820 cm^{-1}. These bands are not seen in the spectrum of the undoped titanium pyrochlore (See figures 2.9 and 2.10 - appendix I). From the SEM analysis results above it does however seem that a large amount of the yttrium is being lost in the calcining process. Table 2.6 A ($Y_2Sn_2O_7$) and table 2.6 B ($Y_2Ti_2O_7$) show the amount of yttrium and tin, and yttrium and titanium present before and after calcining.

Table 2.6 A Atom percent of Y and Sn present before and after calcining.

Reaction number	* Atom%Y before	Atom%Sn before	Atom%Y after	Atom%Sn after
1	50.00	50.00	20.19	79.81
2	50.00	50.00	26.21	73.79
3	50.00	50.00	29.88	70.12
4	50.00	50.00	26.63	73.37

* Number of atoms of Y and of Sn as a percentage of the total number of Y and Sn atoms present. For simplification atom percent of dopants, were present, have not been considered.

Table 2.6 B Atom percent of Y and Ti present before and after calcining of the first reaction mixtures.

Reaction number	Atom%Y before	Atom%Ti before	Atom%Y after	Atom%Ti after
1	50.00	50.00	30.59	69.41
2	50.00	50.00	42.40	57.60
3	50.00	50.00	37.25	62.75
4	50.00	50.00	27.56	72.44

* Number of atoms of Y and of Ti as a percentage of the total number of Y and Ti atoms present. For simplification atom percent of dopants, were present, have not been considered.

From the above tables it seems as though roughly half of the yttrium is being lost in the calcining process. This is not desirable since it means that only half the amount of host mineral, the desired reaction product, can be formed assuming the reaction goes to completion. Since the intensity of the colour of the product is as a result of the interaction between the host lattice and the dopant, loss of yttrium will lead to loss of intensity of colour. Also it is reasonable to expect that the unreacted tin or titanium, as the cases may be, might diluted the colour of the pigments.

XRD data was collected on the products of the first reaction mixtures. The results of these XRD data are summarised in table 2.7 A($Y_2Sn_2O_7$) and 2.7 B ($Y_2Ti_2O_7$) below.

Table 2.7 A XRD data for $Y_2Sn_2O_7$ products of the first reaction mixtures.

Reaction number		Y_2O_3	SnO_2	$Y_2Sn_2O_7$	Other
1	*	(yes)	(yes)	yes	none
2		no	no	yes	none
3		no	no	yes	(YVO_4?)
4		no	no	yes	(YVO_4?)

* (yes) - very little present.

(yes?) - might be present but if so, only in very small quantities.

Table 2.7 B XRD data for $Y_2Ti_2O_7$ products of the first reaction mixtures.

Reaction number		Y_2O_3	TiO_2	$Y_2Ti_2O_7$	Other
1	*	no	no	no	none
2		no	(yes?)	yes	none
3		no	no	yes	(YVO_4?)
4		no	no	yes	(YVO_4?)

* (yes?) - might be present but if so, only in very small quantities.

As already stated, the SEM analysis results show that a large amount of yttrium is being lost in the calcination process. One would therefore expect to see signs of large quantities of unreacted tin in the case of the tin pyrochlore, and titanium in the case of the titanium pyrochlore, in the XRD data, or the presence of some sort of tin, or titanium by-product. The XRD data, however, show no signs of any of these materials except in two of the

reaction mixtures in which, if they are present, they are present only in very small quantities; certainly not in the quantities suggested by the SEM analysis results.

Vibrational spectroscopy is very useful for obtaining information about the structure of the pigments. This is discussed in detail in 2.4 below. Vibrational spectroscopy can, however, also be used successfully on a simple empirical basis in determining the products of the above reactions. Although the intensities of the bands give an indication of the amount of a material present, they are not quantitative. IR spectra tend to have rather broad bands as a result of unsymmetrical vibrations (ungerade), and so are not as useful for this type of empirical work. (Raman spectra on the other hand tend to have sharp bands as a result of symmetrical vibrations (gerade)). Raman spectra were recorded of all of the raw materials and of all of the first reaction mixture products. A comparison of the raw material spectra and the spectra of the reaction products show the presence of only very small raw material peaks, not of tin or of titanium as one might expect from the SEM analysis results, but of unreacted yttrium.

In summation then, while the SEM analysis results point towards loss of yttrium in the calcination process, the XRD data and Raman spectra suggest that no yttrium is lost. Given yttrium's thermal properties it is certainly not likely that it would be volatile at 1300°C.

The second reaction mixtures were carried out to test the effect of increasing the amount of yttrium added to the reaction mixtures before calcination in an effort to counter the loss of yttrium in the calcining process,

assuming any loss occurs at all. These reaction mixtures were not doped.

2.3.2 THE SECOND REACTION MIXTURES

The results of the second reaction mixtures are summarised in table 2.2 A ($Y_2Sn_2O_7$) and 2.2 B ($Y_2Ti_2O_7$) above. None of these reaction mixtures were doped with calcium and vanadium. Reaction mixtures were calcined for each of the respective pyrochlores in which the ratios of yttrium to tin, and yttrium to titanium were 2 to 1, 3 to 1, and 4 to 1 respectively. All of the products of the respective reaction mixtures were soft (fine), white powders.

SEM analysis results of the products of the second reaction mixtures of both pyrochlores are summarised in table 2.8 A ($Y_2Sn_2O_7$) and table 2.8 B ($Y_2Ti_2O_7$) below.

Table 2.8 A Atom percent of yttrium and tin before calcining; and SEM analysis results for $Y_2Sn_2O_7$ products of the second reaction mixtures after calcining.

Reaction number	Atom%Y before	Atom%Sn before	Atom%Y after	Atom%Sn after
1	66.66	33.34	66.00	34.00
2	75.00	25.00	74.04	25.96
3	80.00	20.00	77.46	22.54

Table 2.8 B Atom percent of yttrium and titanium before calcining; and SEM analysis results for $Y_2Ti_2O_7$ products of the second reaction mixtures after calcining.

Reaction number	Atom%Y before	Atom%Ti before	Atom%Y after	Atom%Ti after
1	66.66	33.34	71.15	28.85
2	75.00	25.00	75.55	24.45
3	80.00	20.00	81.12	18.88

The SEM results show that, within the experimental error of the SEM analysis technique, none of the starting materials of any of the second reaction mixtures have been lost. This is confirmed by the XRD results summarised in table 2.9 A ($Y_2Sn_2O_7$) and table 2.9 B ($Y_2Ti_2O_7$) below. The XRD data of all of the reaction mixtures show that unreacted yttrium oxide remains after calcination. The relative peak heights of the yttrium peaks show that yttrium oxide is present in large quantities; the peak heights are proportional to the amount of excess yttrium added to the reaction mixtures before calcining.

Table 2.9 A XRD data for $Y_2Sn_2O_7$ products of the second reaction mixtures.

Reaction numbers	Y_2O_3	SnO_2	$Y_2Sn_2O_7$
1	yes	no	yes
2	yes	no	yes
3	yes	no	yes

Table 2.9 B XRD data for $Y_2Ti_2O_7$ products of the second reaction mixtures.

Reaction number	Y_2O_3	TiO_2	$Y_2Ti_2O_7$	Other
1	yes	no	yes	Y_2TiO_5
2	yes	no	yes	Y_2TiO_5
3	yes	no	yes	Y_2TiO_5

Raman spectra were recorded of all of the second reaction mixtures products, and when compared with the spectra of the raw materials on an empirical basis, confirm yttrium oxide to be the only raw material present after calcining. Once again the peak heights of the yttrium peaks increase as the amount of excess yttrium added before calcining increases. The raw material yttrium oxide has characteristic bands at around 376, 469, and 593 cm^{-1}, the band at 376 cm^{-1} being the most intense. $Y_2Sn_2O_7$ has three bands at around 307, 410 and 505 cm^{-1}. Figures 2.1, 2.2 and 2.3 in appendix I show the Raman spectra of $Y_2Sn_2O_7$ synthesised with a ratio of Y:Sn of 4:1, 3:1 and 1:1 respectively. The intensities of the yttrium oxide bands can clearly be seen to diminish in relation to the bands of the pyrochlore as the amount of excess yttrium oxide decreases; in the spectrum of the pyrochlore without an excess of yttrium only pyrochlore bands can be seen. If we compare the Raman spectra of $Y_2Ti_2O_7$ synthesised with a ratio of Y:Ti of 4:1, 3:1 and 1:1 respectively (Figures 2.7, 2.8 and 2.9 in appendix I) we see similar results.

The SEM analysis results of the first reaction mixtures show that yttrium is being lost in the calcining process. This does not seem to be corroborated by

the XRD data or the Raman spectra of these reaction mixtures. In the second reaction mixtures, the SEM analysis results, XRD data and Raman spectra concur that no yttrium is being lost from the reaction mixtures. The only difference between the first and second reaction mixtures, besides the excess yttrium added to the second reaction mixtures, is the dopants added to the first reaction mixtures. The third reaction mixtures were carried out to test the effect of the dopants on the volatility of yttrium in the reaction mixtures.

2.3.3 THE THIRD REACTION MIXTURES

The details of the third reaction mixtures are summarised in table 2.3 A ($Y_2Sn_2O_7$) and table 2.3 B ($Y_2Ti_2O_7$) above. All of these reaction mixtures were doped with 4 atom percent of calcium and vanadium. Reaction mixtures were calcined for each of the respective pyrochlores in which the ratios of yttrium to tin, and yttrium to titanium were 1 to 1, 2 to 1, 3 to 1, and 4 to 1 respectively.

The colour of the reaction products of both the tin pyrochlores and titanium pyrochlores was strongest when the ratio of yttrium to tin or yttrium to titanium was 1 to 1 before calcining. As the amount of excess yttrium added to the reaction mixtures increased, so the intensity of the colour of the product decreased.

SEM analysis was done on the reaction products of the third reaction mixtures. The results are summarised in table 2.10 A ($Y_2Sn_2O_7$) and table 2.10 B ($Y_2Ti_2O_7$) below along with the amount of yttrium and tin, and yttrium and titanium respectively present before calcining for comparative purposes.

Table 2.10 A Atom percent of Y and Sn present before and after calcining of the third reaction mixtures.

Reaction number	* Atom%Y before	Atom%Sn before	Atom%Y after (SEM)	Atom%Sn after (SEM)
1	50.00	50.00	32.16	67.84
2	66.66	33.34	42.12	57.88
3	75.00	25.00	51.28	51.32
4	80.00	20.00	50.50	43.50

* Number of atoms of Y and of Sn as a percentage of the total number of Y and Sn atoms present. For simplification atom percent of dopants have not been considered.

Table 2.10 B Atom percent of Y and Ti present before and after calcining of the third reaction mixtures.

Reaction number	Atom%Y before	Atom%Ti before	Atom%Y after (SEM)	Atom%Ti after (SEM)
1	50.00	50.00	31.42	68.58
2	66.66	33.34	46.77	53.23
3	75.00	25.00	55.34	44.66
4	80.00	20.00	69.10	30.90

* Number of atoms of Y and of Ti as a percentage of the total number of Y and Ti atoms present. For simplification atom percent of dopants have not been considered.

As in the first reaction mixtures, the SEM analysis results show that large amounts of yttrium have been lost in the calcining process.

The XRD data of the third reaction mixtures are summarised in table 2.11 A

($Y_2Sn_2O_7$) and table 2.11 B ($Y_2Ti_2O_7$) below.

Table 2.11 A XRD data for $Y_2Sn_2O_7$ products of the third reaction mixtures.

Reaction number	Y_2O_3	SnO_2	$Y_2Sn_2O_7$	Other
1	no	no	yes	none
2	yes	no	yes	none
3	yes	no	yes	none
4	yes	no	yes	none

Table 2.11 B XRD data for $Y_2Ti_2O_7$ products of the third reaction mixtures.

Reaction number	Y_2O_3	TiO_2	$Y_2Ti_2O_7$	Other
1	no	no	yes	(YVO_4)
2	yes	no	yes	Y_2TiO_5
3	yes	no	yes	Y_2TiO_5
4	yes	no	yes	Y_2TiO_5

* (yes) - very little present.

The SEM results closely resemble those of the first reaction mixtures in that they show that a large amount of yttrium has been lost in the calcining process. The XRD data closely resembles that of the first and second reaction mixtures in that they show that in those reaction mixtures were excess yttrium was added, excess unreacted yttrium remains after calcining;

and in the reaction mixtures were equimolar quantities of yttrium and tin, and yttrium and titanium were used, no raw materials remain after calcining. Once again Raman spectra were recorded of all of the products of the third reaction mixtures and these, once again, support the XRD data.

From all of the above evidence, it would appear that when dopants in the form of calcium and vanadium are present, the SEM analysis results are unreliable, and that no yttrium is lost in the calcining process in any of these reactions. This is definitely substantiated by the intensity of the colours of the reaction mixtures which are strongest when the ratio of yttrium to tin, and yttrium to titanium are one to one before calcining. This is also substantiated by the XRD data of these reaction mixtures which show the pyrochlore to be the only product of these reactions, and the Raman spectra of these products. The SEM technique is sometimes influenced by the chemical state of the material being analysed.

2.3.4 THE FOURTH REACTION MIXTURES

Only one yttrium-tin reaction mixture was calcined at 1450°C for two hours. The reaction mixture contained one atom percent of calcium and vanadium as dopants respectively, in the form of $CaCO_3$ and NH_4VO_3. XRD data showed the only product formed in this reaction to be $Y_2Sn_2O_7$. This was confirmed by the Raman spectra of the reaction mixture. The colour of this reaction mixture product was a very intense yellow/orange, the most intense colour of all of the products prepared. The product was in the form of a soft lump that was easily broken down to powder form by the water leaching process.

2.3.5 THE FIFTH REACTION MIXTURES

In pigment synthesis, mineralisers or catalysts are often used to facilitate the formation of the host lattice or the entrance of the chromophore into the host lattice, or both, at a lower temperature. This is a desirable effect since it lowers production costs; cheaper equipment can be used to synthesis the pigment and less power is required. A host of different compounds, known to catalyse other solid state reactions, were tested on both the tin and the titanium pyrochlores at temperatures ranging from 900°C to 1150°C; the temperatures at which the reaction mixtures were fired being determined by the thermal stability of the mineralisers. None of these catalysts were found to have any effect on the formation of the host pyrochlore. This was seen clearly from the XRD results which showed that only starting materials were present after calcining. Both these pyrochlores show great resistance to any form of catalysis what so ever. It is most likely that this is due to yttrium oxides extreme thermal stability (melting point >2300°C), and yttrium oxide's rather poorly developed coordination chemistry that results in it's forming very weak coordination bonds even with elements like fluorine. With this in mind, the fifth reaction mixtures were carried out in an attempt to synthesis the pigment at lower temperatures.

The details of the fifth reaction mixtures are summarised in table 2.4 A ($Y_2Sn_2O_7$) and table 2.4 B ($Y_2Ti_2O_7$) above. One reaction mixture of each of the respective pyrochlores was not doped. The colour of these reaction products were white as expected. One of each of the respective pyrochlores was doped with 2 and with 4 atom percent of calcium and vanadium respectively. The colours of these reaction mixtures were all the same shade of pale yellow. The colours were not at all well developed. The XRD data of

these reaction mixtures are summarised in table 2.12 A ($Y_2Sn_2O_7$) and 2.12 B ($Y_2Ti_2O_7$) below.

Table 2.12 A XRD data for the $Y_2Sn_2O_7$ products of the fifth reaction mixtures.

Reaction number	Y_2O_3	SnO_2	$Y_2Sn_2O_7$	Other
1	(yes)	(yes)	yes	none
2	(yes)	(yes)	yes	none
3	(yes)	(yes)	yes	none

* (yes) - very little present.

Table 2.12 B XRD data for the $Y_2Ti_2O_7$ products of the fifth reaction mixtures.

Reaction number	Y_2O_3	TiO_2	$Y_2Ti_2O_2$	Other
1	(yes)	(yes)	yes	none
2	(yes)	(yes)	yes	none
3	(yes)	(yes)	yes	none

* (yes) - very little present.

From the above XRD data it is clear that the desired pyrochlore has been formed at the relatively low temperature of 1150°C. This is favourable since it cuts down on the manufacturing costs of the ceramic pigment. Unfortunately, even with the high concentrations of dopants used, the intensity of the colour of the pigments is low. Further work may include

attempting to synthesis the pigment using the above 'aqueous technique' in conjunction with a mineraliser mixture.

2.4 SPECTROSCOPY

2.4.1 ELECTRONIC SPECTROSCOPY

Diffuse reflectance electronic spectra were recorded of each of the first reaction numbers of the third reaction mixtures of the tin pyrochlore and of the titanium pyrochlore respectively. (See figures 2.17 and 2.18 - appendix I) Both of these reaction mixtures had intense colours and were made up entirely of the pyrochlore host lattice (no raw materials or by-products present). The vanadium is most likely to be in its fifth and most stable oxidation state [16]. Vanadium in its fifth oxidation state does not have any electrons in its 3d orbitals. Consequently, we do not expect to see any bands in the visible region. From the literature, we expect to see a band in the near infrared region (not a d-d transition) at 271 nm for the free transition metal ion [17]. The spectra of both of the pyrochlore compounds show no absorption maxima in the visible range of the electromagnetic spectrum (ie. 400-700nm) and a band at approximately 300nm. This is in good accordance with the literature.

2.4.2 VIBRATIONAL SPECTROSCOPY

Raman spectra were recorded of all of the pyrochlore reaction products prepared. Some of these appear in appendix I (see figures 2.1-2.12). Infrared spectra were also recorded, but only of selected reaction mixtures.(See figures 2.13 - 2.16). The vibrational spectra and the force fields have been reported by Vandenborre et al. for various pyrochlore compounds including the yttrium/tin and yttrium/titanium pyrochlores [9;10]. Facer et al. have

refined the structure of the yttrium/tin pyrochlore [15]. They have found that the tin atoms are in a nearly octahedral coordination state. It therefore follows that the titanium atoms in the yttrium titanium pyrochlore are also in a nearly octahedral coordination state. The yttrium in both pyrochlores has a distorted eight fold symmetry (ie. The Y atoms are coordinated to eight oxygen atoms placed at the vertices of a scalenohedron). The Raman and infrared data are summarised in tables 2.13 and 2.14 below.

Table 2.13 Raman bands of $Y_2Sn_2O_7$ and $Y_2Ti_2O_7$ observed in this study, and in the literature and the modes and bond contributions from the literature [9;10].

Band No.	$Y_2Sn_2O_7$ undoped	1Atom %	2Atom %	4Atom %	Literature undoped	$Y_2Ti_2O_7$ undoped	1Atom %	2Atom %	4Atom %	Literature undoped	Literature modes	Literature * Bonds
1	-	806	809	811	-	-	823	836	815	-	-	-
2	-	755	762	757	-	-	753	751	-	-	-	-
3	-	-	-	-	-	706	708	704	-	717	-	-
4	505	505	506	507	505	520	523	521	525	527	F_{2g}&A_{1g}	2(&1)
5	410	408	408	409	418	-	-	-	-	333	E_g	1&2(&3)
6	-	-	-	-	355	307	307	306	297	318	F_{2g}	1&2(&3)
7	307	307	305	307	315	-	-	-	-	227	F_{2g}	3

* M = Ti or Sn; 1 = M -O stretch; 2 = O-M-O bend; 3 = Y-O stretch; 4 = O-Y-O bend

Table 2.14 Infrared bands of $Y_2Sn_2O_7$ and $Y_2Ti_2O_7$ observed in this study, and in the literature, and the modes and bond contributions, from the literature [9;10].

Band No.	$Y_2Sn_2O_7$ undoped	1Atom%	Literature undoped	$Y_2Ti_2O_7$ undoped	1Atom%	Literature undoped	literature Modes	literature bonds
1	-	668	-	-	602	-	-	-
2	641	641	640	577	570	568	F_{1u}	1
3	449	451	454	463	461	462	F_{1u}	1&2
4	391	390	396	418	424	410	F_{1u}	2&(1&3)
5	-	375	-	-	376	-	-	-
6	350	354	350	239	232	248	F_{1u}	3&4
7	221	222	227	281	286	285	F_{1u}	1&2&(3)
8	179	177	176	176	170	176	F_{1u}	3&4
9	123	123	125	112	110	105	F_{1u}	3&4

* M = Sn or Ti; 1 = M-O stretch; 2 = O-M-O bend; 3 = Y-O stretch; 4 = O-Y-O bend

The following representation for the vibrations of the pyrochlore structure $A_2B_2O_6O'$ were determined in this study and are in accordance with those determined by Vandenborre et al. (except for one of the inactive modes).

$$\Gamma_{opt} = \underset{(Raman)}{A_{1g}} + \underset{(Raman)}{E_g} + \underset{(inactive)}{2F_{1g}} + \underset{(Raman)}{4F_{2g}} +$$

$$\underset{(inactive)}{3A_{2u}} + \underset{(inactive)}{E_u} + \underset{(Infrared)}{7F_{1u}} + \underset{(inactive)}{4F_{2u}}$$

In accordance with most pyrochlore compounds, the Raman spectra of the yttrium\tin and yttrium\titanium pyrochlores show only three intense bands, and the infrared spectra show seven bands. All of these bands are in accordance with those found in the study of these compounds by Vandenborre. The details of these are summarised in tables 2.13 and 2.14 above.

In the Raman spectra of the undoped reaction mixtures, all three bands in both cases correlate closely with bands reported by Vandenborre et al. In addition, two more bands are seen at around 808 cm^{-1} and 755 cm^{-1} in the case of the doped yttrium/tin pyrochlore; and 820 cm^{-1} and 752 cm^{-1} in the case of the doped yttrium/titanium pyrochlore (table 2.13, band numbers 1 and 2). The direct relationship between the concentration of the dopants and the intensities of these two bands and their absence in the undoped reaction mixtures indicates that they are dopant bands. The relationship between the concentration of the dopant and the intensities of these bands can be seen in the Raman spectra of $Y_2Sn_2O_7$ doped with 1, 2 and 4 atom percent of dopant respectively (figures 2.4, 2.5 and 2.6 - appendix I), and in the

Raman spectra of $Y_2Ti_2O_7$ doped with 1, 2 and 4 atom percent of dopant respectively (figures 2.10, 2.11 and 2.12 - appendix I). Their intensities should be seen relative to the intensities of the pyrochlore bands (table 2.13 band numbers 4, 5 and 7 for the tin pyrochlore, and band numbers 3, 4 and 6 for the titanium pyrochlores).

They are in the region in which one would expect to find vanadium stretching bands, most certainly not calcium stretching bands.

A comparison of the infrared spectra of the undoped and doped reaction mixtures reveal two additional bands; at 668 cm^{-1} and 375 cm^{-1} in the case of the yttrium/tin pyrochlore (table 2.14, band numbers 1 and 5; figures 2.13 and 2.14 - appendix I), and 602cm^{-1} and 376 cm^{-1} in the case of the yttrium/titanium pyrochlore (table 2.14, band numbers 1 and 5; figures 2.15 and 2.16 - appendix I). The additional bands in the infrared spectra are more difficult to see than those in the Raman spectra since infrared bands tend to be broad. Once again these are most likely dopant bands.

An empirical correlation has been developed by Hardcastle et al. for relating the Raman stretching frequencies of vanadium-oxygen (V-O) bonds to their bond lengths in vanadium oxygen reference compounds [18]. In their study, a least squares exponential fit of crystallographically determined V-O bond lengths to V-O Raman stretching frequencies was presented along with a relationship between V-O bond strengths (in valence units) and Raman stretching frequencies. These empirical correlations lead to a very useful, systematic method for determining the coordination and bond lengths of vanadates. The empirical mathematical formula (formula 1 below) was

determined by Hardcastle et al. and relates Raman stretching frequencies to coordination and bond lengths of vanadates.

$$v = 21\ 349 \exp(-1.9176R) \qquad \text{...Formula 1}$$

where v = *position of the band in* cm^{-1}.

R = *bond length in* Å.

Hence, from the bands observed in the Raman spectra of these compounds, we can calculate the bond lengths of the bonds responsible for the respective Raman bands. We can then compare them with the bond lengths of reference compounds of vanadium (V) in the fourth, the fifth and the sixth coordination state to determine in which coordination state the vanadium finds itself.

The bond lengths calculated in this fashion are summarised in table 2.15 below.

Table 2.15 bond lengths of V-O bonds calculated for the tin and titanium pyrochlores using the formula derived by Hardcastle et al.

	Raman Stretching Frequency (cm^{-1})	**Bond Length (Å)**
$Y_2Sn_2O_7$	807	1.708
	760	1.739
$Y_2Ti_2O_7$	820	1.700
	745	1.750

The bands are very intense Raman stretching frequencies. There are only two bands. Comparing the above bands with those of the reference compounds in the work done by Hardcastle et al., we see that the vanadium (V) in the yttrium\tin and yttrium\titanium pyrochlores are in tetrahedral coordination (fourth coordination state). Compounds in tetrahedral coordination have two or three bands in the 700-900 cm^{-1} region. It is in this coordination state that vanadium (V) is in its least distorted coordination state. Compounds in pentacoordinated or octahedrally coordinated states tend to have many more bands (they have more bonds) and the stretching frequency ranges of the bands are much larger. For pentacoordinated vanadium (V) we expect to find bands (up to five) in the range 950-200 cm^{-1} (bond lengths in the range 1.60 - 2.80 Å), and for octahedrally coordinated vanadium (V), we expect to find bands in the range 1000 to 200 cm^{-1} (bond lengths in the range 1.58 - 2.80 Å).

If one compares the Raman bands of the undoped pyrochlores and the pyrochlores doped with various concentrations of dopant (table 2.13 above), one notes very slight shifts in the band positions of the bands that result from tin or titanium stretches and/or bends. This points towards the vanadium substituting for the tin or titanium as the case may be. (The bands in the infrared spectra are too broad to be useful in this way). This may at first seem strange since (as already stated) the tin or titanium atoms, as the case may be, are in octahedral coordination. If, however, we look at the various vanadium pyrochlores used by Hardcastle et al. in their study as reference compounds ($Cd_2V_2O_7$ and α-$Zn_2V_2O_7$), we note that while the vanadium is in its fifth oxidation state (and tetrahedral coordination), the other metal of the pyrochlore is in its second oxidation state; as is calcium.

Since the vanadium is in tetrahedral coordination in the yttrium\tin and yttrium\titanium pyrochlores and the Raman band shifts point towards its being substituted for the tin or titanium as the case may be, the calcium is most likely substituted for the yttrium; the structure around the substituted calcium and vanadium resembling that of the $Cd_2V_2O_7$ and α-$Zn_2V_2O_7$ type pyrochlores.

2.5 CONCLUSION

2.5.1 SYNTHESIS

Bright yellow yttrium/tin and yttrium/titanium pyrochlores doped with calcium and vanadium were synthesised. While the best colour development was found in reaction mixtures calcined at 1450°C very good colour development was also found at 1300°C - a temperature more readily accesable on an industrial scale. The synthesis of the pigment was found to be unreceptive to the mineraliser mixtures tested.

2.5.2 SPECTROSCOPY

The vibrational spectra of the undoped pyrochlores were recorded and found to be in good agreement with those found in the literature. The dopant was found to have a marked effect on the vibrational spectra of the pyrochlores. These spectra along with the electronic spectra of these compounds were used successfully to study the chemical state of the dopants. The dopant responsible for the colour in both of these pigments, vanadium, was found to be in its fifth oxidation state in tetrahedral coordination. The vanadium seems most likely to have substituted for the tin or titanium in the respective pyrochlores, with the calcium having substituted for the yttrium.

CHAPTER 3

The Malayaite and Titanite Compounds

3.1 INTRODUCTION

Malayaite (calcium tin silicate) is a naturally occurring mineral with the general chemical formula $CaSnOSiO_4$ (or simply $CaSnSiO_5$). Malayaite was first found at Perak, Malay Peninsula by Ingham and Bradfood in 1960, and was named by Alexander and Flinter in 1965 [19]. Since then the malayaite mineral has been found in a number of places around the world including Southern Africa. It has been reported that naturally occurring malayaite often contains 10 to 20 percent of titanium [19]. This is not surprising since there is a natural mineral titanium analogue of malayaite called titanite, with the general chemical formula $CaTiOSiO_4$ (or simply $CaTiSiO_5$).

In earlier days malayaite and titanite were thought to be isostructural. With the improvement of XRD techniques it became apparent, however, that there is a structural difference between the two, albeit small. The details of the structures will be discussed in the spectroscopic part of this chapter.

Malayaite shows very good properties of thermal stability and this makes it a good candidate for the host lattice of ceramic pigments. Titanite is not as thermally stable but due to the structural similarities between itself and malayaite, it is also of interest here. Malayaite has been synthetically prepared by Takenouchi using hydrothermal techniques (ie. conditions of high temperature and pressure) in an attempt to emulate the natural formation of malayaite. These conditions are not practical for the bulk synthesis of a material to be used as a ceramic pigment since, by the nature of their being, they are expensive. Alternative methods of synthesis have been reported in which malayaite was synthesised under conditions of high temperature but at atmospheric pressure. These methods which make use of a catalyst

mixture (or mineraliser) are far more suited to the formation of ceramic pigments since they require far less harsh conditions of synthesis, and consequently, are cheaper and easier. Eppler [20], Sanghani et al.[21]; and Carda et al.[22] have used techniques of this nature to investigate the effects of doping malayaite with various guest chromophores. A method similar to those described by Eppler, Sanghani et al., and Carda et al. was used to prepare initial reaction mixtures in this study.

3.2 EXPERIMENTAL

3.2.1 SYNTHESIS OF THE MALAYAITE COMPOUNDS

Stoichiometric quantities of calcium, tin and silicon, in the form of $CaCO_3$ (calcium carbonate; the mineral calcite), SnO_2 (tin oxide; the mineral cassiterite), and SiO_2 (silicon oxide; the mineral quartz), were intimately wet mixed. The reaction mixture was then dried and dry mixed with a mortar and pestle, and then calcined. The reaction mixture was heated from room temperature to 1550°C. This temperature was held constant for two hours after which the reaction mixture was allowed to cool slowly to room temperature inside the oven. The reaction mixture was found to have shrunk considerably and, due to the initial onset of sintering, had formed a solid mass with the shape of the crucible which could not be broken down to a powder form with a mortar and pestle. The Raman spectrum of the reaction product was recorded.

The reaction was repeated under the same conditions but at the slightly lower temperature of 1500°C. The product of this reaction out of the oven was also found to have shrunk considerably, but not to the extent of the reaction calcined out at 1550°C. The product of the 1500°C reaction was

softer than that of the 1550°C reaction and was broken down to powder form with a mortar and pestle. The Raman and infrared spectra of the product were recorded. XRD data were also collected, and a SEM analysis carried out on the reaction product.

A number of other reactions were carried out under various conditions of temperature, with various mineraliser mixtures and mineraliser mixture concentrations, and with different dopants and different dopant concentrations. A number of mineraliser mixtures were tested. A mixture of boric acid (H_3BO_3) and potassium nitrate (KNO_3) was found to produce the best results and was used extensively for the malayaite and titanite reactions. (No other mineraliser mixtures tested were found to have any effect on the reaction at all). Chromium in the form of potassium dichromate ($K_2Cr_2O_7$) and cobalt in the form of cobalt carbonate ($CoCO_3$) were used as dopants in the respective reactions. Unless otherwise stated, the reaction products were washed in boiling water (water leached) to remove any water soluble materials that might have been formed in the calcination process and, in those cases where a mineraliser mixture was used, to remove the mineraliser mixture as well. The details of all of these reactions are summarised in the tables that follow.

Table 3.1 Malayaite reaction mixtures calcined at 1450°C for two hours.

Reaction number	* Ca	: Sn	: Si	dopant %Cr	dopant %Co	min ser %H_3BO_3	min ser %KNO_3
1	1	1	1	-	-	-	-
2	1	1	1	1.00	-	-	-

Reaction number	* Ca	: Sn	: Si	dopant %Cr	dopant %Co	min ser $\%H_3BO_3$	min ser $\%KNO_3$
3	1	1	1	4.00	-	-	-
4	1	1	1	8.00	-	-	-
5	1	1	1	-	0.50	-	-
6	1	1	1	-	2.00	-	-
7	1	1	1	-	4.00	-	-

* Ratio of Ca to Sn to Si; and atom percent of dopants and mineraliser used. (Atom percent of total number of atoms of Ca, Sn and Si before calcining.)

Table 3.2 Malayaite reaction mixtures calcined at 1300°C for two hours.

Reaction number	* Ca	: Sn	: Si	dopant %Cr	dopant %Co	min ser $\%H_3BO_3$	min ser $\%KNO_3$
1	1	1	1	1	-	-	-
2	1	1	1	1	-	5	1
3	1	1	1.33	0.5	-	-	-
4	1	1	1.33	0.5	-	5	1
5	1	1	1.33	1	-	-	-
6	1	1	1.33	1	-	5	1
7	1	1	1.33	4	-	-	-
8	1	1	1.33	4	-	5	1
9	1	1	1	-	2	5	1
10	1	1	1.33	-	2	-	-
11	1	1	1.33	-	2	5	1

* Ratio of Ca to Sn to Si; and atom percent of dopants and mineraliser used. (Atom percent of total number of atoms of Ca, Sn and Si before calcining.)

Table 3.3 Malayaite reaction mixtures calcined at 1200°C for two hours.

Reaction number	* Ca	: Sn	: Si	dopant %Cr	dopant %Co	min ser $\%H_3BO_3$	min ser $\%KNO_3$
1	1	1	1	-	-	-	-
2	1	1	1	-	-	5	1
3	1	1	1	0.25	-	-	-
4	1	1	1	0.25	-	5	1
5	1	1	1	0.50	-	-	-
6	1	1	1	0.50	-	5	1
7	1	1	1.33	0.50	-	5	1
8	1	1	1	1.00	-	-	-
9	1	1	1	1.00	-	5	1
10	1	1	1.33	1.00	-	5	1
11	1	1	1	-	2	-	-
12	1	1	1	-	2	5	1

* Ratio of Ca to Sn to Si; and atom percent of dopants and mineraliser used. (Atom percent of total number of atoms of Ca, Sn and Si before calcining.)

Table 3.4 Malayaite reaction mixtures calcined at 1150°C for two hours.

Reaction number	* Ca	: Sn	: Si	dopant %Cr	dopant %Co	min ser $\%H_3BO_3$	min ser $\%KNO_3$
1	1	1	1	-	-	-	-
2	1	1	1	-	-	5	1
3	1	1	1	2	-	-	-
4	1	1	1	2	-	5	1
5	1	1	1.33	2	-	-	-

Reaction number	* Ca	: Sn	: Si	dopant %Cr	dopant %Co	min ser $\%H_3BO_3$	min ser $\%KNO_3$
6	1	1	1.33	2	-	5	1
7	1	1	1	-	2	-	-
8	1	1	1	-	2	5	1
9	1	1	1.33	-	2	-	-
10	1	1	1.33	-	2	5	1

* Ratio of Ca to Sn to Si; and atom percent of dopants and mineraliser used. (Atom percent of total number of atoms of Ca, Sn and Si before calcining.)

Table 3.5 Malayaite reaction mixtures calcined at 1150°C for twelve hours.

Reaction number	* Ca	: Sn	: Si	dopant %Cr	dopant %Co	min ser $\%H_3BO_3$	min ser $\%KNO_3$
1	1	1	1	-	-	-	-
2	1	1	1	-	-	5	1
3	1	1	1	2	-	-	-
4	1	1	1	2	-	5	1
5	1	1	1.33	2	-	-	-
6	1	1	1.33	2	-	5	1
7	1	1	1	-	2	-	-
8	1	1	1	-	2	5	1
9	1	1	1.33	-	2	-	-
10	1	1	1.33	-	2	5	1

* Ratio of Ca to Sn to Si; and atom percent of dopants and mineraliser used. (Atom percent of total number of atoms of Ca, Sn and Si before calcining.)

Table 3.6 Malayaite reactions calcined at 1300°C for two hours. Reactions carried out to test the effect of the mineraliser concentration on the reaction.

Reaction number	* Ca : Sn : Si	dopant %Cr	min ser $\%H_3BO_3$	min ser $\%KNO_3$
1	1 : 1 : 1	0.5	-	-
2	1 : 1 : 1	0.5	0.5	0.5
3	1 : 1 : 1	0.5	1.0	1.0
4	1 : 1 : 1	0.5	2.0	2.0
5	1 : 1 : 1	0.5	3.5	3.5
6	1 : 1 : 1	0.5	5.0	0.0
7	1 : 1 : 1	0.5	0.0	5.0
8	1 : 1 : 1	0.5	5.0	1.0

* Ratio of Ca to Sn to Si; and atom percent of dopants and mineraliser used. (Atom percent of total number of atoms of Ca, Sn and Si before calcining.)

3.2.2 SYNTHESIS OF TITANITE

Stoichiometric quantities of calcium, titanium and silicon, in the form of $CaCO_3$ (calcium carbonate; the mineral calcite), TiO_2 (titanium dioxide; the mineral rutile) and SiO_2 (silicon dioxide; the mineral quartz), were intimately wet mixed. The reaction mixture was then dried and dry mixed with a mortar and pestle, and then calcined. The reaction mixture was heated from room temperature to 1200°C. This temperature was held constant for two hours after which the reaction mixture was allowed to cool slowly to room temperature inside the oven. (Initially this reaction was attempted at 1450°C but the reaction mixture sintered.) The product was found to have shrunk slightly and was crystalline and hard. The product was broken down to

powder form with a mortar and pestle. The reaction was repeated a number of times under the same conditions as the previous reaction but at the lower temperature of 1150°C. A mineraliser mixture was used in some of the reaction mixtures. The Raman and infrared spectra of selected reaction products were recorded. XRD data were also collected, and a SEM analysis carried out, also on selected reaction products. The details of all of the titanite reactions are summarised in table 3.7 below.

Table 3.7 Titanite reaction mixtures.

Reaction number	* Ca : Ti : Si	min ser $\%H_3BO_3$	min ser $\%KNO_3$	Temp. °C	Time hours
1	1 : 1 : 1	-	-	1200	2
2	1 : 1 : 1	-	-	1150	2
3	1 : 1 : 1	5	1	1150	2
4	1 : 1 : 1	-	-	1150	10
5	1 : 1 : 1	5	10	1150	10

* Ratio of Ca to Ti to Si; and atom percent of mineraliser used; and calcination temperatures and times.
(Atom percent of total number of atoms of Ca, Ti and Si before calcining.)

XRD results of the above reaction mixtures of malayaite and titanite showed that various reaction mixtures contained unreacted raw materials, and in some cases other by-products, along with, or instead of the desired reaction products (these results are discussed below). In the malayaite reactions, these by-products were found to be $CaSiO_3$ (calcium silicate; the mineral wollastonite) and $CaSnO_3$ (calcium tin oxide), and in the titanite reactions,

$CaTiO_3$ (calcium titanium oxide). Consequently, $CaSiO_3$, $CaSnO_3$ and $CaTiO_3$ were synthesised in order to study their properties and the effect that they have on the formation of, and on the vibrational spectra of malayaite and titanite respectively.

3.2.3 SYNTHESIS OF $CaSnO_3$ AND $CaTiO_3$

Stoichiometric quantities of calcium and tin, in the form of $CaCO_3$ (calcium carbonate; the mineral calcite) and SnO_2 (tin oxide; the mineral cassiterite), were intimately wet mixed. The reaction mixture was then dried and dry mixed with a mortar and pestle, and then calcined. The reaction mixture was heated from room temperature to 1300°C. This temperature was held constant for two hours after which the reaction mixture was allowed to cool slowly to room temperature inside the oven. The product was found to have shrunk considerably and was crystalline and hard. The reaction product was broken down to powder form with a mortar and pestle. The Raman spectrum was recorded of the product and the XRD data were collected.

The $CaTiO_3$ was prepared in the same way as the $CaSnO_3$ above except that titanium, in the form of TiO_2 (titanium dioxide; the mineral anatase), was substituted for tin oxide.

3.2.4 SYNTHESIS OF $CaSiO_3$

Stoichiometric quantities of calcium and silicon, in the form of $CaCO_3$ (calcium carbonate; the mineral calcite) and SiO_2 (silicon oxide; the mineral quartz), were intimately wet mixed. The reaction mixture was then dried and dry mixed with a mortar and pestle, and then calcined. The reaction mixture was heated from room temperature to 1150°C. This temperature was held

constant for two hours after which the reaction mixture was allowed to cool slowly to room temperature inside the oven. (The product was initially calcined at a higher temperatures but sintered in each case.) The product was found to have shrunk slightly and to be a soft powder. A number of other reactions were carried out, some with dopants and some with mineralisers. The details of these reactions are summarised in table 3.8 below.

Table 3.8 $CaSiO_3$ reaction mixtures calcined at 1150°C for various time periods.

Reaction number	* Time hours	Ca : Si	dopant %Cr	min ser %H_3BO_3	min ser %KNO_3
1	2	1 : 1	-	-	-
2	2	1 : 1	0.5	-	-
3	2	1 : 1	0.5	5	1
4	2	1 : 1	2	-	-
5	2	1 : 1	2	5	1
6	10	1 : 1	-	-	-
7	10	1 : 1	0.5	-	-
8	10	1 : 1	0.5	5	1
9	10	1 : 1	2	-	-
10	10	1 : 1	2	5	1

* Calcination times of reactions; ratio of Ca to Si; and atom percent of dopant and of mineralisers used.
(Atom percent of total number of atoms of Ca, Ti and Si before calcining.)

3.3 RESULTS AND DISCUSSION

3.3.1 MALAYAITE REACTIONS AT 1550°C AND AT 1500°C FOR TWO HOURS

These reaction products were synthesised in order to produce undoped reference samples for comparison with doped reaction mixtures of malayaite using SEM analysis, XRD and the various forms of spectroscopy. The high temperatures at which these reactions were calcined also give useful information about the thermal stability of the starting materials, and of coarse, the reaction products.

The product of the reaction calcined at 1550°C showed signs of considerable shrinkage, though no significant loss in weight was observed (ie. weight of product expected, calculated on the basis of number of moles of starting materials assuming malayaite to be the only product formed.). In fact, the product was one solid mass which could not be broken down to powder form with a mortar and pestle. At 1550°C the reaction mixture was apparently on the verge of sintering. Consequently, SEM analysis and XRD were not used to characterise the reaction product. The Raman spectrum of the reaction product was recorded (figure 3.1 - appendix I).

The product of the reaction calcined at 1500°C also showed signs of considerable shrinkage, though not to the extent of the reaction at 1550°C. The shrinkage was approximately half that of the product of the reaction calcined at 1550°C. While this product was also in the form of a solid mass, it was possible to break it down to powder form with a mortar and pestle. A SEM analysis was done, and XRD data collected on the reaction product. The results of the SEM analysis and XRD data are summarised in table 3.9 and table 3.10 below.

Table 3.9 SEM analysis results for the malayaite reaction calcined at 1500°C for two hours.

REACTION NUMBER	ATOM %		
	Ca	Sn	Si
1	27.58	31.93	40.48

Table 3.10 XRD results of the malayaite reaction calcined at 1500°C.

Reaction number	SnO_2	SiO_2	$CaSnSiO_5$	Other compounds
1	none	none	yes	none

The accuracy of the SEM technique has been mentioned before and is discussed in appendix III. The reproducibility of the results is good to within approximately ten atom percent. So it is not surprising that, while the SEM analysis indicates an excess of silicon in the reaction product, the XRD data shows that no unreacted silicon oxide nor any other silicon containing by-products are present in any measurable quantities. The reaction can therefore be said to have gone to completion at 1500°C, without loss of any of the starting materials. Raman and infrared spectra of the product were recorded. (See figures 3.2 and 3.22 - appendix I). The results of the spectra recorded will be discussed later.

As already stated, the Raman spectrum of the product of the reaction

calcined at 1550°C was recorded. A comparison between this spectrum and that of the product of the 1500°C shows that the only product of the 1550°C reaction is malayaite.

Consequently, the only difference between the reaction product of the 1500°C reaction and that of the 1550°C reaction is their physical properties coming out of the oven. Both were very hard, but the 1500°C reaction product was not as hard. The harder the reaction product, the larger the particle sizes of the particles, and the more they are agglomerated. As far as the desirable properties of ceramic pigments are concerned, the softer the product coming out of the oven the better since this cuts down on the milling required to get the pigment to the size required for application to the ceramic product. This consequently cuts down on production costs. Synthesising a pigment at a lower temperature also reduces production costs. Consequently, doped reaction mixtures were prepared at temperatures lower than 1500°C. The first doped reaction products were prepared at 1450°C with good results overall. Subsequent reactions were carried out at temperatures ranging from 1300°C to 1150°C. The effect of various mineraliser mixtures on the reaction were also tested. The results of all of these reaction mixtures are discussed below.

3.3.2 MALAYAITE REACTIONS CALCINED AT 1450°C FOR TWO HOURS

The details of these reactions are summarised in table 3.1 above. Reaction number 1 contains no dopants or mineraliser. It is however clear from the reaction products maroon/pink colour that the product was contaminated with chromium in the calcining process. The chromium had diffused uniformly throughout the whole reaction mixture. The the Raman spectrum

of this reaction mixture (figure 3.3 - appendix I) when compared to that of the undoped malayaite synthesised at 1500°C (figure 3.2 - appendix I) shows three extra bands at 741 cm^{-1}, 940 cm^{-1} and 983 cm^{-1} respectively (for further discussion, these bands will be referred to as 'the chromium bands'). These bands are due to chromium and are associated with the pink colour. The spectroscopic details of the doped and undoped malayaite will be discussed later in this chapter. The chromium can only have come, via the vapour phase, from the other reaction mixtures calcined at the same time, inside the same oven as reaction number one. The contamination could not have come from the oven since the reactions calcined at 1550°C and at 1500°C were calcined inside the same oven. Clearly, the chromium is volatile at 1450°C. None of the reaction mixtures calcined at this temperature contained any mineraliser mixture.

Reaction numbers 2, 3 and 4 were doped with 1, 4 and 8 atom percent of chromium respectively. The Raman spectrum of reaction number 2 can be seen in appendix I - figure 3.14. If one compares this spectrum to that of reaction number 1 (figure 3.3 - undoped but contaminated malayaite) the three bands that are present as a result of the chromium are far more intense in relation to the malayaite bands (572 cm^{-1}, 512 cm^{-1}, 443 cm^{-1}, 363 cm^{-1} and 323 cm^{-1} - referred to as 'the malayaite bands' for further discussion) indicating (not surprisingly) that the intensity of these bands is a function of, and proportional to the amount of chromium present in the reaction product. All three reaction products had shrunk considerably, and were hard. They were broken down with a mortar and pestle to produce coarse, hard powders. Under the microscope the reaction products were crystalline in nature. In addition, they were all very darkly coloured maroon, with the odd

particle having a crystalline green phase as part of it. The intensity of the colour of the chromium doped reaction mixtures was a function of, and proportional to the amount of chromium with which they were doped.

Reaction numbers 5, 6 and 7 were doped with 0.5, 2 and 4 atom percent of cobalt respectively. The Raman spectrum of reaction number 2 can be seen in appendix I - figure 3.11. No cobalt bands seem to be present; only the malayaite bands. Possible reasons for this are discussed in the spectroscopy section of this chapter. The product mixtures were shrunk to a far greater extent than those doped with chromium, and unlike their chromium doped counterparts, were shrunk to various degrees; the amount of shrinkage appearing to be a function, and proportional of the amount of cobalt present in the reaction mixture. Reaction numbers 5 (0.5 atom% Co) and 6 (2 atom% Co) were broken down to powder form with a mortar and pestle. Reaction number 7 (4 atom% Co) was in the process of sintering at 1450°C and was one solid mass that could not be broken down to powder form with a mortar and pestle. The shrinkage of this reaction product was considerable. The cobalt seemed to lower the temperature required to cause malayaite to sinter. The reaction products were all blue, the intensity of the colour once again being a function of, and proportional to the amount of dopant present in the reaction mixture. The mixture containing 0.5 atom% of cobalt was a blue/white colour with a strong undertone of pink. This reaction mixture too had been contaminated with chromium. The reaction mixture containing 4 atom% of cobalt was a very dark shade of blue. Although an undertone of pink could not be seen in reaction mixtures 6 and 7 (the blue was too intense), they to were contaminated with chromium. The evidence for this is found in the Raman spectra of these reaction mixtures which show the

presence of the chromium pink bands (figure 3.11 - appendix I).

As stated in the experimental section of this chapter, all reaction products were water leached to remove any water soluble products of the calcination process. The supertinants that remained after the reaction products had been filtered off, in all of the chromium doped mixtures (reaction numbers 2, 3 and 4), were clear and bright yellow in colour. The supertinant of reaction number 1 (the undoped but contaminated reaction product) and of reaction mixtures 5, 6 and 7 (the cobalt doped reaction mixtures) were transparent and colourless. The yellow supertinants of the chromium doped reaction mixtures were evaporated to dryness and a SEM analysis was carried out on the solid yellow material that remained. The SEM analysis revealed that the yellow material was composed of potassium and silicon in roughly equal quantities, and approximately 10% of chromium. The yellow colour is therefore a result of the chromium in this water soluble compound. Consequently, the intensity of the yellow supertinant can be used as an indication of the amount of chromium that has not reacted to form the maroon pigment. It was found, in the three chromium doped reaction mixtures above, that the intensity of the yellow supertinant is also a function of the amount of chromium used to dope the reaction mixtures.

SEM analysis was done, and XRD data collected on selected reaction products that were calcined at 1450°C. The results are summarised in table 3.11 and table 3.12 below. As in the SEM analysis results of the pyrochlore compounds, while the dopants were also analysed, these results are not reported since, at such low concentrations, they are grossly inaccurate.

Table 3.11 SEM analysis results for selected malayaite reactions calcined at 1450°C for two hours.

Reaction number	ATOM%		
	Ca	Sn	Si
1	31.27	34.09	34.64
2	30.91	33.15	35.94
3	30.92	30.62	38.46

Table 3.12 XRD results of selected malayaite reaction calcined at 1450°C.

Reaction number		SnO_2	SiO_2	$CaSnSiO_5$	Other compounds
2	*	(yes)	no	yes	none
6		(yes)	no	yes	none

* (yes) - very little present.

The SEM analysis results show that no apparent loss of calcium tin or silicon starting materials has occurred. The SEM analysis is unfortunately not sensitive enough to give reliably results as to the concentration of dopants present since the concentrations of these are too low. But it is clear from the contamination of some of the reaction mixtures that some of the chromium is lost to the vapour phase in the calcination process and that some reacts to form a water soluble by product. None of the cobalt appeared to be lost to the vapour phase but the cobalt did seem to catalyse the formation or the sintering of malayaite since the cobalt doped products were far more coarse

than their chromium doped counterparts.

3.3.3 MALAYAITE REACTIONS CALCINED AT 1300°C FOR TWO HOURS

The details of these reactions are summarised in table 3.2 above. Reaction numbers one and two contained 1 atom percent of chromium as dopant. In addition reaction number two also contained a mineraliser mixture in the form boric acid (H_3BO_3) and potassium nitrate (KNO_3), the concentration of which were optimised. This is discussed later in this chapter. The colour of reaction number one was a light pink/maroon. The colour of reaction number two was a dark maroon; far more intense than that of reaction number one. The mineraliser has a marked effect on the reaction product.

In addition to the effect that the mineraliser has on the colour of the pigment, the effect that it has on the physical properties of the pigments after it has been calcined is also noteworthy. The reaction mixtures containing mineraliser show signs of shrinkage and are hard and crystalline. The reaction mixtures without mineraliser are soft powders with particle sizes that are visibly smaller. Unfortunately this effect of the mineraliser is undesirable for reasons already discussed.

The colour of malayaite based ceramic pigment doped with chromium and synthesised with a ratio of calcium to tin to silicon of one to one to one, tend to fade when leached with acid. Silicon is used extensively as a material for coating powders in order to increase their resistance to chemical attack, amongst other things. It is also a cheap and readily available raw material and since it is a starting material of this reaction, it was seen as a prime candidate for protecting this pigment. It was therefore added to reaction

numbers 3 to 8, in the form of quartz, to try to increase the resistance of these pigments colours to acid leaching.

Reaction numbers 3 and 4, 5 and 6, and 7 and 8 contained 0.5, 1 and 4 atom percent of chromium as dopant respectively. One of each of these reaction mixtures (reaction numbers 4, 6 and 8) also contained a mineraliser mixture; the same as that used in reaction number 2. The colours of the reaction mixtures that did not contain the mineraliser mixture (reaction numbers 3, 5 and 7) were all lighter shades of pink/maroon. Furthermore, their colours were almost indistinguishable from one another, irrespective of the fact that some of the reaction mixtures contained more chromium than others. The reaction mixtures that did contain mineraliser (reaction numbers 4, 6 and 8) were all shades of maroon, the intensity of their colours being a function of, and proportional to the amount of dopant in the reaction mixture before calcining.

The Raman spectra of reaction numbers 2 (1 atom %Cr with mineraliser) and 1 (1 atom %Cr without mineraliser) can be seen in appendix I - figures 3.5 and 3.6. While the colours of the two reaction products may differ, the Raman spectra of the reaction products prepared at this temperature do not.

A comparison of the reaction mixtures with extra quartz and those without yields the following results. Both reaction mixtures 2 and 6 contained the same amount of dopant and mineraliser but reaction mixture 6 contained an excess of quartz. Reaction mixture 6 was found to have a colour that was very slightly stronger and brighter than that of reaction mixture 2. This is an interesting result since one might have expected the excess of quartz to

dilute the colour instead of apparently strengthening it.

All of the above reaction mixtures were water leached before the acid leaching tests. The resulting supertinants of reaction numbers 1 and 2 (those without excess of quartz) were transparent and bright yellow in colour indicating the loss of some of the dopant as described earlier. The resulting supertinants of reaction numbers 3 to 8 (those with an excess of quartz) were transparent and colourless.

Comparative acid leaching tests done on those reaction mixtures with, and those without an excess of quartz, show that the reaction mixtures with an excess of quartz have a much higher resistance to acid leaching treatment than those without. The acid leaching treatment gives a good indication of how the pigment will respond when applied to a ceramic article and processed since the processing procedure is very corrosive. The loss of colour in the reaction mixtures with excess quartz was not detectable with the eye. A small loss of dopant is apparent from the feint yellow colour of the mother liquor of the acid leaching treatment after the pigment has been filtered off.

The results of the water leaching and acid leaching tests show that the addition of an excess of quartz to reaction mixtures calcined at 1300°C has favourable effects.

Reaction numbers 9, 10 and 11 each contained 2 atom percent of cobalt respectivly. Reaction numbers 10 and 11 also contained an excess of quartz. Reaction numbers 9 and 11 also contained the mineraliser mixture. All three

reaction mixture products were hard and crystalline, the reaction mixture without mineraliser included. As already noted, this seems to be due to the presence of the cobalt since the reaction mixtures doped with chromium and without mineraliser are soft powders. The cobalt doped reaction mixture without mineraliser had a pink undertone indicating that it was contaminated with chromium. The contamination by the chromium can be seen clearly in the Raman spectra of this reaction mixture (figure 3.12 - appendix I). The reaction mixtures containing mineraliser showed a much more intense colour development than the reaction mixture without mineraliser. Consequently, these reaction mixtures did not show visible signs of chromium contamination (a pink undertone). Very small chromium contamination could however be seen in the Raman spectra of these two reaction mixtures. In the case of the cobalt doped reaction mixtures, unlike that of the chromium doped reaction mixtures, the addition of excess quartz did serve to noticeably dilute the colour of the reaction product.

SEM analysis was done, and XRD data collected on selected reaction products that were calcined at 1300°C. The SEM analysis results are in line with those of the reaction products prepared at 1450°C and are not discussed further. The XRD results are summarised in table 3.13 below.

TABLE 3.13 XRD results of selected malayaite reaction calcined at 1300°C.

Reaction number	SiO_2	SnO_2	$CaSnO_3$	$CaSiO_3$	$CaSnSiO_3$
1	yes	yes	yes	yes	yes
2	yes	yes	no	no	yes

Reaction number	SiO_2	SnO_2	$CaSnO_3$	$CaSiO_3$	$CaSnSiO_3$
5	yes	yes	yes	yes	yes
6	yes	yes	no	no	yes
8	yes	yes	no	no	yes

The XRD data shows that the predominant product in all of the reaction mixtures calcined at this temperature was malayaite (the desired product). The relative peak heights of a strong malayaite peak that does not overlap with the peak of a raw material or by-product, of reaction mixtures without mineraliser (1 & 5) are 68.89 and 69.66 respectively. The relative peak heights of the same peak of reaction mixtures with mineraliser (reaction mixtures 2, 6 & 8) are all 100.00 respectively. Clearly, more malayaite is formed when the mineraliser is used. The fact that all three peaks are the same height, taken into consideration the fact that there is an excess of quartz (SiO_2) present in the reaction mixtures 6 & 8, indicates that there is even more malayaite formed in the reaction mixtures with an excess of quartz. The relative intensities of the quartz peaks in the reaction mixtures that started out with excess quartz are higher than those that did not by roughly a third indicating that the excess quartz has not reacted, but is still present as quartz. The relative peak heights of all the malayaite peaks show that the reaction mixtures (2, 6 & 8) containing mineraliser (in the form of H_3BO_3 and KNO_3) have far more malayaite present than those reaction mixtures (1 & 5) without mineraliser. Also noteworthy from table 3.13 are the presence of other products besides malayaite but only in the reaction mixtures without mineraliser.

3.3.4 MALAYAITE REACTIONS CALCINED AT 1200°C FOR TWO HOURS

The details of these reactions are summarised in table 3.3 above. Reaction numbers 1 and 2 contain no dopant. Reaction number 2 contains a mineraliser mixture in the form of boric acid and potassium nitrate. Both reaction mixtures showed signs of chromium contamination, but only on the top of the crucible.

Reaction numbers 3 and 4, were doped with 0.25 atom percent of chromium. Reaction number 4 contained a mineraliser mixture. Reaction numbers 5, 6 and 7 were doped with 0.5 atom percent of chromium. Two of these mixtures contained a mineraliser mixture, one of which also contained an excess of quartz. Reaction numbers 8, 9 and 10 were doped with 1 atom percent of chromium. Two of these mixtures contained a mineraliser mixture, one of which also contained an excess of quartz. As with the reaction mixtures calcined at 1300°C, the reaction mixtures calcined at 1200°C with a mineraliser mixture showed considerable shrinkage inside their crucibles. In addition, these reaction mixtures were hard and crystalline with larger particle sizes than the reaction mixtures calcined without a mineraliser mixture, which were soft powders.

Once again the reaction mixtures without mineraliser were pink in colour and almost indistinguishable from one another irrespective of the amount of chromium with which they were doped. The reaction mixtures with a mineraliser mixture showed a much more intense colour development with the colour being a function of, and proportional to the amount of chromium used to dope the reaction mixtures. The addition of excess quartz to reaction mixtures with a mineraliser mixture also did not have a detrimental effect on

the colour of the reaction mixtures calcined at this temperature. The colours of these reaction mixtures were virtually indistinguishable from the colours of the reaction mixtures with the same concentrations of dopant and mineraliser mixture. As might be expected from the results of the reaction mixtures calcined at 1300°C, the water leaching process yielded a transparent yellow supertinant in the case of the chromium doped reaction mixtures without excess quartz, and a colourless transparent mother liquor in the case of the reaction mixtures with excess quartz.

The Raman spectra of reaction numbers 9 (1 atom %Cr with mineraliser) and 8 (1 atom %Cr without mineraliser) can be seen in appendix I - figures 3.7 and 3.8. A comparison of the two spectra shows clearly that at 1200°C malayaite is not the favoured reaction product unless the mineraliser mixture is present. As one might expect, this is the trend for all reactions calcined at 1200°C and below.

Reaction numbers 11 and 12 were doped with 2 atom percent of cobalt. Reaction number 12 contained a mineraliser mixture, the same as that used in the other reaction mixtures calcined at 1200°C. At this temperature the cobalt did not seem to have much of an effect on the physical properties of the product of reaction mixture 11 (without mineraliser) which was a soft powder with a very poorly developed sky blue colour. In contrast, reaction mixture 12 (with mineraliser) was hard and crystalline and was broken down to powder form with a mortar and pestle. Once again, this is the trend for all reactions calcined at 1200°C and below. The colour of this reaction mixture was well developed.

XRD data were collected on selected reaction products that were calcined at 1200°C and are summarised table 3.14 below.

TABLE 3.14 XRD results of selected malayaite reaction calcined at 1200°C.

Reaction number	SiO_2	SnO_2	$CaSnO_3$	$CaSiO_3$	$CaSnSiO_5$
8	no	yes	yes	(yes)	(yes)
9	no	(yes)	no	no	yes
12	no	(yes)	no	no	yes

* (yes) - very little present.

The XRD results show that in the reaction mixture calcined at 1200°C without mineraliser (reaction mixture 8), very little malayaite has been formed. Instead, judging from the relative peak heights of the XRD, a lot of tin oxide remains unreacted and a lot of $CaSnO_3$ and a little $CaSiO_3$ have been formed as by-products. As already stated, the colours of these reaction mixtures were poorly developed. The reaction mixtures containing a mineraliser mixture (reaction numbers 9 an 12), on the other hand, show malayaite as the major product, with the only other mineral present, a small amount of unreacted tin oxide. The empirical Raman results are confirmed by the XRD data.

3.3.5 MALAYAITE REACTIONS CALCINED AT 1150°C FOR TWO HOURS

The details of these reactions are summarised in table 3.4 above. Reaction numbers 1 and 2 contained no dopant. Reaction number 2 contained a mineraliser mixture in the form of boric acid (H_3BO_3) and potassium nitrate

(KNO_3). Reaction mixtures 3, 4, 5 and 6 contained 2 atom% of chromium as dopant. Reaction mixtures 5 and 6 contained an excess of quartz. One of the reaction mixtures with extra quartz (reaction mixture 5), and one of the reaction mixtures without extra quartz (reaction mixture 3) contained the same mineraliser mixture as reaction number 2. Reaction mixtures 7, 8, 9 and 10 were doped with 2 atom percent of cobalt. Reaction mixtures 9 and 10 contained excess quartz. One of the reaction mixtures with excess quartz (reaction mixture 10) and one of the reaction mixtures without extra quartz (reaction mixture 8) contained the same mineraliser mixture as reaction number 2.

Once again the reaction mixtures containing mineraliser had shrunk in the calcination process, but only very slightly at this temperature. These reaction mixtures were also only very slightly harder (more crystalline) than the reaction mixtures without mineraliser, which were soft as expected. The undoped reaction mixture with mineraliser showed very slight chromium contamination but only on top. From this it is deduced that although the chromium is still volatile at the lower temperature of 1150°C, it is so to a much lesser extent.

The colour intensity of all of the chromium and cobalt doped reaction mixtures was low. This is especially true if on considers the relatively large amount of dopant used to dope these reaction mixtures with. The reaction mixtures containing an excess of quartz showed a colour that was very diluted and very poorly developed in both the chromium and cobalt doped reaction mixtures.

XRD data was collected on selected reaction products that were calcined at 1150°C for two hours. The XRD data are summarised table 3.15 below.

TABLE 3.15 XRD results of selected malayaite reaction calcined at 1200°C.

Reaction number	SnO_2	SiO_2	$CaSnO_3$	$CaSiO_3$	$CaSnSiO_5$
1	* yes	yes	yes	(yes)	no
2	yes	no	no	no	yes
3	yes	no	yes	(yes)	no
4	yes	no	no	(yes)	yes
5	yes	(yes?)	(yes)	yes	no
6	yes	(yes?)	(yes?)	(yes)	(yes)

* (yes) - very little present.

(yes?) - might be present but if so, only in very small quantities.

From the XRD results, it is clear that no malayaite was formed at this temperature in the reaction mixtures without a mineraliser mixture. In the reaction mixtures with mineraliser, the two reaction mixtures without an excess of quartz showed the best results as far as the formation of malayaite is concerned. The amount of malayaite formed judging from the relative peak heights of the XRD data, however, was roughly only fifty percent. The rest was mostly unreacted tin oxide. In the reaction with an excess of quartz, the reaction products also included large amounts of $CaSiO_3$. The colour development in all of the reaction mixtures was poor, with the exception of the reaction mixture with mineraliser but without an excess of quartz. This reaction mixture's colour was however also weakly developed relative

compared to reaction mixtures with the same quantities of starting materials and dopant, fired at higher temperatures. In addition, this reaction mixture did not show very good resistance to acid attack in the leaching process as one might expected. The XRD and results are supported by the Raman spectra of the respective reaction mixtures. (figures 3.9 and 3.10 - appendix I).

3.3.6 MALAYAITE REACTIONS CALCINED AT 1150°C FOR TWELVE HOURS

The reactions calcined at 1150°C for two hours were not very successful. This set of reactions was carried out to test the effect of increasing the length of the calcination time on the reaction products. The details of these reactions are summarised in table 3.5 above. Lengthening the calcination time did not improve the colour development of the reaction products in the chromium or the cobalt doped reaction mixtures. If anything, the effect of lengthening the calcining time caused the colour to weaken slightly. Perhaps this is due to greater loss of chromium to the vapour phase. There was also no improvement in the quantity of malayaite formed.

XRD data collected on selected reaction products that were calcined at 1150°C for twelve hours. The XRD data are summarised in table 3.16 below.

TABLE 3.16 XRD results of selected malayaite reaction calcined at 1150°C for twelve hours.

Reaction number	SiO_2	SnO_2	$CaSnO_3$	$CaSiO_3$	$CaSnSiO_5$
1	* yes	yes	yes	(yes)	no
2	no	(yes)	no	no	yes

Reaction number	SiO_2	SnO_2	$CaSnO_3$	$CaSiO_3$	$CaSnSiO_5$
4	no	yes	no	(yes)	yes
8	no	yes	(yes?)	(yes?)	yes

* (yes) - very little present.

(yes?) - might be present but if so, only in very small quantities.

The XRD data are very similar to those of the reaction mixture calcined at 1150°C for two hours. Clearly calcining the mixture for an extra ten hours has little or no effect on the reaction products.

3.3.7 MALAYAITE REACTIONS CARRIED OUT TO TEST THE EFFECT OF THE MINERALISER CONCENTRATION ON THE REACTION PRODUCT

The details of these reactions are summarised in table 3.6 above. The reactions were calcined at 1300°C for two hours. All of the reaction mixtures contained the relatively low dopant concentration of 0.5 atom percent of chromium. The reaction mixtures were mixed with various concentrations of boric acid (H_3BO_3) and potassium nitrate (KNO_3) as mineralisers.

A comparison of the colour of all of these reaction mixtures revealed the following results. The reaction mixture without any mineraliser mixture had the colour with the lowest intensity except for the reaction mixture that contained only potassium nitrate as mineraliser. (The colour of this reaction mixture was an off white grey\pink.) Reaction numbers 2, 3, 4 and 5 contained increasing concentrations of boric acid and potassium nitrate, ranging from 0.5 to 3.5 atom percent. The intensity of their colours was a

function of, and proportional to the concentration of boric acid and potassium nitrate present. Reaction mixture 6 contained only 5 atom percent of boric acid as mineraliser. The intensity of the colour of this reaction mixture was slightly weaker than that of the reaction mixtures containing both boric acid and potassium nitrate as mineraliser mixture (irrespective of the concentrations). Reaction number 8 contained 5 atom percent of boric acid and, 1 atom percent of potassium nitrate. This reaction mixture showed the best colour development of all the reaction mixtures produced to test the effect of the mineraliser concentration on the product of the reactions. Consequently, it was this concentration of boric acid and potassium nitrate that was used in all of the malayaite reaction mixtures already discussed. Various other compounds, known to catalyse the reaction of other pigments, were tested on the malayaite reaction without success.

XRD data was collected on selected reaction products of these reaction mixtures. The results of the XRD data are summarised in table 3.17 below.

TABLE 3.17 XRD results of selected malayaite reactions carried out to test the effect of the mineraliser concentration on the reaction products.

Reaction number	SiO_2	SnO_2	$CaSnO_3$	$CaSiO_3$	$CaSnSiO_5$
1	* no	yes	(yes)	(yes)	yes
4	no	(yes)	no	no	yes
8	no	(yes)	no	no	yes

* (yes) - very little present.

The XRD results are interesting. Reaction number 1 contained no mineraliser. The XRD results of this reaction mixture show the presence of a large amount of unreacted tin oxide, and the formation of calcium silicate and calcium tin oxide as by-products, relative to the other reaction mixtures. Reaction number 4 contained 2 atom percent of boric acid and of potassium nitrate. Reaction 8 contained 5 atom percent of boric acid and 1 atom percent of potassium nitrate. The relative peak heights of the malayaite peaks in the XRD data of reaction numbers 4 and 8 indicate that reaction number 8 has the most malayaite formed of all the reactions in this batch. This is in line with it having the most intensely developed colour as well.

3.3.8 TITANITE REACTIONS

The details of these reactions are summarised in table 3.7 above. XRD data was collected on selected reaction products of these reaction mixtures. The results are summarised in table 3.18 below.

Table 3.18 XRD results of selected titanite reactions.

Reaction number		SiO_2	TiO_2	$CaTiO_3$	$CaTiSiO_5$
1	*	yes	(yes)	yes	yes
3		(yes)	(yes)	yes	yes

* (yes) - very little present.

The XRD results show that there is a small amount of $CaTiO_3$ formed in both reaction mixtures and that there are very small quantities of unreacted raw materials left as well. Reaction number 3 contains a mineraliser mixture in the form of boric acid and potassium nitrate; reaction number 1 does not.

Reaction mixture 3 contains roughly double the amount of titanite than reaction mixture 1 judging from the relative peak heights of the XRD data. The Raman spectra of these reaction mixtures shows titanite as the only product in the reaction mixtures containing the mineraliser mixture, and the presence of large amounts of by-products in the reaction mixtures without the mineraliser (figures 3.17 and 3.18 - appendix I).

3.3.9 BY-PRODUCT REACTIONS

The details of the synthesis of these reaction are discussed in sections 3.2.3 and 3.2.4 above. The $CaSnO_3$ was not doped and was white in colour. XRD confirmed its make up. $CaTiO_3$ was also not doped and was a slightly off-white colour. Both doped and undoped reaction mixtures of $CaSiO_3$ were synthesised. The undoped reaction product was white in colour, while the doped reaction mixture produced a avocado green coloured pigment. The Raman spectra of all of these reaction products were recorded. In addition, the electronic spectra (diffuse reflectance) of the doped $CaSiO_3$ was also recorded. The details of these spectra are discussed latter in this chapter.

3.4 SPECTROSCOPY

3.4.1 INTRODUCTION

The chemical state of the dopants of all of the pigments discussed in this work are of primary importance since it is the chemical state of the dopants that is directly responsible for the colour of the reaction products. Spectroscopy was very successful in deciphering the chemical state of the vanadium doped pyrochlores in chapter 2. The chemical state of the dopants of the pigments of this chapter were also studied with the various forms of spectroscopy with very interesting results.

3.4.2 ELECTRONIC SPECTROSCOPY

3.4.2.1 MAROON/PINK CHROMIUM DOPED MALAYAITE

The electronic spectrum of chromium doped malayaite prepared in this study was recorded (figure 3.26 - appendix I). It is most likely that the chromium is in its third oxidation state and in octahedral coordination, since this is the most stable chemical state of chromium.

For Cr(III) in octahedral coordination, we find the following transitions [23;24].

ν_1: A_{2g} (F) → T_{2g} (F)

ν_2: A_{2g} (F) → T_{1g} (F)

ν_3: A_{2g} (F) → T_{1g} (P)

For Cr(III) in tetrahedral coordination, we find the following transitions [23;24].

ν_1: T_1 (F) → T_2 (F)

ν_2: T_1 (F) → A_2 (F)

ν_3: T_1 (F) → T_1 (P)

Clearly then, in both tetrahedral and octahedral coordination there will be three bands. The energy states of these transitions are shown schematically in figure 1 below. From figure 1 it is clear that not all three bands in tetrahedrally and octahedrally coordinated d^3 ions will have the same energy. Consequently, although there will be three bands in both spectra, the band gaps will be different. The band gaps are characteristic of the coordination state and can therefore be used to determine the coordination state of the respective ion.

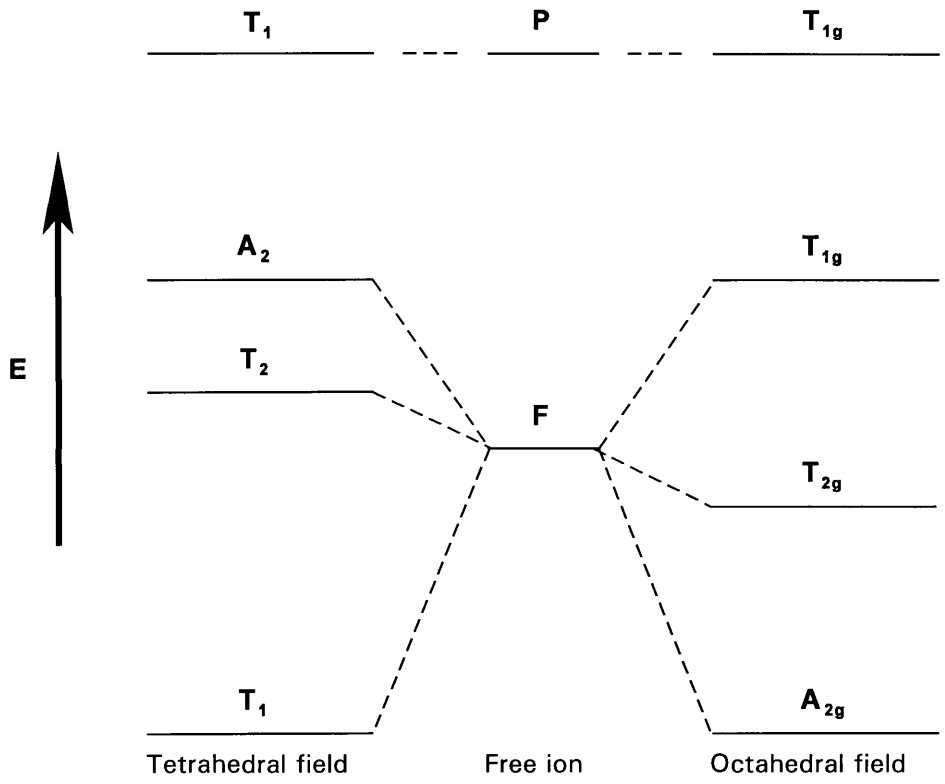

FIGURE 1 Energy level scheme for the maximum multiplicity term splitting in tetrahedral and octahedral complexes in d^3 configurations.

The electronic spectra of the chromium doped malayaite, recorded in this study, show three bands as expected (figure 3.26 - appendix I). The bands are assigned to the most probable transitions and then the assignment is tested using the Tanabe-Sugano diagram for a transition metal element in the d^3 state in octahedral coordination [23]. Consequently the empirically observed bands are assigned as follows.

ν_1: 15 385 cm^{-1} (650 nm)

ν_2: 18 870 cm^{-1} (530 nm)

ν_3: 33 333 cm^{-1} (300 nm)

The Tanabe-Sugano diagram for a transition metal element in the d^3 state shows good correlation for $\nu 1$ and $\nu 3$ at $\Delta/B = 15$. This correlates to $B' = 0.9B$ for Cr(III). From the Tanabe-Sugano diagrams at $\Delta/B = 15$, the

theoretical position for ν_2 is 19 467 cm^{-1}. The theoretical value correlates very well with the empirical value of 18 870 cm^{-1} obtained in this study. Consequently, as expected from the electronic spectra, the chromium is in its Cr(III) oxidation state in octahedral coordination.

3.4.2.2 BLUE COBALT DOPED MALAYAITE

The electronic spectra of cobalt doped malayaite prepared in this study was recorded (figure 3.27 - appendix I). The electronic spectra of the blue cobalt doped malayaite has been reported by Carda et al [22].The UV-VIS spectra of a cobalt doped blue pigment with the spinel structure has also been published; by J. Alarcon et al [25]. (For many years ceramic pigments with the spinel structure have been used extensively in the ceramic industry [26;27;28]).In both the cobalt-malayaite blue and the cobalt-spinel blue the cobalt is in the Co(II) oxidation state [22;25]. Alarcon et.al. place the Co(II) in the spinel pigment in tetrahedral coordination through calculations involving Tanabe-Sugano diagrams. This goes along with the simple observation that tetrahedral complexes of cobalt most commonly have an intense blue colour. Octahedral complexes of cobalt, on the other hand, are typically pale red or purple in colour [24]. And it is this very same observation that makes the findings of Carda et al. suspect. Through the same type of calculations, also involving Tanabe-Sugano diagrams, Carda et al. place the Co(II) in the malayaite pigment in octahedral coordination. Their spectra show a very broad band between approximately 500nm and 700nm, the local maxima on this broad band being very weak. The spectra obtained in this study show a very broad band between approximately 450nm and 700nm but with very clearly defined local maxima on this broad band. In addition, the spectra obtained in this study bare a very close

resemblance to those in the study of the Co(II)-spinel blue [25]. Both papers are suspect from the point of view that they have reported using spectra in the range of 800nm to 300nm. From the discussion that follows it is clear that both tetrahedrally and octahedrally coordinated Co have only the ν_3 band in this region. Calculations involving Tanabe-Sugano diagrams are impossible when only one band can be observed.

The electronic spectra of the cobalt blue malayaite synthesised were recorded (figure 3.26 - appendix I). Typical electronic spectra of tetrahedrally coordinated Co(II) in the form of $[CoCl_4]^{2-}$, and octahedrally coordinated Co(II) in the form of $[Co(H_2O)_6]^{2+}$ have been published [29;24] and are reproduced in figure 2 below.

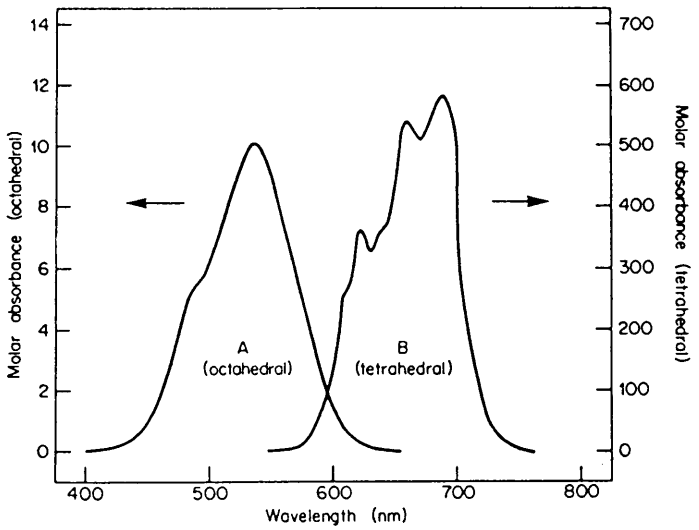

FIGURE 2 The electronic spectra of $[Co(H_2O)_6]^{2+}$ (spectrum A) and $[CoCl_4]^{2-}$ (spectrum B).

The spectrum of the tetrahedrally coordinated Co(II) shows very close resemblance to the spectra obtained in this study, and of the spectra obtained in the study of the cobalt doped spinel by Alarcon et al.

For Co(II) in octahedral coordination, we find the following transitions [24].

ν_1: T_{1g} (F) → T_{2g} (F)

ν_2: T_{1g} (F) → A_{2g} (F)

ν_3: T_{1g} (F) → T_{1g} (P)

The visible spectrum is dominated by the highest energy transition; ν3. The transition with the next highest energy (ν_2) is essentially a two electron process and is consequently weaker by a factor of about 10^{-2}. The third and last spin allowed transition (ν_1) generally occurs in the near infrared region [24].

For Co(II) in tetrahedral coordination, we find the following transitions [24].

ν_1: A_2 (F) → T_2 (F)

ν_2: A_2 (F) → T_1 (F)

ν_3: A_2 (P) → T_1 (P)

Once again the visible region is dominated by the highest energy transition (ν_3). For tetrahedral complexes there is also a transition in the near infrared region (ν_2), as well as one of quite low energy (ν), which is seldom observed because it is in an inconvenient region of the spectrum (1000-2000 nm), and it is orbitally forbidden [24].

Consequently, we expect to see only one band in the visible region for

tetrahedral and maybe two for the octahedral Co(II) complexes with one of the bands being about 100 times weaker than the other. The visible transitions in both cases, but particularly in the tetrahedral case, generally have complex envelopes because a number of transitions to doublet exited states occur in the same region, and these acquire some intensity by means of spin-orbit coupling. In tetrahedral systems, as illustrated in figure 2 above, the visible transition is generally an order of magnitude more intense and displaced to lower energies, in accordance with the observed colours mentioned above. From the above evidence, it seems very likely that the Co(II) species is in tetrahedral coordination rather than in octahedral coordination as suggested by Carda et al.

3.4.2.3 GREEN CHROMIUM DOPED WOLLASTONITE

The electronic spectrum was recorded of chromium doped wollastonite (figure 3.25 - appendix I). As with the chromium doped malayaite (3.4.2.1 above) we expect to find the chromium in its most stable state (ie. Cr(III) d^3) and in Cr(III)'s stable coordination state (ie. Octahedral). All the details of Cr(III) in tetrahedral and octahedral coordination have been discussed above (3.4.2.1). Following the procedure used above, we assign the three bands found in the electronic spectra of the chromium doped wollastonite as follows.

ν_1: 14 164 cm^{-1} (706 nm)

ν_2: 16 835 cm^{-1} (600 nm)

ν_3: 26 316 cm^{-1} (380 nm)

Once again, the Tanabe-Sugano diagram for a transition metal element in the d^3 state shows good correlation for ν_1 and ν_3 at $\Delta/B = 15$ [23]. This

correlates to $B' = 0.75B$. From the Tanabe-Sugano diagrams at $\Delta/B = 15$, the theoretical position for ν_2 is 16 223 cm^{-1}. The theoretical value correlates very well with the empirical value of 16 835 cm^{-1}. Consequently, as expected, the electronic spectrum indicates that the chromium is in its Cr(III) oxidation state in octahedral coordination.

3.4.3 VIBRATIONAL SPECTROSCOPY

3.4.3.1 THE SELECTION RULES

If one takes the complexity of the structure of malayaite and titanite into account, it is hardly surprising that the vibrational spectra of the respective compounds have not yet been fully assigned. It is also not the aim of this study to undertake such an operation. Instead, a some what simpler method was employed to shed some light on the properties of spectra recorded in this study. As will become evident, this was done so very successfully.

Factor group analysis is generally performed by operating upon all of the atoms in the appropriate primitive unit cell at the same time. Both malayaite and titanite have four molecules per unit cell ($Z = 4$), and two molecules per Bravais unit cell (Primitive unit cell). Consequently, separation of this task into a set of similar tasks , each dealing with a complete set of equivalent points (Wyckoff sites) allows much simpler tabulation of results that are in a suitable form for general purposes.

Table 3.19 and 3.20 were taken from the literature [30]. They were computed using a table of site group symmetries derived from the "International Tables for X-Ray Crystallography".

Table 3.19 Data derived for space group 15 (C2\c) for factor group analysis [30].

Wyckoff	Space Group 15 C2/c (C_{2h})			
letter	A_g	B_g	A_u	B_u
2a-2d	0	0	3	3
2e	1	2	1	2
4f	3	3	3	3

Table 3.20 Data derived for rotatory modes of space group 15 (C2/c) for factor group analysis [30].

Wyckoff	Space Group 15 C2/c (C_{2h})			
letter	A_g	B_g	A_u	A_u
2a-2d	3	3	0	0
2e	1	2	1	2
4f	3	3	3	3

The results of the factor group analysis are summarised in table 3.21 below, and were obtained as follows. The relevant row of table 3.19 corresponding to the Wyckoff letter of the respective atom was tabulated, for each atom. These rows were then summed to yield the total number of modes for $CaSnSiO_5$ (N(total)). The unit cell vibrations of molecules and complex ionic crystals may be further divided into internal and external (or lattice) modes. Optical branch translatory modes (T) are calculated by considering only the translationally independent components of the unit cell. Thus, $(T + T_A)$ is obtained by summing the rows in table 3.19 which correspond to the centres of gravity of any molecules, complexes or monatomic ions present. If we

look at malayaite (and/or titanite), there are not any molecules, complexes or monatomic ions that can be isolated. These are after all solid state materials. One can however 'break' up the complex into nearest neighbour components. Malayaite consists of corner sharing SnO_6 octahedra cross linked by silicate tetrahedra to form a $SnOSiO_4$ framework that accommodates Ca in irregular 7-coordination polyhedra [31]. The structure of titanite is almost exactly the same as that of malayaite. In fact, at temperatures in excess of 220°C the two compounds are isostructural [32;33]. They are both in space group 15. At temperatures below 220°C, titanite has a structure in space group 14 (slightly less symmetrical). This is because there is a slightly 'off-centred' displacement of the titanium atoms from the geometric centre of each octahedron resulting in long and short Ti-O bonds alternating along the chains of the TiO_6 octahedra. Consequently, we can look at the structure of malayaite (and titanite) in distinct, isolated units. That is, SnO_6 octahedra (or TiO_6 octahedra), and SiO_4 tetrahedra. The Ca polyhedra are not important as far as substitution by these chromophores is concerned. Thus, $T+T_A$ is the sum of rows of table 3.19, representing Sn (or Ti) and Si (the centres of gravity of the translatory independent components). They are 4d for Sn (or Ti) and 4e for Si. T_A is the sum of the translatory modes obtained from the character table for C_{2h} symmetry group (space group 14 and 15) (ie. A_u+2B_u). R for Sn (or Ti) and Si, the rotatory modes, are obtained from table 3.20. $T+T_A$ and the rotatory modes of the atoms representing the centres of gravity of the 'discrete components' of these compounds are subtracted from the total number of modes (N(total)) to yield the number of internal modes (N (internal)). The data described above are tabulated below.

Table 3.21 Selection rules for $CaSnOSiO_4$ (Malayaite)

Element & Wyckoff symbol	A_g	B_g	A_u	B_u
Ca 4e	1	2	1	2
Si 4e	1	2	1	2
Sn 4d	0	0	3	3
O 4e	1	2	1	2
O_4 8f	3	3	3	3
N (total)	6	9	9	12
$T + T_A$	1	2	4	5
T_A	0	0	1	2
R (Si 4e)	1	2	1	2
R (Sn 4d)	3	3	0	0
N (internal)	1	2	4	5

Consequently, we expect to see three Raman bands ($1A_g$ band and 2 less intense B_g bands) and 9 infrared bands ($4A_u$ and 5 B_u bands) due to internal modes in the spectrum of malayaite. The same procedure was followed for titanite and the results are summarised in table 3.22 below. The data derived for space group 14 is not reproduced here [30].

Table 3.22 Selection rules for $CaTiOSiO_4$ (Titanite)

Element & Wyckoff symbol	A_g	B_g	A_u	B_u
Ca 4e	3	3	3	3
Si 4e	3	3	3	3

Element & Wyckoff symbol	A_g	B_g	A_u	B_u
Ti 4d	3	3	3	3
O(1)4e	3	3	3	3
O(4)4e	6	6	6	6
N (total)	18	18	18	18
$T + T_A$	6	6	6	6
T_A	0	0	1	2
R (Si 4e)	3	3	3	3
R (Ti 4d)	3	3	3	3
N (internal)	6	6	6	6

Consequently, we expect to see twelve Raman bands ($6A_g$ band and 6 less intense B_g bands) and 12 infrared bands ($6A_u$ and 6 B_u bands) due to internal modes.

Raman spectra were recorded of all of the malayaite reaction mixtures prepared (figures 3.1 - 3.18 - appendix I), and of all of the related reaction mixtures; and of all of the raw materials. Infrared spectra were recorded of selected reaction mixtures only(figures 3.19 - 3.22 - appendix I). As already discussed, the crystal structure of malayaite and titanite have been previously reported [11;31;32;33].

3.4.3.2 RAMAN AND INFRARED SPECTRA

Raman spectra were recorded of all of the malayaite, titanite and by-product reaction products. Selected spectra appear in appendix I (figures 3.1 - 3.18). Infrared spectra were also recorded, but only of selected reaction mixtures. These can also be seen in appendix I (figures 3.19 - 3.22).The bands observed in the Raman and infrared spectra of these compounds are summarised in tables 3.23 and 3.24 below.

Table 3.23 Raman and infrared bands of malayaite observed in this study.

RAMAN BANDS (cm^{-1})			IR BANDS (cm^{-1})		
Undoped	Cr doped	Co doped	Undoped	Cr doped	Co doped
-	980	-	910	907	908
-	938	-	865	860	867
-	741	-	811	820	820
571	571	571	668	668	670
511	490	511	566	566	564
443	452	443	530	532	530
363	362	362	470	470	468
323	322	323	420	423	422
			343	340	341
			315	315	315
			256	257	259
			217	214	215
			140	157	141
			123	132	122

Table 3.24 Raman and infrared bands of titanite observed in this study and Raman bands reported in the literature [34].

RAMAN BANDS cm^{-1}		**IR BANDS cm^{-1}**
This study	Literature	This study
606	594	897
535	522	874
465	453	676
424	412	668
384	374	563
350	341	470
313	306	436
286	279	340
257	251	314
		282
		232
		121

It is clear from the discussion in 3.4.3.1 above that many more bands are expected in both the Raman and infrared spectra of titanite than in that of malayaite. This is to be expected since titanite, as already stated, is in a less symmetrical space group than malayaite. This is in fact what we observe in the spectra of malayaite and titanite. In the Raman spectrum of malayaite, one very intense band is seen at 572 cm^{-1}, the A_g band. Two bands with roughly half the intensity of the band at 572 cm^{-1} are seen at 363 cm^{-1}, and 323 cm^{-1}, and two bands with roughly a fifth of the intensity of the 572 cm^{-1} band at 512 cm^{-1}. Two of these bands are the internal B_u modes predicted in 3.4.3.1 above (figures 3.1 and 3.21 - appendix I). In addition,

there are a number of bands at around 900 cm^{-1} of very low intensity. The details of all these bands are summarised in table 3.23 above.

The spectra of titanite (figure 3.17 - appendix I) shows a very intense band at 606 cm^{-1} and a number of relatively intense bands between 250 and 600 cm^{-1}. In addition, there are some very weak bands at around 900 cm^{-1}. The details of all of these bands are summarised in table 3.24 above along with the bands observed by Salje et al. [34] and it is clear that the spectra of the two studies are very similar. The details of the infrared spectra of titanite are also summarised in table 3.24 above (figure 3.24 - appendix I).

A comparison of the infrared spectra of undoped malayaite with those of chromium and cobalt doped malayaite that the doping has no apparent effect on the spectra of these compounds. This is not surprising since the quantity of dopants used was very small which will result in dopant bands that are of very low intensity. This in addition to the phenomena that leads to the band of infrared spectra being broad makes it very difficult for the bands of the dopants to be seen.

The fact that the dopants are in such low concentrations might suggest that their bands might also be difficult to see in the Raman spectra of these compounds. This indeed appears to be the case with the cobalt doped malayaite. A comparison of the Raman spectra of undoped malayaite with that of cobalt doped malayaite shows that the two spectra are for all practical purposes, identical (figures 3.1 and 3.11 - appendix I). This does not mean that Raman spectroscopy is obsolete as a tool for the study of this compound. Rather, the excitation line (514.5 nm laser beam) used in this

study may not be capable of exiting the cobalt(II)-oxide bands. It is in fact found empirically that cobalt(II) compounds are often not responsive to the 514.5 nm excitation line. So, further studies might include recording the Raman spectra of this compound with a different excitation line.

It is in the spectra of chromium doped malayaite that we see Raman spectroscopy coming to its full potential. These spectra show the emergence of some extremely intense bands (relative to the malayaite bands) at 740 cm^{-1}, 935 cm^{-1} and 980 cm^{-1}. These bands are due to the chromium in the doped reaction mixtures. The intensity of these bands is abnormally high. This is due to a phenomenon known as *Resonance Raman* (see appendix II). The sensitivity of Raman for these bands is so high that chromium was detected in undoped reaction mixtures and cobalt reaction mixtures that had been contaminated with chromium that had come from chromium doped reaction mixtures, via the vapour phase, during calcining and in many cases the concentration was so low that it could not be detected by the naked eye. It is from these bands that a number of very interesting questions arise.

From the electronic spectra of these compounds it appears that the chromium is in its third oxidation state, and in octahedral coordination. We also know that the compound yields a pink to maroon colour depending on the concentration of chromium with which the reaction mixture was doped. The gem stone ruby has a similar colour to that of the chromium doped malayaite. The colour results from α-alumina (Al_2O_3) doped with chromium in its third oxidation state which, not surprisingly, is also in octahedral coordination [24]. The environment of the Cr (III) in ruby is a slightly distorted octahedron of oxide ions. The frequency of the spin allowed

electronic transitions of Cr(III) in ruby indicate that the chromium ions are under considerable compression. This results in the maroon colour observed in ruby.

If chromium in the ruby and that in malayaite are in a very similar chemical state (Cr(III) in octahedral coordination), and it is clear that their colours are very similar, then one could reasonable expect to find chromium bands in the Raman spectra of the two compounds in similar positions. With this in mind, the Raman spectra of undoped synthetic α-alumina, chromium doped synthetic α-alumina, and natural ruby were recorded (figures 3.19 - 3.21 - appendix I). The Raman spectrum of α-alumina has been assigned [35]. α-alumina has an E_g band at 751 cm^{-1}. Unfortunately, this corresponds to the position of the most intense chromium band in malayaite. There is also an A_{1g} alumina band at 418 cm^{-1}. The Raman spectra of undoped synthetic α-alumina, chromium doped synthetic α-alumina and natural chromium doped α-alumina (ruby) all show the intense A_{1g} alumina band at around 418 cm^{-1}. In addition, they all have a band at around 750 cm^{-1}; the α-alumina E_g band as expected. The intensity of this band in the undoped synthetic alumina is very small in comparison to that of the A_{1g} band. In the doped synthetic alumina, the intensities of the to bands are roughly equal. So the intensity of the 750 cm^{-1} band has increased in the chromium doped alumina. In addition, there is an extra band at around 785 cm^{-1} in the spectrum of the doped α-alumina of the same intensity as the 750 cm^{-1} band. All of these bands are seen in the spectrum of natural ruby, but the 418 cm^{-1} band is by far the most intense band. This could very well be due to the extremely high crystallinity of the natural ruby. It is crystalline to the point that it is transparent. The synthetic alumina is white. While these bands do occur in

the right area to be chromium bands that are similar to those in the chromium doped malayaite, it is not possible to state unequivocally at this point that they arise from bonds that are similar to those that give rise to the bands in the spectra of chromium doped malayaite.

There is another question which needs to be addressed; the question of electro neutrality. The evidence so far points to the chromium being in its third oxidation state, in octahedral coordination. If this is the case, then the chromium atom will most likely be occupying the tin position. The tin in malayaite, as already stated, is in octahedral coordination, and is in its fourth oxidation state. Consequently, the substitution will lead to the loss of a positive charge. This loss needs to be countered for in some way or another. It is not clear how this is done though certain mechanisms may be speculated upon. It is interesting to note however that natural titanite contains aluminium and iron as substituents for titanium, and consequently it is likely that the same mechanism that is responsible for maintaining electro neutrality in aluminium doped titanite, is responsible for maintaining electro neutrality in chromium (III) doped malayaite. The fact that the Al(III) is capable of substituting Ti(IV) in titanite and that Cr(III) is capable of substituting Al(III) in ruby is strong circumstantial evidence that Cr(III) is capable of substituting Sn(IV) in malayaite.

Another possibility is that chromium (IV) is responsible for the colour in this ceramic pigment, as suggested by Gohshi [36]. It is necessary at this stage to point out that the work performed by Gohshi et al. in the early seventies does not seem to be totally accurate. The technique that they employed is not in general use thirty odd years latter. In addition, the apparatus used by

these researchers is probably not capable of yielding the resolution that they report. Nonetheless, chromium (IV) is certainly a possibility. It would certainly maintain electro neutrality in malayaite without any complicated mechanism being involved. It has also to be noted, however, that chromium (IV) is not a preferred chemical state of chromium since it is rather unstable. This seen against the back drop of the extreme temperatures at which these pigments are synthesised makes it very unlikely that the chromium is present in its fourth oxidation state. Unfortunately, the Raman spectrum of CrO_2 could not be found in the literature. It is unlikely that this is due to an oversight. CrO_2 is of coarse well known for its ferromagnetic properties [37] and is widely used in cassettes amongst other things. The infrared spectra of this compound has been reported and shows only one very broad band [38]. CrO_2 has the rutile structure and consequently, the chromium is in octahedral coordination [37].

The only other possibility for the chemical state of chromium is of coarse the well characterised Cr(VI). Once again, this is not a very stable state of chromium although it is most certainly more stable than Cr(IV). Invariable, Cr(VI) is found in tetrahedral coordination. If it is present in malayaite, it is therefore most likely substituted for silicon. This is certainly not impossible. This of course does not solve the problem of electro neutrality. There is another reason why Cr(VI) is an unlikely candidate. Cr(VI) has no electrons in its d-orbitals. Consequently, if it has any colour at all, it is likely to be pale, and its electronic spectrum is likely to resemble that of the pyrochlores.

As already stated, the chromium bands are found at 740 cm^{-1}, 940 cm^{-1} and 980 cm^{-1} respectively. From the literature [39], we expect to find Cr(III)-

oxide bands in the region 625-446 cm^{-1} and Cr(VI)-oxide bands between 950-500 cm^{-1}. While the chromium bands of malayaite initially appear to be too high to be Cr(III) bands, the shift might very well be accounted for by the fact that, as in ruby, the chromium atoms have to be under considerable compression to account for the 'ruby like' colour. This would most certainly result in a shift of a chromium bands to a higher wave number, around 740 cm^{-1} perhaps, but they are unlikely to be shifted as far as far as 940 and 980 cm^{-1}. It therefore seems as though chromium might be present in two chemical states, Cr(III) with a band at 740 cm^{-1} and responsible for the maroon colour; and Cr(VI) with bands at 940 cm^{-1} and 980 cm^{-1}, and not contributing much to the colour of the pigment. This being the case, the problem of electro neutrality might be solved by having one Cr(VI) atom for every two Cr(III) atoms present. The ratios of the intensities of the three bands, relative to each other, are constant in all of the spectra recorded of chromium doped malayaite. The electronic spectra of Cr(VI)-oxide compounds and of Cr(III)-oxide compounds show that both types of chromium complexes are candidates for being influenced by the resonance Raman effect [40].

From all the evidence above, it is clear that the problem is complex, and that further work in this area is required. This may include the follow.

1. Adding another dopant (phosphoric acid perhaps) in addition to the chromium to counter the loss of the positive charge when chromium is substituted for tin to test the effect that this has on the conditions of synthesis of this pigment, the spectra of the reaction product, and of coarse the colour of the reaction product.

2. Doping the titanite with chromium. As already stated, titanite has a crystal structure that is more compact than that of malayaite. This, added to the fact that chromium is most likely under considerable compression in the malayaite crystal structure may mean that the chromium will not substitute for titanium in titanite at all. The chromium bands of malayaite may of coarse appear in titanite indicating that the chromium may be sitting in another position.

3. Replace the calcium with a rare earth cation. This will have an effect on the charge balance of the compound.

4. Attempt to synthesis single crystals of chromium doped malayaite for detailed crystallographic studies.

3.5 CONCLUSION

3.5.1 SYNTHESIS

Chromium doped malayaite with the most intense colour was synthesised at 1450°C without a mineraliser. It was found that a mineraliser mixture of boric acid and potassium nitrate significantly reduced the temperature required to produce pigment with a sufficiently intense colour. Pigments with good colour intensity were produced at 1200°C with the mineralizer mixture, the concentration of which was optimised. An excess of quartz was found to improve the chemical and thermal stability of the pigment.

Cobalt doped malayaite with the most intense colour was synthesised at 1450°C. The products at this temperature were highly agglomerated. At temperatures above 1200°C, cobalt was found to increase the amount of

agglomeration in the reaction product. Excess quartz did adversely affect the colour of this pigment, but since this pigment was stable to acid leaching, excess quartz was not required. It was found that a mineraliser mixture of boric acid and potassium nitrate significantly reduced the temperature required to produce pigment with a sufficiently intense colour. The pigments with the best quality were produced at 1300°C.

Titanite was synthesise for spectroscopic purposes.

Certain by-products of the malayaite and titanite reaction were also synthesised and investigated.

3.5.2 SPECTROSCOPY

The electronic spectra of chromium and cobalt doped malayaite were recorded. They indicated that the chromium is in its third oxidation state, in octahedral coordination. Consequently the chromium is most likely substituted for the tin in malayaite. The cobalt is in its second oxidation state, in tetrahedral coordination, and most probably substituted for the silicon in malayaite.

The vibrational spectra of undoped malayaite and titanite were recorded and the number of internal modes associated with them calculated. Spectra of chromium and cobalt doped malayaite were also recorded. The Raman spectra of chromium doped malayaite showed the presence of chromium bands. The origin of these bands were investigated. Although they seem to support the electronic spectra, this could not be shown unequivocally. Further experimental work is required in this respect.

CHAPTER 4

Conclusion

4.1 SOLID STATE CHEMISTRY

Material science and studies in the solid state are often regarded as the domain of physics or metallurgy. While physics tends to concentrate on the characterization of solid state materials, metallurgy tends to concentrate on extracting and working with metals. Chemistry is able to combine these two fields with synthesis. An understanding of the chemical properties of the elements allows the chemist to synthesis solid state materials. The chemist is then able to characterise the reaction products by combining an intimate knowledge of the chemistry of the elements with sophisticated equipment.

4.2 SYNTHESIS

Synthesis formed an integral part of this study. The approach used in the synthesis of the materials in this study had to satisfy two criteria. Firstly, the pigments synthesised had to have the best possible chemical and aesthetic properties required of ceramic pigments. Secondly, the synthesis techniques used had to be viable on an industrial scale. These two factors are often not complimentary. We see, for example, in both pigments investigated, that the higher the temperature at which they are prepared, the better the colour development. Unfortunately, high temperatures are expensive. Invariable, a compromise has to be made.

4.3 CHARACTERIZATION

Characterisation of these pigments was divided into two parts. Firstly, characterisation of the bulk host material, and secondly, characterisation of the guest dopant(s) (or chromophore(s)). The host lattice materials investigated in this study were all naturally occurring minerals and

consequently, through geology, they have been well characterised. The structural and electronic properties of small amounts of dopants added to these minerals have, on the other hand, not been well characterised. This is because most techniques are not sensitive enough to detect such small quantities of dopants in a host lattice. XRD and SEM analysis were used effectively to investigate the host materials in this study but not the dopants. Spectroscopy was found to be very useful in studying the chemical state of the dopants and was also useful as an empirical tool.

In the study of the pyrochlore compounds, electronic spectroscopy and vibrational spectroscopy were used successfully to study the chemical state of the vanadium and calcium (the dopants). A novel empirical relationship between vanadium-oxygen bond lengths and the vibrational frequency of their Raman bands was used to determine the coordination states of the dopants and their positions inside the host lattice.

The usefulness of spectroscopy as a tool for studying small quantities of dopants inside a host material was also illustrated in the study of the chromium and cobalt doped malayaite, titanite and other related compounds. Electronic spectroscopy was used successfully to investigate the chemical state of all of the doped reaction products. An empirical relationship between chromium-oxygen bond lengths and the vibrational frequency of their Raman bands has not been reported and the bands of the Raman spectra of malayaite and titanite have also not been fully assigned due to their complexity. Consequently a different approach to that used in the study of the pyrochlores was used. Resonance Raman effects were seen in the Raman spectra of chromium doped malayaite. The chemical state of the

dopants and their position inside the host lattice could not be solved unequivocally. The resonance Raman effects will almost certainly be instrumental in determining the chemical state of the dopants and their position inside the host lattice in further studies. Recording Raman spectra using a different excitation line could also be useful in this respect. Synthesising other related compounds may also be useful in further studies (these are discussed in chapter 3).

The limitation of infrared spectroscopy as a tool for studying these compounds when compared with Raman spectroscopy is the broadness of the bands (as with most compounds). Further studies will most certainly also include investigating both pigment types under the newly acquired microscope infrared apparatus. Broad bands are also a major draw back in electronic spectroscopy (The bands can be narrowed using a cryostat).

Many different techniques are required when studying compounds of this nature since different compounds tend to react differently to different techniques. We see for example that while SEM analysis was useful in the studies of malayaite and titanite, it was not accurate in the studies of the doped pyrochlores. Also, while XRD was very useful in studying the host lattices, it could not be used to study the dopants. (It should be noted that more advanced XRD equipment than that used in this study might well be useful in the study of the dopants.) Spectroscopy was very useful in this respect. Spectroscopy too has its drawbacks. Not least of all, the broad bands characteristic of electronic and infrared spectroscopy, and the expensive equipment and complex nature of vibrational spectroscopy.

Finally, while the pigments were tested on ceramic articles from time to time, the results of these tests are not discussed here. The glaze, which is used as the glass binder on ceramic products, is a complex mixture of metal oxides. Optimising the glaze formulation to suit the pigment is a study in itself.

APPENDIX I

Vibrational

and

Electronic

Spectra

1.1 Vibrational and Electronic Spectra of Chapter 2

1.1.1 VIBRATIONAL SPECTRA

1.1.1.1 RAMAN SPECTRA

FIGURE 2.1 Raman spectrum of undoped $Y_2Sn_2O_7$ synthesised with a ratio of Y:Sn of 4:1.

FIGURE 2.2 Raman spectrum of undoped $Y_2Sn_2O_7$ synthesised with a ratio of Y:Sn of 3:1.

FIGURE 2.3 Raman spectrum of undoped $Y_2Sn_2O_7$ synthesised with a ratio of Y:Sn of 1:1.

FIGURE 2.4 Raman spectrum of $Y_2Sn_2O_7$ doped with 1 atom percent of Ca and V.

FIGURE 2.5 Raman spectrum of $Y_2Sn_2O_7$ doped with 2 atom percent of Ca and V.

FIGURE 2.6 Raman spectrum of $Y_2Sn_2O_7$ doped with 4 atom percent of Ca and V.

FIGURE 2.7 Raman spectrum of undoped $Y_2Ti_2O_7$ synthesised with a ratio of Y:Ti of 4:1.

FIGURE 2.8 Raman spectrum of undoped $Y_2Ti_2O_7$ synthesised with a ratio of Y:Ti of 3:1.

FIGURE 2.9 Raman spectrum of undoped $Y_2Ti_2O_7$ synthesised with a ratio of Y:Ti of 1:1.

FIGURE 2.10 Raman spectrum of $Y_2Ti_2O_7$ doped with 1 atom percent of Ca and V.

FIGURE 2.11 Raman spectrum of $Y_2Ti_2O_7$ doped with 2 atom percent of Ca and V.

FIGURE 2.12 Raman spectrum of $Y_2Ti_2O_7$ doped with 4 atom percent of Ca and V.

1.1.1.2 INFRARED SPECTRA

FIGURE 2.13 a Mid-Infrared spectrum of undoped $Y_2Sn_2O_7$.
b Far-Infrared spectrum of undoped $Y_2Sn_2O_7$.

FIGURE 2.14 a Mid-Infrared spectrum of $Y_2Sn_2O_7$ doped with 4 atom percent of Ca and V.

b Far-Infrared spectrum of $Y_2Sn_2O_7$ doped with 4 atom percent of Ca and V.

FIGURE 2.15 a Mid-Infrared spectrum of undoped $Y_2Ti_2O_7$.

b Far-Infrared spectrum of undoped $Y_2Ti_2O_7$.

FIGURE 2.16 a Mid-Infrared spectrum of $Y_2Ti_2O_7$ doped with 4 atom percent of Ca and V.

b Far-Infrared spectrum of $Y_2Ti_2O_7$ doped with 4 atom percent of Ca and V.

1.1.2 ELECTRONIC SPECTRA

FIGURE 2.17 Diffuse electronic spectrum of $Y_2Sn_2O_7$ doped with 4 atom percent of Ca and V.

FIGURE 2.18 Diffuse electronic spectrum of $Y_2Ti_2O_7$ doped with 4 atom percent of Ca and V.

1.2 Vibrational and Electronic Spectra of Chapter 3

1.2.1 VIBRATIONAL SPECTRA

1.2.1.1 RAMAN SPECTRA

FIGURE 3.1 Raman spectrum of undoped malayaite ($CaSnSiO_5$) prepared at a temperature of 1550°C.

FIGURE 3.2 Raman spectrum of undoped malayaite ($CaSnSiO_5$) prepared at a temperature of 1500°C.

FIGURE 3.3 Raman spectrum of undoped malayaite ($CaSnSiO_5$), contaminated with chromium, and prepared at a temperature of 1450°C.

FIGURE 3.4 Raman spectrum of malayaite ($CaSnSiO_5$), doped with 1 atom% of chromium, and prepared at a temperature of 1450°C.

FIGURE 3.5 Raman spectrum of malayaite ($CaSnSiO_5$), doped with 1 atom% of chromium, and prepared at a temperature of 1300°C with mineraliser.

FIGURE 3.6 Raman spectrum of malayaite ($CaSnSiO_5$), doped with 1 atom% of chromium, and prepared at a temperature of 1300°C without mineraliser.

FIGURE 3.7 Raman spectrum of malayaite ($CaSnSiO_5$), doped with 1 atom% of chromium, and prepared at a temperature of 1200°C with mineraliser.

FIGURE 3.8 Raman spectrum of malayaite ($CaSnSiO_5$), doped with 1 atom% of chromium, and prepared at a temperature of 1200°C without mineraliser.

FIGURE 3.9 Raman spectrum of malayaite ($CaSnSiO_5$), doped with 2 atom% of chromium, and prepared at a temperature of 1150°C with mineraliser.

FIGURE 3.10 Raman spectrum of malayaite ($CaSnSiO_5$), doped with 2 atom% of chromium, and prepared at a temperature of 1150°C without mineraliser.

FIGURE 3.11 Raman spectrum of malayaite ($CaSnSiO_5$), doped with 2 atom% of cobalt, and prepared at a temperature of 1450°C without mineraliser.

FIGURE 3.12 Raman spectrum of malayaite ($CaSnSiO_5$), doped with 2 atom% of cobalt, and prepared at a temperature of 1300°C without mineraliser.

FIGURE 3.13 Raman spectrum of malayaite ($CaSnSiO_5$), doped with 2 atom% of cobalt, and prepared at a temperature of 1200°C with mineraliser.

FIGURE 3.14 Raman spectrum of a reaction mixture that did not form malayaite ($CaSnSiO_5$); doped with 2 atom% of cobalt, and prepared at a temperature of 1200°C without mineraliser.

FIGURE 3.15 Raman spectrum of malayaite ($CaSnSiO_5$), doped with 2 atom% of cobalt, and prepared at a temperature of 1150°C with mineraliser.

FIGURE 3.16 Raman spectrum of a reaction product that did not form malayaite ($CaSnSiO_5$); doped with 2 atom% of cobalt, and prepared at a temperature of 1150°C without mineraliser.

FIGURE 3.17 Raman spectrum of undoped titanite ($CaTiSiO_5$) prepared at a temperature of 1150°C with mineraliser.

FIGURE 3.18 Raman spectrum of product of reaction to synthesis undoped ($CaTiSiO_5$) at a temperature of 1150°C without mineraliser. Reaction did not go to completion.

FIGURE 3.19 Raman spectrum of synthetic α-alumina.

FIGURE 3.20 Raman spectrum of synthetic α-alumina doped with chromium.

FIGURE 3.21 Raman spectrum of natural α-alumina (ruby) doped with chromium.

1.2.1.2 INFRARED SPECTRA

FIGURE 3.22 Infrared spectrum of undoped malayaite ($CaSnSiO_5$) prepared at a temperature of 1500°C without mineraliser.

FIGURE 3.23 Infrared spectrum of malayaite ($CaSnSiO_5$) doped with 4 atom% of chromium, prepared at a temperature of 1300°C with mineraliser.

FIGURE 3.24 a Mid-infrared spectrum of malayaite ($CaSnSiO_5$) doped with 2 atom% of cobalt, prepared at a temperature of 1200°C without mineraliser.

b Far-infrared spectrum of malayaite ($CaSnSiO_5$) doped with 2 atom% of cobalt, prepared at a temperature of 1200°C without mineraliser.

FIGURE 3.25 Infrared spectrum of undoped titanite ($CaTiSiO_5$) prepared at a temperature of 1150°C with mineraliser.

1.2.2 ELECTRONIC SPECTRA

FIGURE 3.26 Diffuse reflectance electronic spectrum of malayaite ($CaSnSiO_5$), doped with 1 atom% of chromium, and prepared at a temperature of 1300°C with mineraliser.

FIGURE 3.27 Diffuse reflectance electronic spectrum of malayaite ($CaSnSiO_5$), doped with 2 atom% of cobalt, and prepared at a temperature of 1300°C without mineraliser.

FIGURE 3.28 Diffuse reflectance electronic spectrum of wollastonite ($CaSiO_3$), doped with 2 atom% of chromium, and prepared at a temperature of 1150°C with mineraliser.

1.1.1 Vibrational Spectra (CHAPTER 2)

1.1.1.1 RAMAN SPECTRA

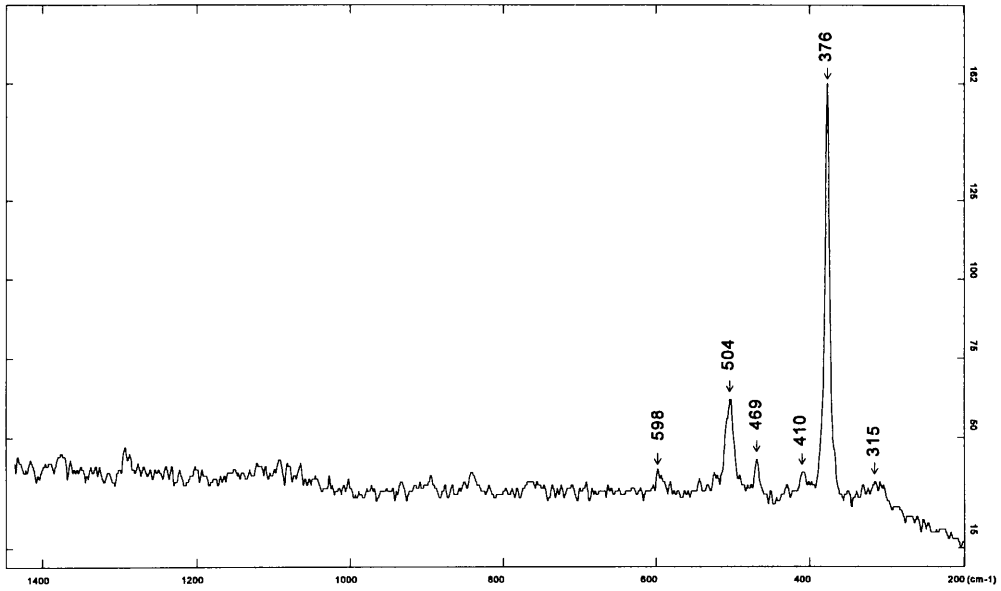

FIGURE 2.1 Raman spectrum of undoped $Y_2Sn_2O_7$ synthesised with a ratio of Y:Sn of 4:1. (Reaction number 2, second reaction mixtures, table 2.2 A.)

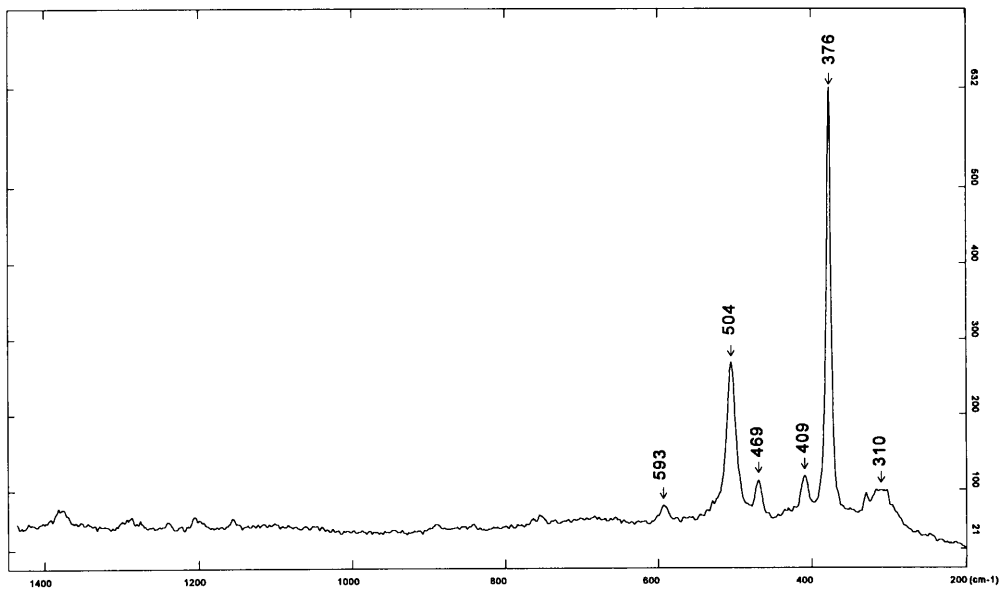

FIGURE 2.2 Raman spectrum of undoped $Y_2Sn_2O_7$ synthesised with a ratio of Y:Sn of 3:1. (Reaction number 3, second reaction mixtures, table 2.2A.)

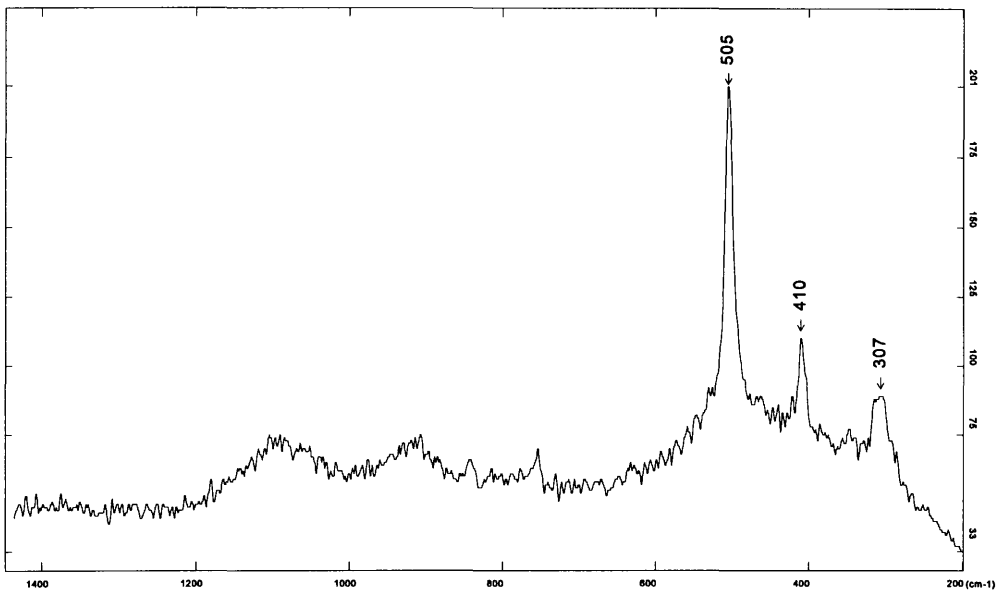

FIGURE 2.3 Raman spectrum of undoped $Y_2Sn_2O_7$ synthesised with a ratio of Y:Sn of 1:1. (Reaction number 1, first reaction mixtures, table 2.1 A.)

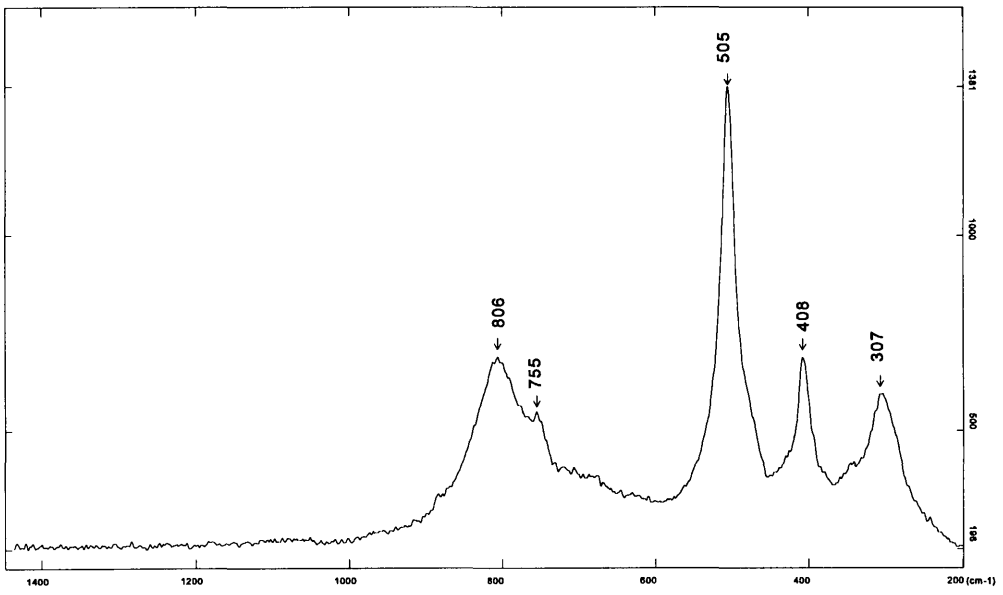

FIGURE 2.4 Raman spectrum of $Y_2Sn_2O_7$ doped with 1 atom percent of Ca and V. (Reaction number 2, first reaction mixtures, table 2.1 A.)

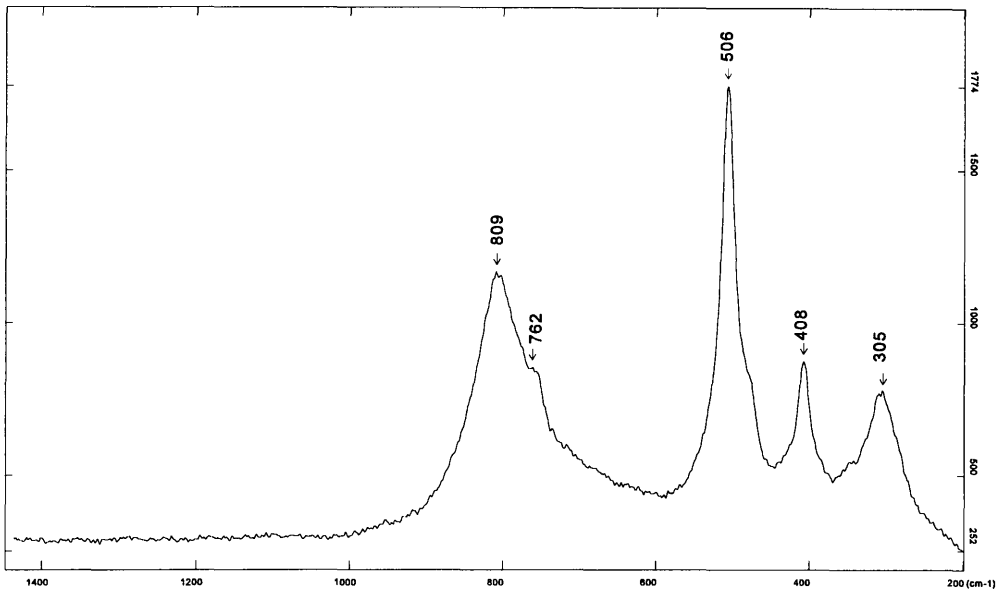

FIGURE 2.5 Raman spectrum of $Y_2Sn_2O_7$ doped with 2 atom percent of Ca and V. (Reaction number 3, first reaction mixtures, table 2.1 A.)

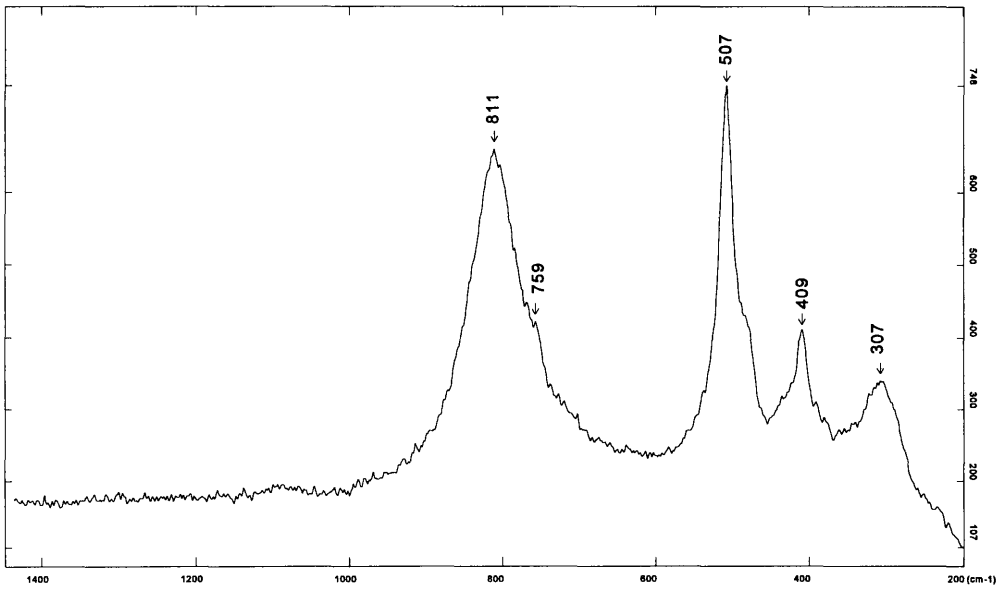

FIGURE 2.6 Raman spectrum of $Y_2Sn_2O_7$ doped with 4 atom percent of Ca and V. (Reaction number 4, first reaction mixtures, table 2.1 A.)

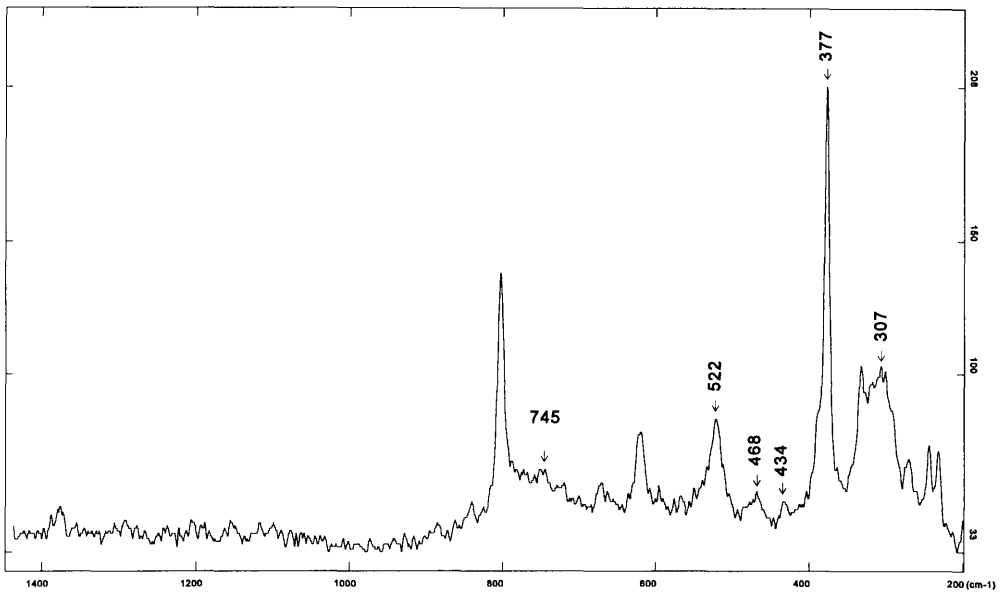

FIGURE 2.7 Raman spectrum of undoped $Y_2Ti_2O_7$ synthesised with a ratio of Y:Ti of 4:1. (Reraction number 3, second reaction mixtures, table 2.2B.)

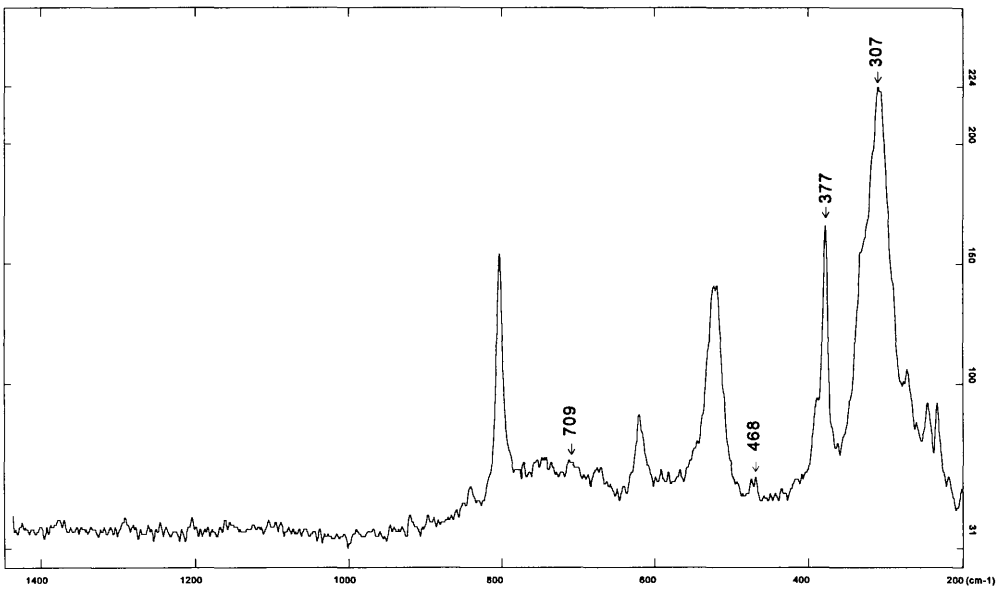

FIGURE 2.8 Raman spectrum of undoped $Y_2Ti_2O_7$ synthesised with a ratio of Y:Ti of 3:1. (Reaction number 2, second reaction mixtures, table 2.2 B.)

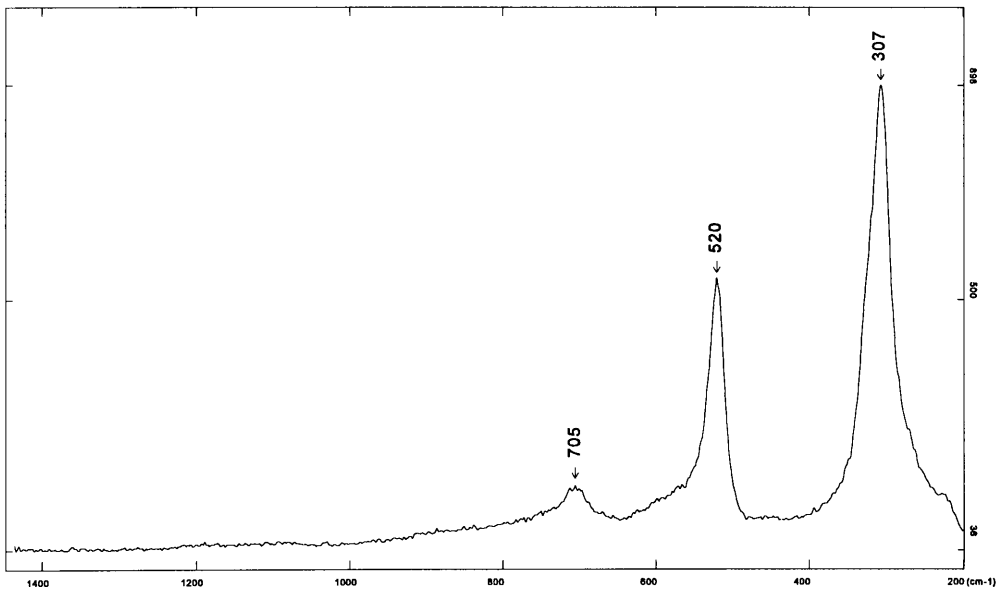

FIGURE 2.9 Raman spectrum of undoped $Y_2Ti_2O_7$ synthesised with a ratio of Y:Ti of 1:1. (Reaction number 1, first reaction mixtures, table 2.1 B.)

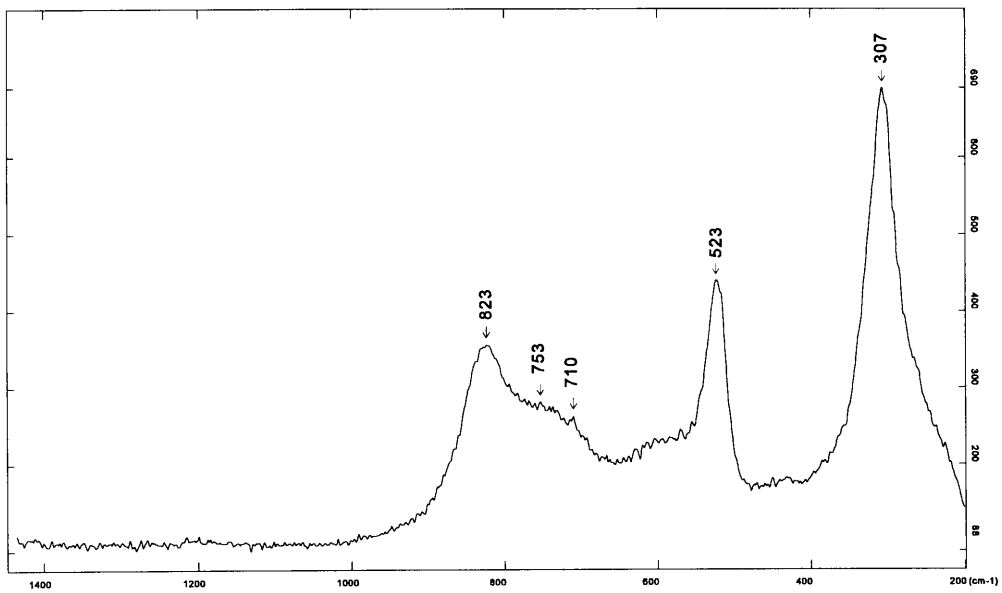

FIGURE 2.10 Raman spectrum of $Y_2Ti_2O_7$ doped with 1 atom percent of Ca and V. (Reaction number 2, first reaction mixtures, table 2.1 B.)

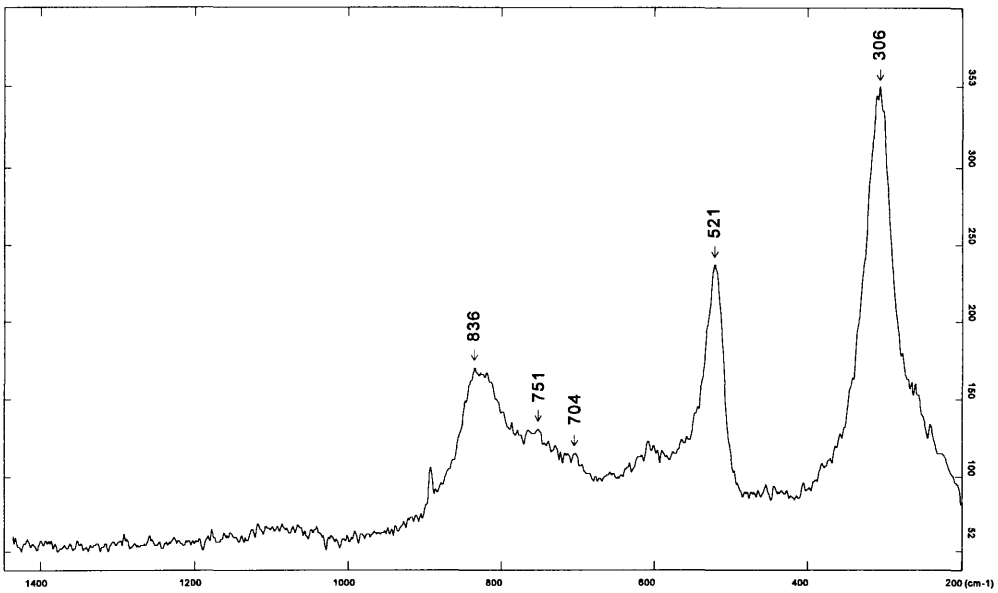

FIGURE 2.11 Raman spectrum of $Y_2Ti_2O_7$ doped with 2 atom percent of Ca and V. (Reaction number 3, first reaction mixtures, table 2.1 B.)

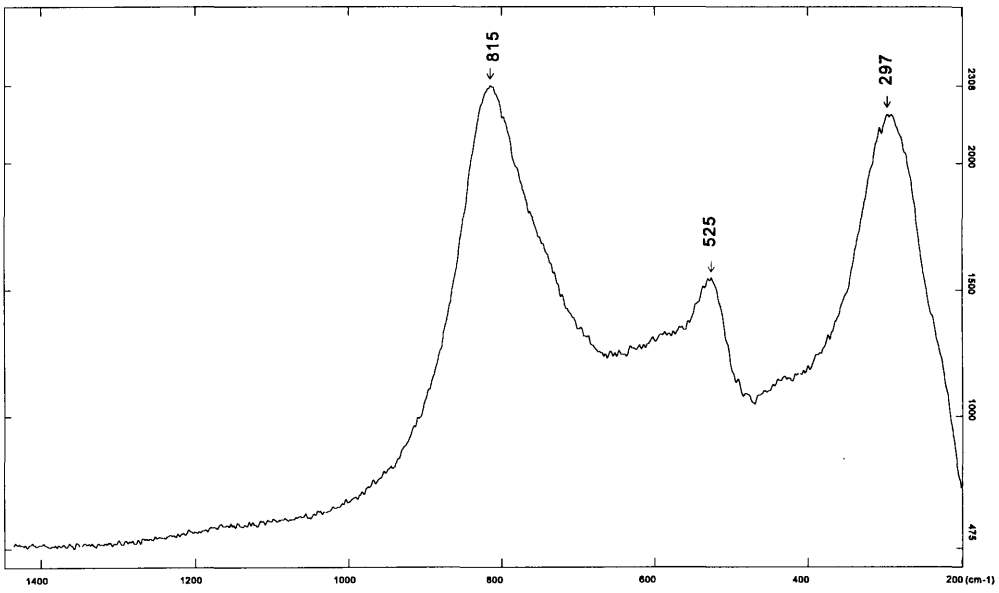

FIGURE 2.12 Raman spectrum of $Y_2Ti_2O_7$ doped with 4 atom percent of Ca and V. (Reaction number 4, first reaction mixtures, table 2.1 B.)

1.1.1.2 INFRARED SPECTRA (CHAPTER 2)

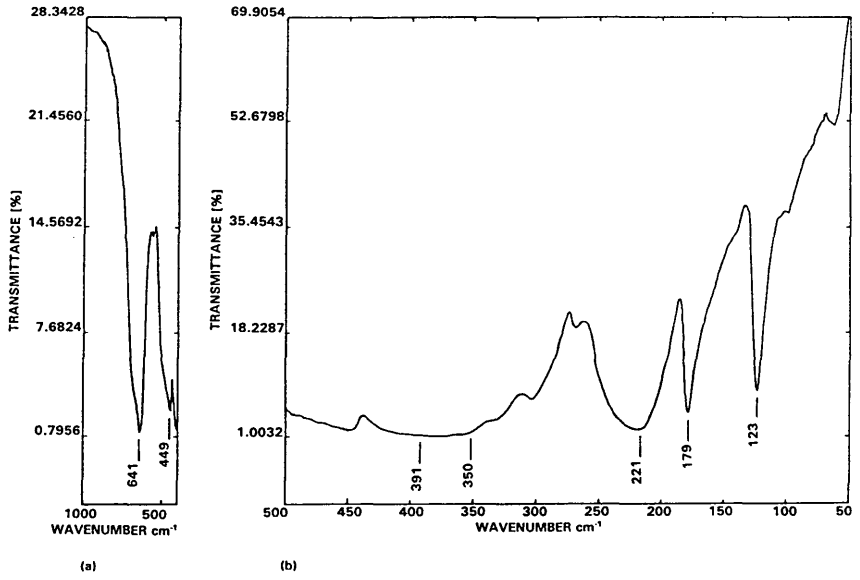

Figure 2.13 a&b Mid-Infrared (a) and Far-Infrared (b) spectrum of undoped $Y_2Sn_2O_7$. (Reaction number 1, first reaction mixtures, table 2.1 A.)

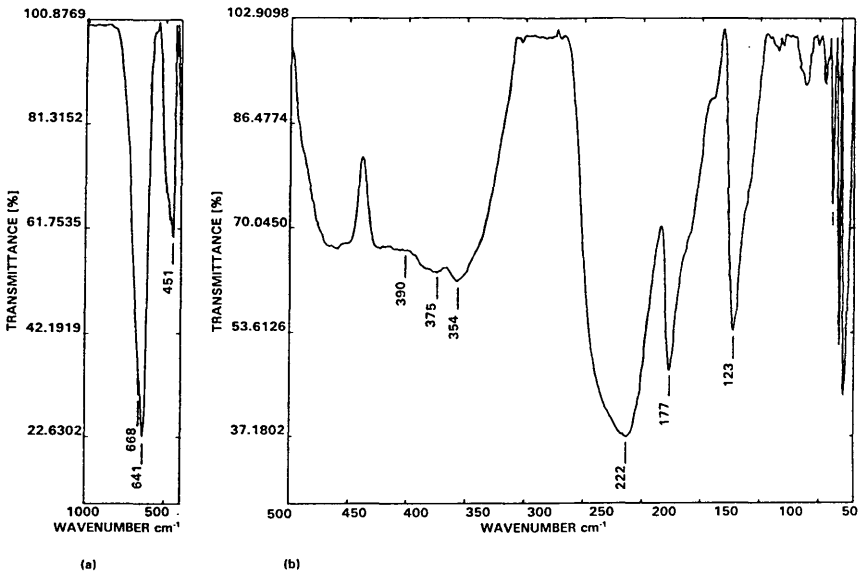

Figure 2.14 a&b Mid-Infrared (a) and Far-Infrared (b) spectrum of $Y_2Sn_2O_7$ doped with 4 atom percent of Ca and V.
(Reaction number 4, third reaction mixtures, table 2.3 A.)

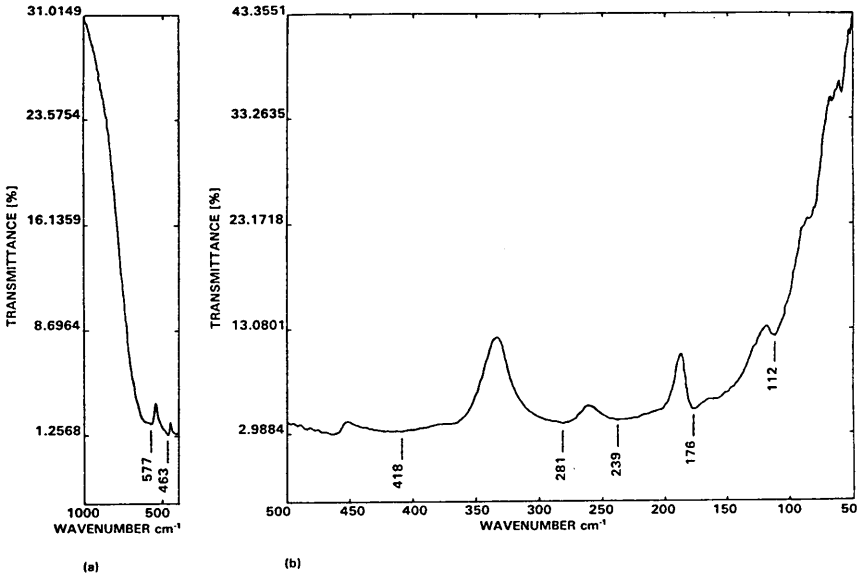

Figure 2.15 a&b Mid-Infrared (a) and Far-Infrared (b) spectrum of undoped $Y_2Ti_2O_7$. (Reaction number 1, first reaction mixtures, table 2.1 B.)

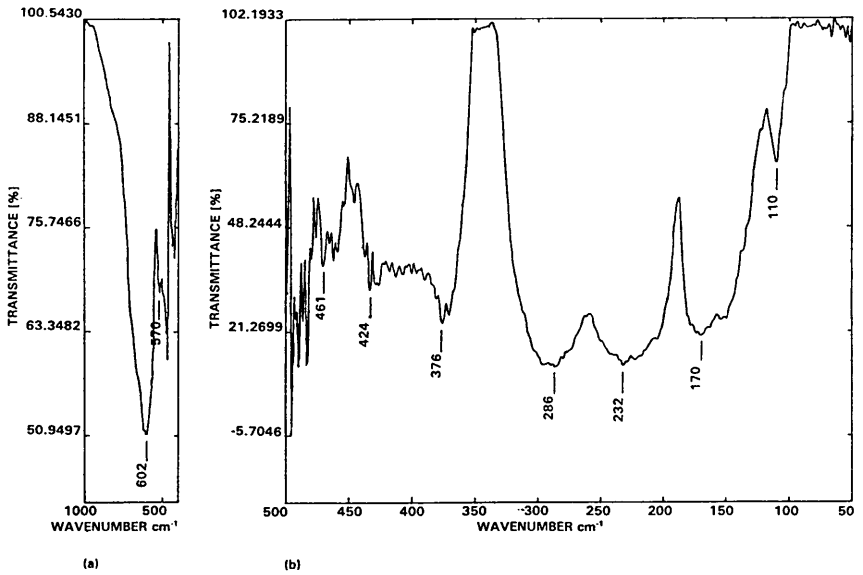

Figure 2.16 a&b Mid-Infrared (a) and Far-Infrared (b) spectrum of $Y_2Ti_2O_7$ doped with 4 atom percent of Ca and V.
(Reaction number 4, third reaction mixtures, table 2.3 B.)

1.1.2 ELECTRONIC SPECTRA (CHAPTER 2)

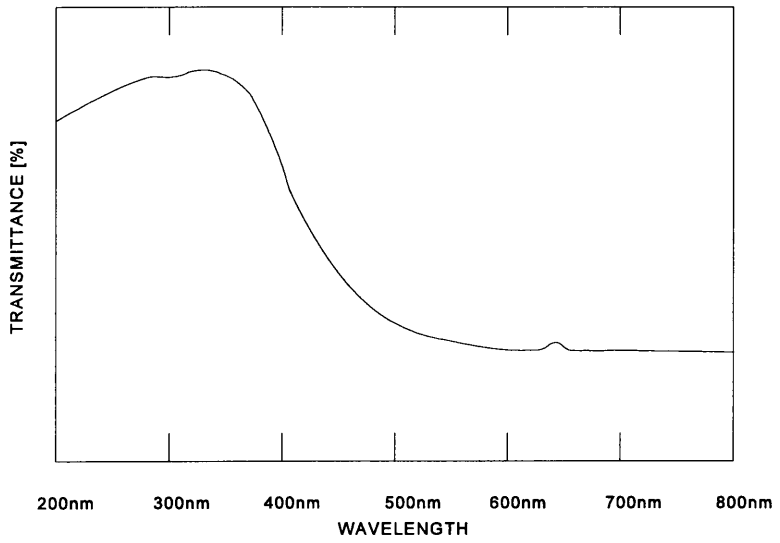

Figure 2.17 Diffuse reflectance electronic spectrum of calcium and vanadium doped $Y_2Sn_2O_7$. (Reaction number 1, third reaction mixtures, table 2.3 A.)

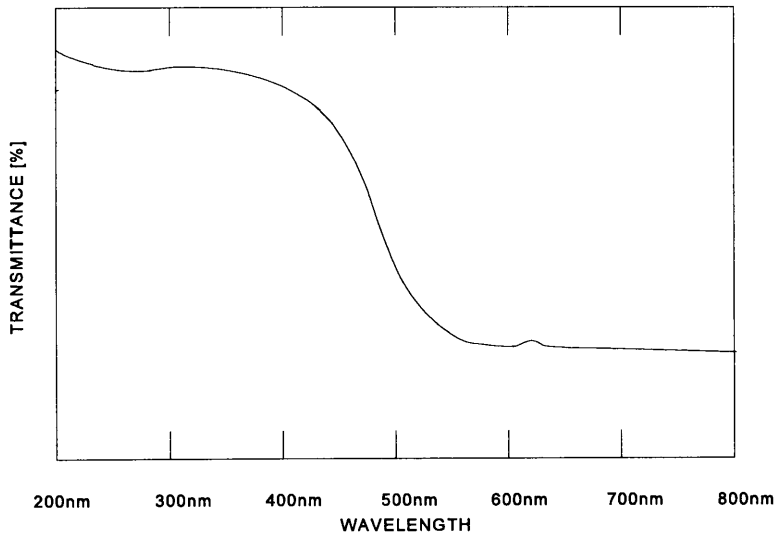

Figure 2.18 Diffuse reflectance spectrum of calcium and vanadium doped $Y_2Ti_2O_7$. (Reaction number 1, third reaction mixtures, table 2.3 B.)

1.2 Vibrational and Electronic Spectra of Chapter 3

1.2.1 VIBRATIONAL SPECTRA

1.2.1.1 RAMAN SPECTRA

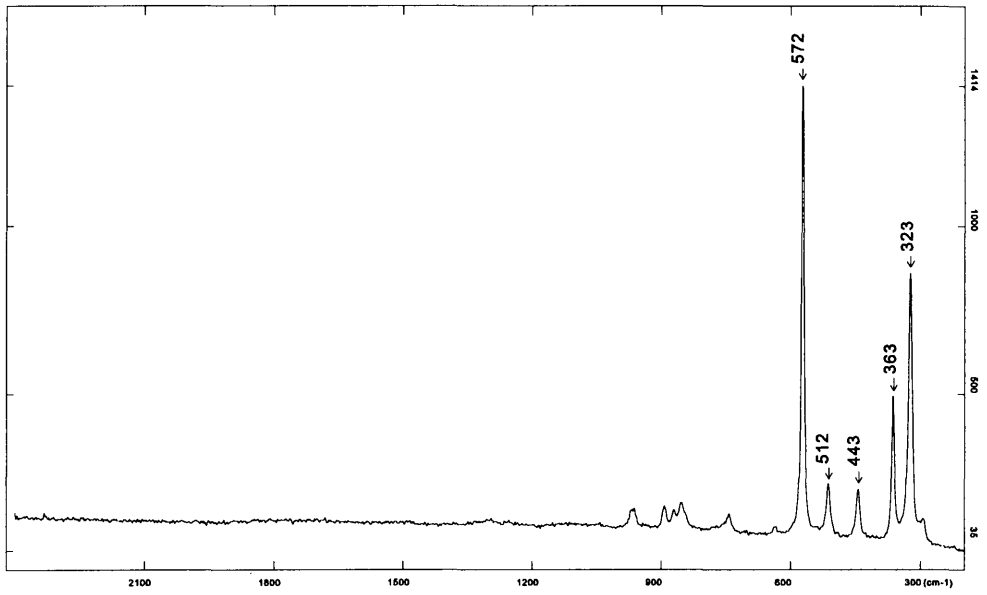

FIGURE 3.1 Raman spectrum of undoped malayaite ($CaSnSiO_5$) prepared at a temperature of 1550°C.
(3.2.1 - Chapter 3)

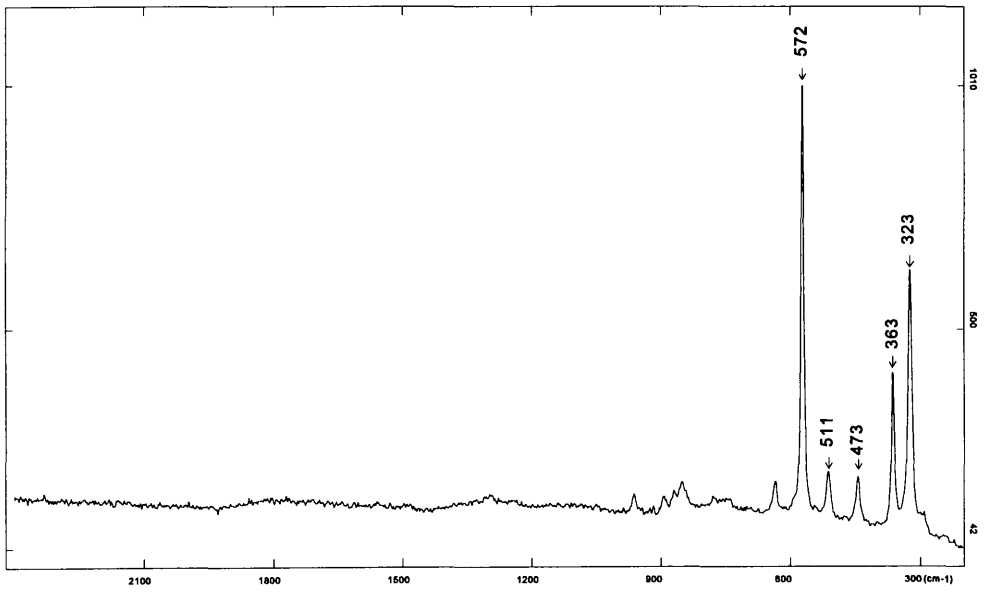

FIGURE 3.2 Raman spectrum of undoped malayaite ($CaSnSiO_5$) prepared at a temperature of 1500°C.
(3.2.1 - Chapter 3)

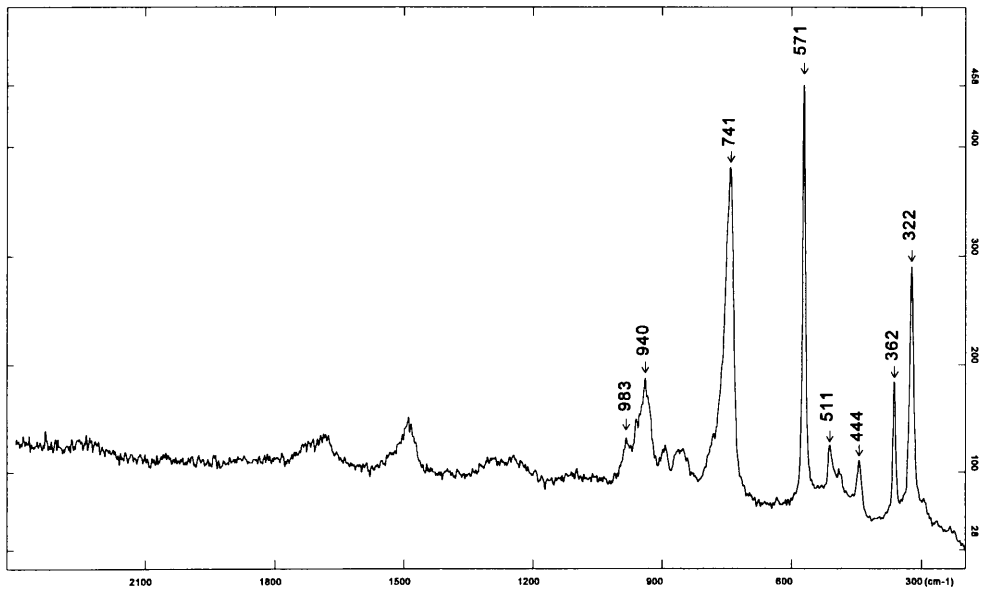

FIGURE 3.3 Raman spectrum of undoped malayaite ($CaSnSiO_5$), contaminated with chromium, and prepared at a temperature of 1450°C.
(Reaction number 1, table 3.1)

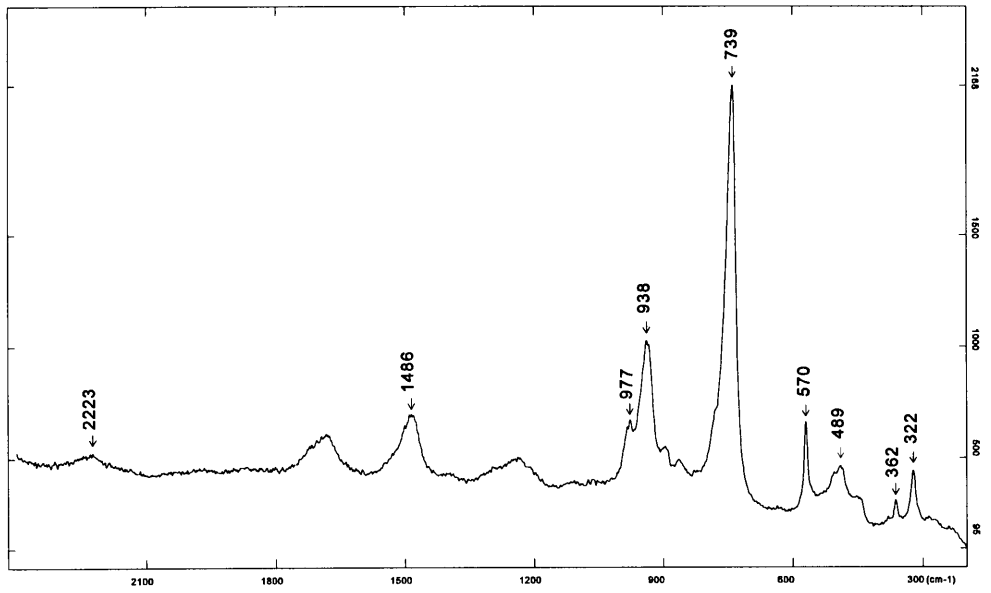

FIGURE 3.4 Raman spectrum of malayaite ($CaSnSiO_5$), doped with 1 atom% of chromium, and prepared at a temperature of 1450°C.
(Reaction number 2, table 3.1)

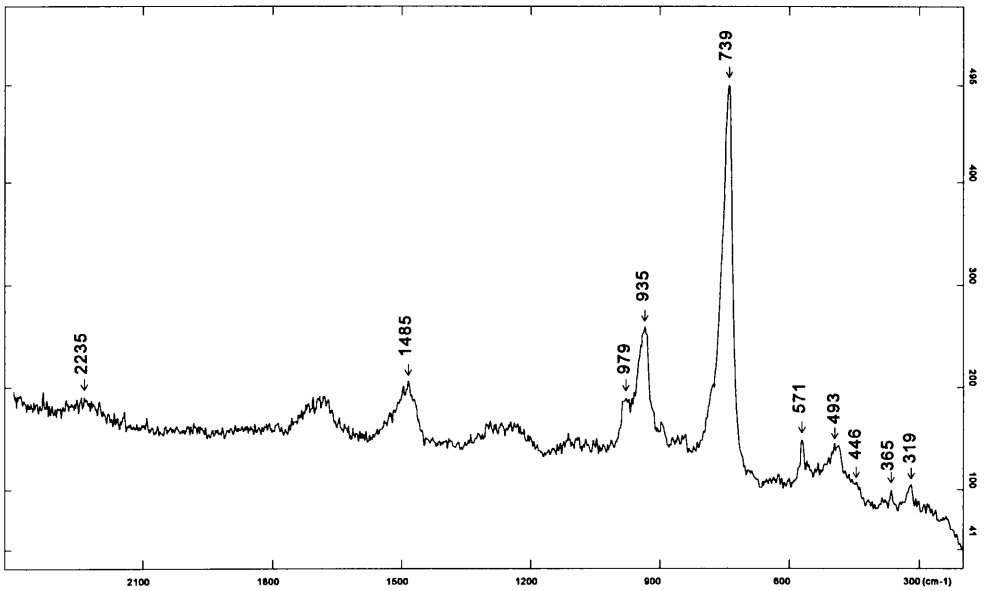

FIGURE 3.5 Raman spectrum of malayaite ($CaSnSiO_5$), doped with 1 atom% of chromium, and prepared at a temperature of 1300°C with mineraliser.
(Reaction number 2, table 3.2)

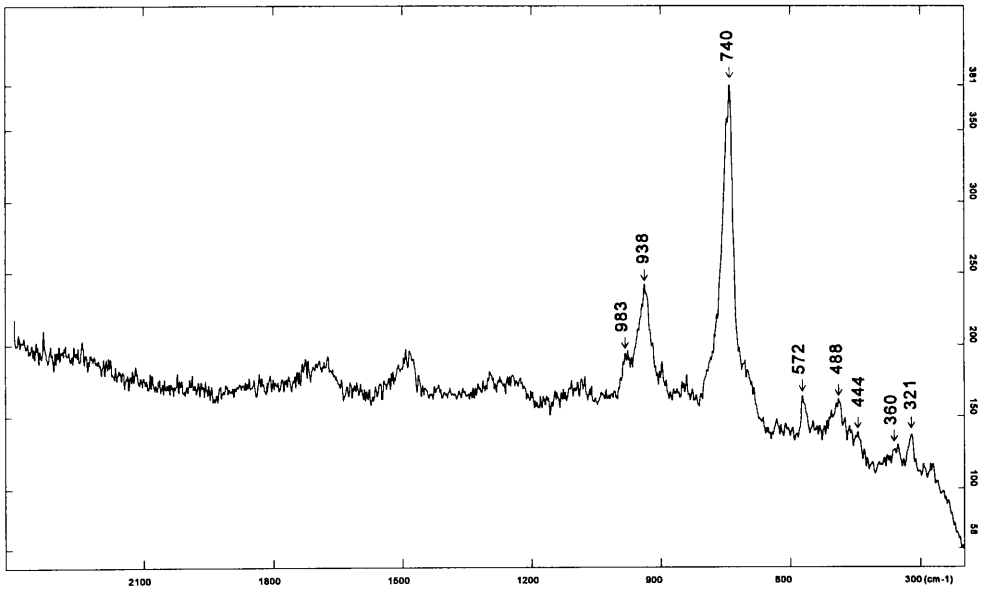

FIGURE 3.6 Raman spectrum of malayaite ($CaSnSiO_5$), doped with 1 atom% of chromium, and prepared at a temperature of 1300°C without mineraliser.
(Reaction number 1, table 3.2)

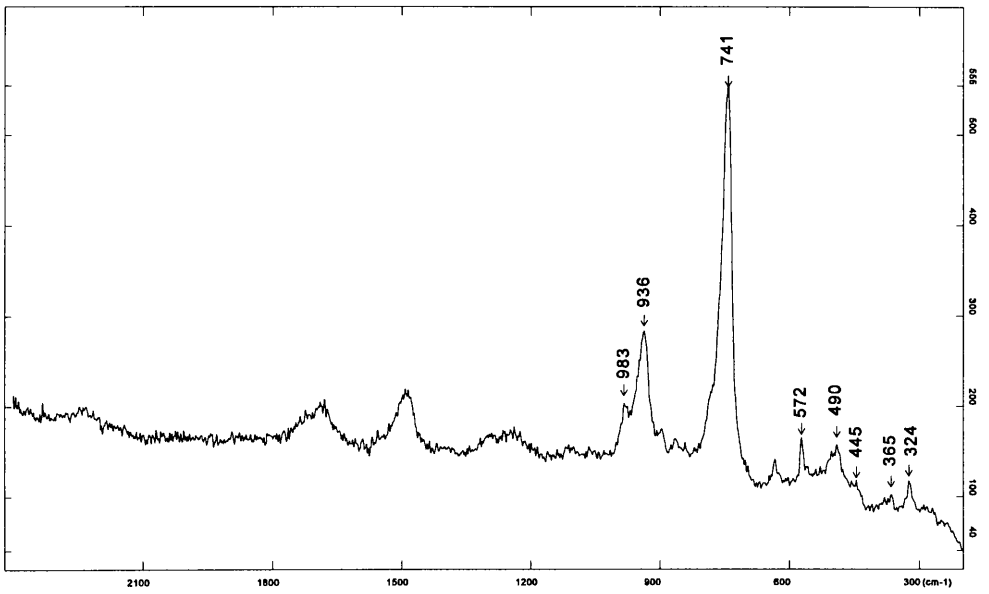

FIGURE 3.7 Raman spectrum of malayaite ($CaSnSiO_5$), doped with 1 atom% of chromium, and prepared at a temperature of 1200°C with mineraliser.
(Reaction number 9, table 3.3)

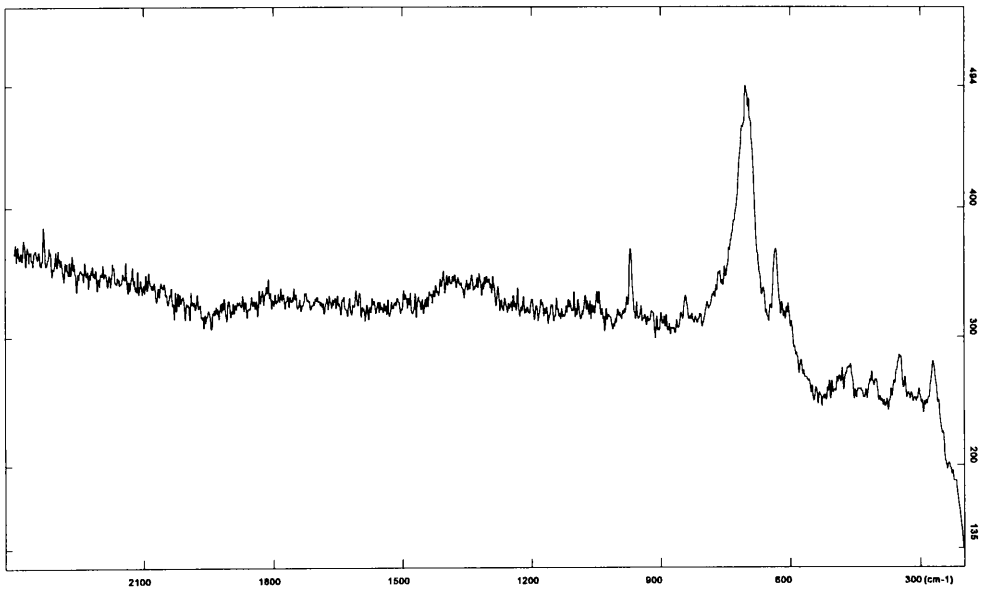

FIGURE 3.8 Raman spectrum of malayaite ($CaSnSiO_5$), doped with 1 atom% of chromium, and prepared at a temperature of 1200°C without mineraliser.
(Reaction number 8, table 3.3)

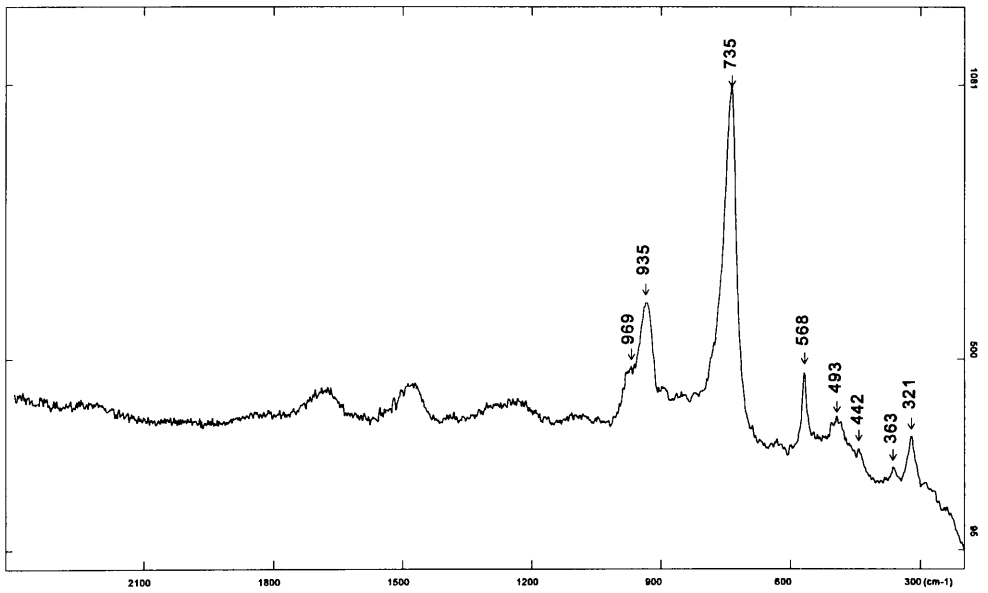

FIGURE 3.9 Raman spectrum of malayaite ($CaSnSiO_5$), doped with 2 atom% of chromium, and prepared at a temperature of 1150°C with mineraliser.
(Reaction number 4, table 3.4)

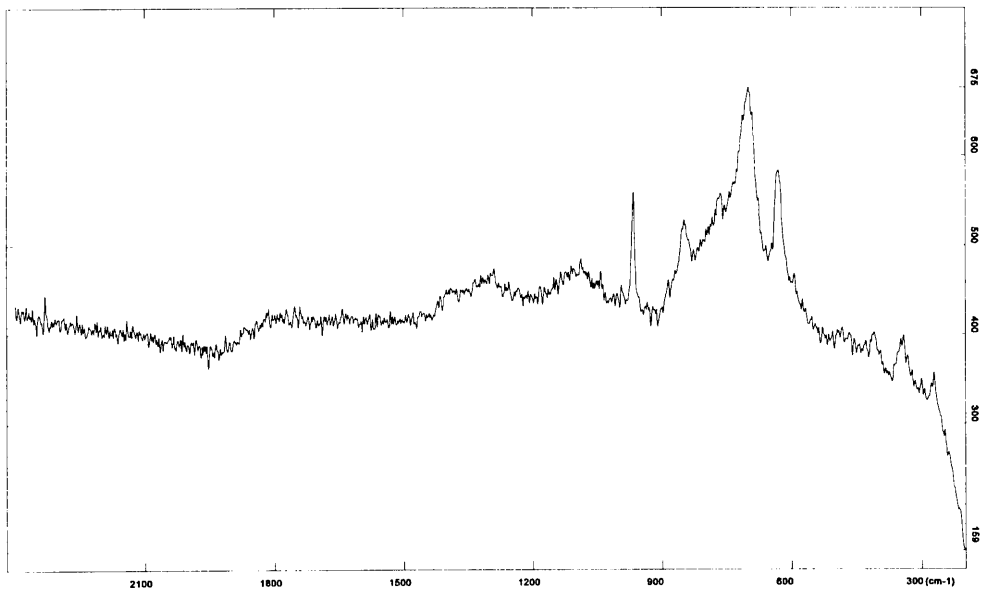

FIGURE 3.10 Raman spectrum of malayaite ($CaSnSiO_5$), doped with 2 atom% of chromium, and prepared at a temperature of 1150°C without mineraliser.
(Reaction number 3, table 3.4)

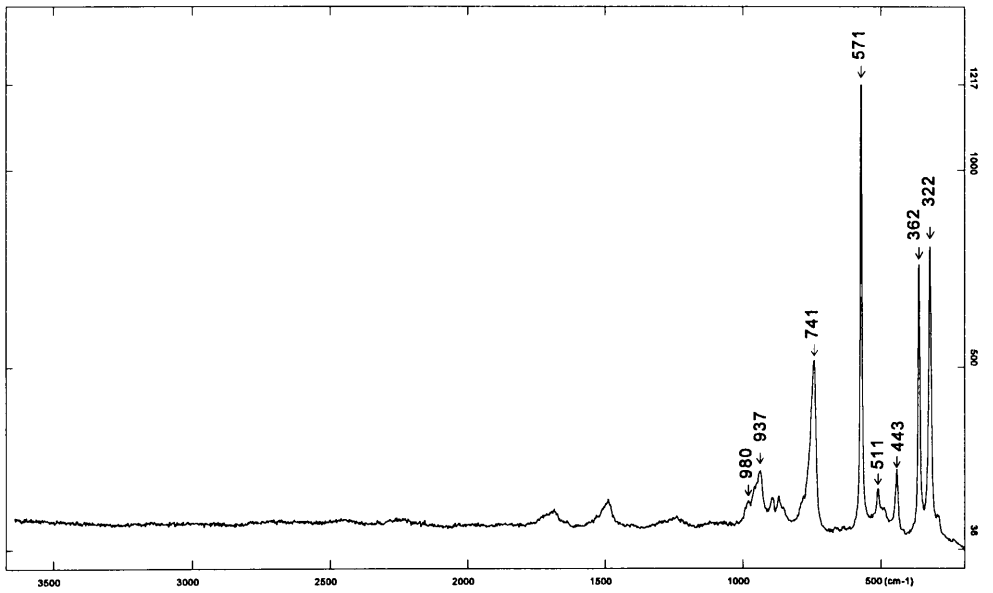

FIGURE 3.11 Raman spectrum of malayaite ($CaSnSiO_5$), doped with 2 atom% of cobalt, and prepared at a temperature of 1450°C without mineraliser.
(Reaction number 6, table 3.1)

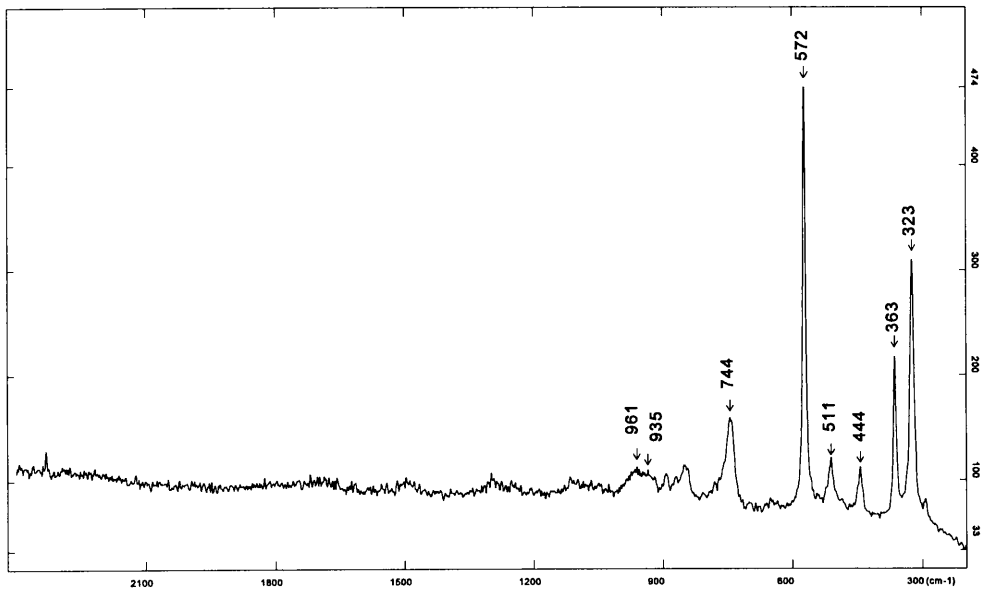

FIGURE 3.12 Raman spectrum of malayaite ($CaSnSiO_5$), doped with 2 atom% of cobalt, and prepared at a temperature of 1300°C without mineraliser.
(Reaction number 10, table 3.2)

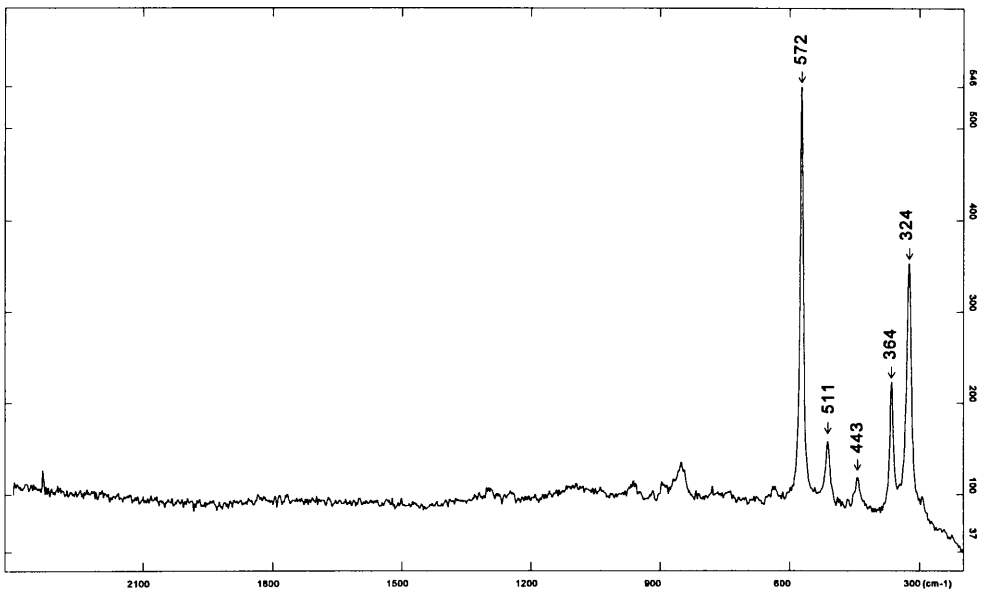

FIGURE 3.13 Raman spectrum of malayaite ($CaSnSiO_5$), doped with 2 atom% of cobalt, and prepared at a temperature of 1200°C with mineraliser.
(Reaction number 11, table 3.3)

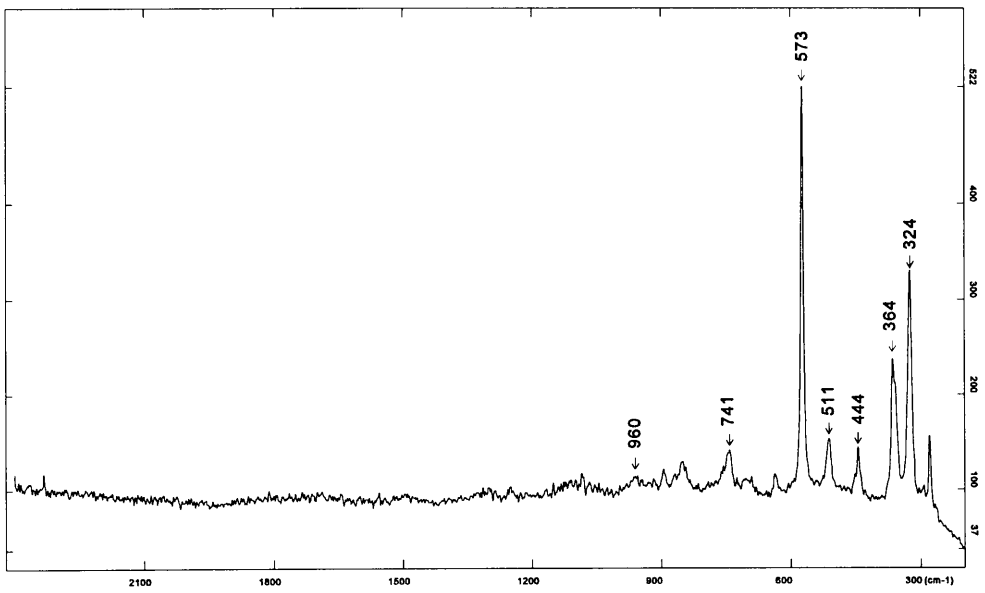

FIGURE 3.14 Raman spectrum of a reaction mixture that did not form malayaite ($CaSnSiO_5$); doped with 2 atom% of cobalt, and prepared at a temperature of 1200°C without mineraliser.
(Reaction number 12, table 3.3)

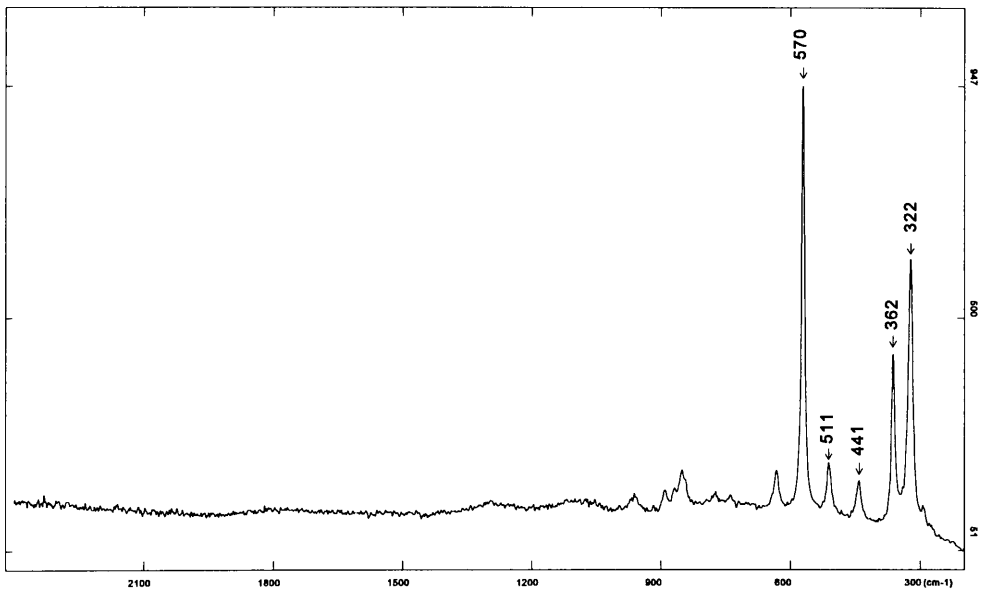

FIGURE 3.15 Raman spectrum of malayaite ($CaSnSiO_5$), doped with 2 atom% of cobalt, and prepared at a temperature of 1150°C with mineraliser.
(Reaction number 8, table 3.4)

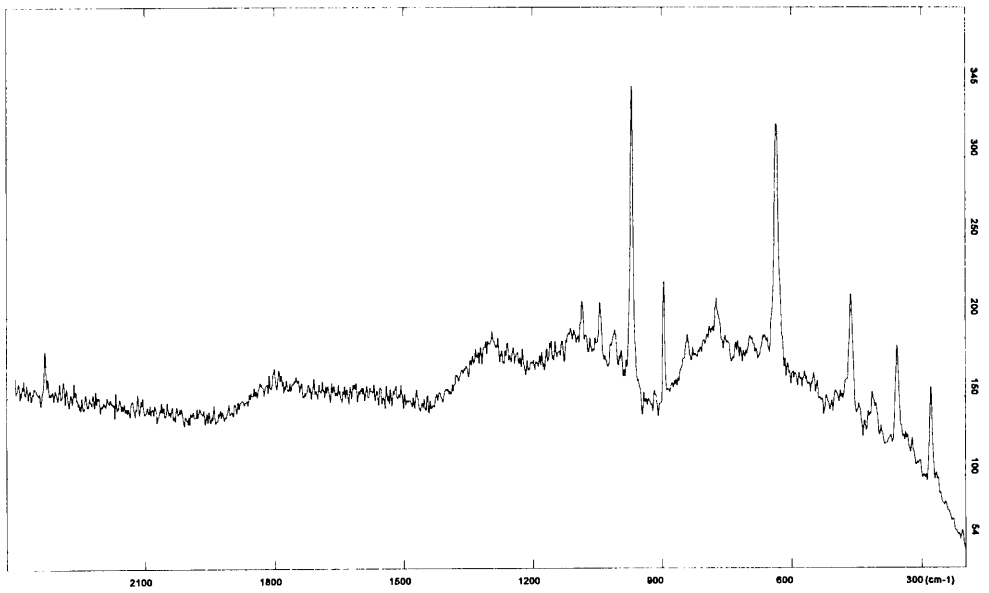

FIGURE 3.16 Raman spectrum of a reaction product that did not form malayaite ($CaSnSiO_5$); doped with 2 atom% of cobalt, and prepared at a temperature of 1150°C without mineraliser.
(Reaction number 7, table 3.4)

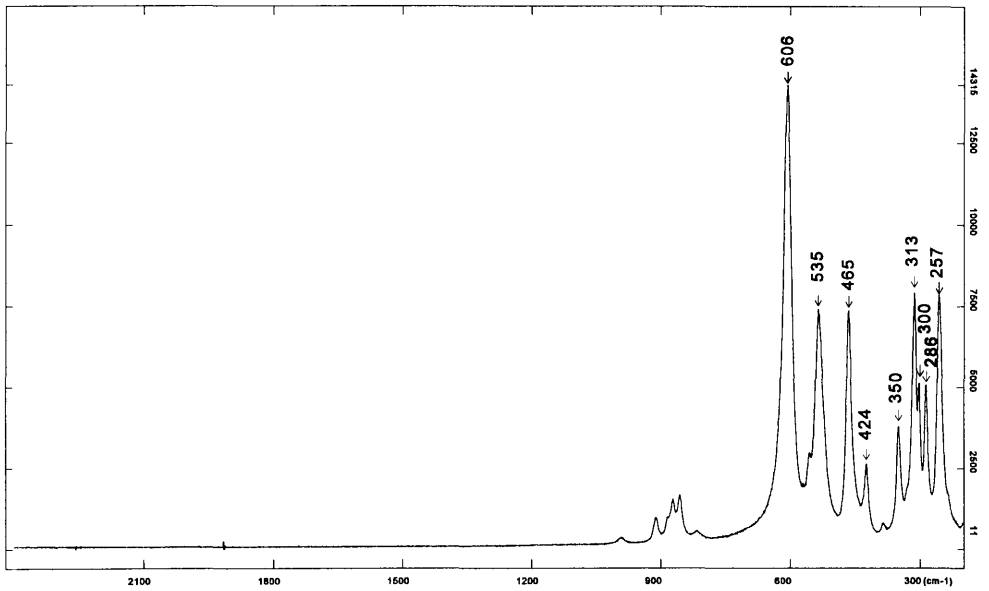

FIGURE 3.17 Raman spectrum of undoped titanite ($CaTiSiO_5$) prepared at a temperature of 1150°C with mineraliser.
(Reaction number 3, table 3.7)

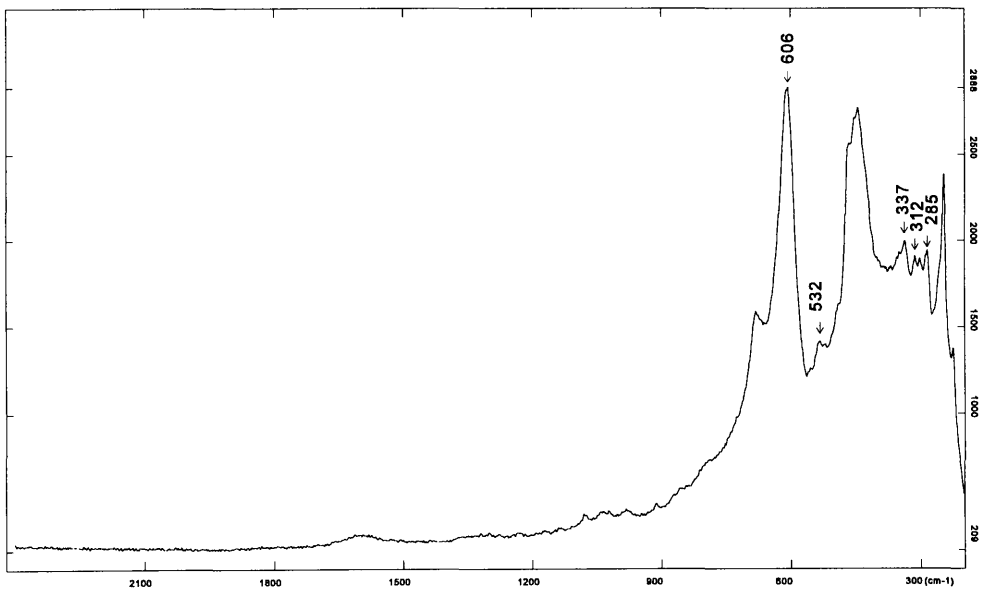

FIGURE 3.18 Raman spectrum of product of reaction to synthesis undoped ($CaTiSiO_5$) at a temperature of 1150°C without mineraliser. Reaction did not go to completion.
(Reaction number 2, table 3.7)

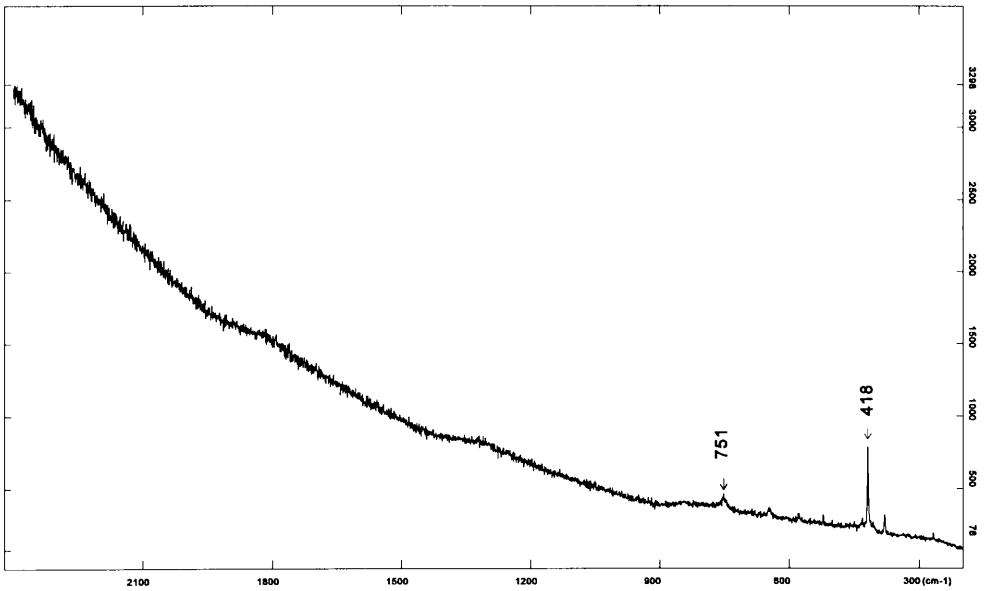

FIGURE 3.19 Raman spectrum of synthetic α-alumina.

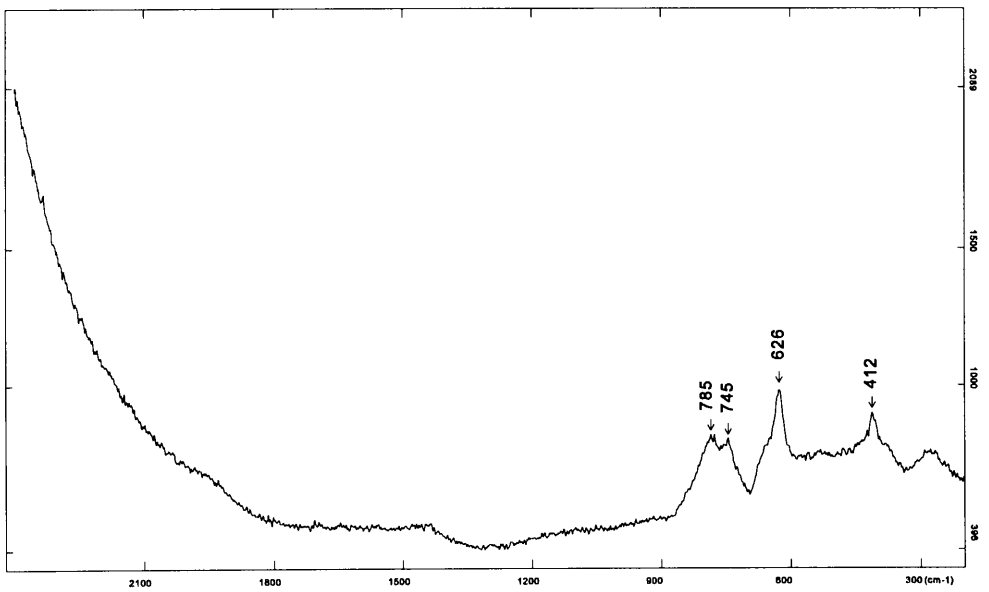

FIGURE 3.20 Raman spectrum of synthetic α-alumina doped with chromium.

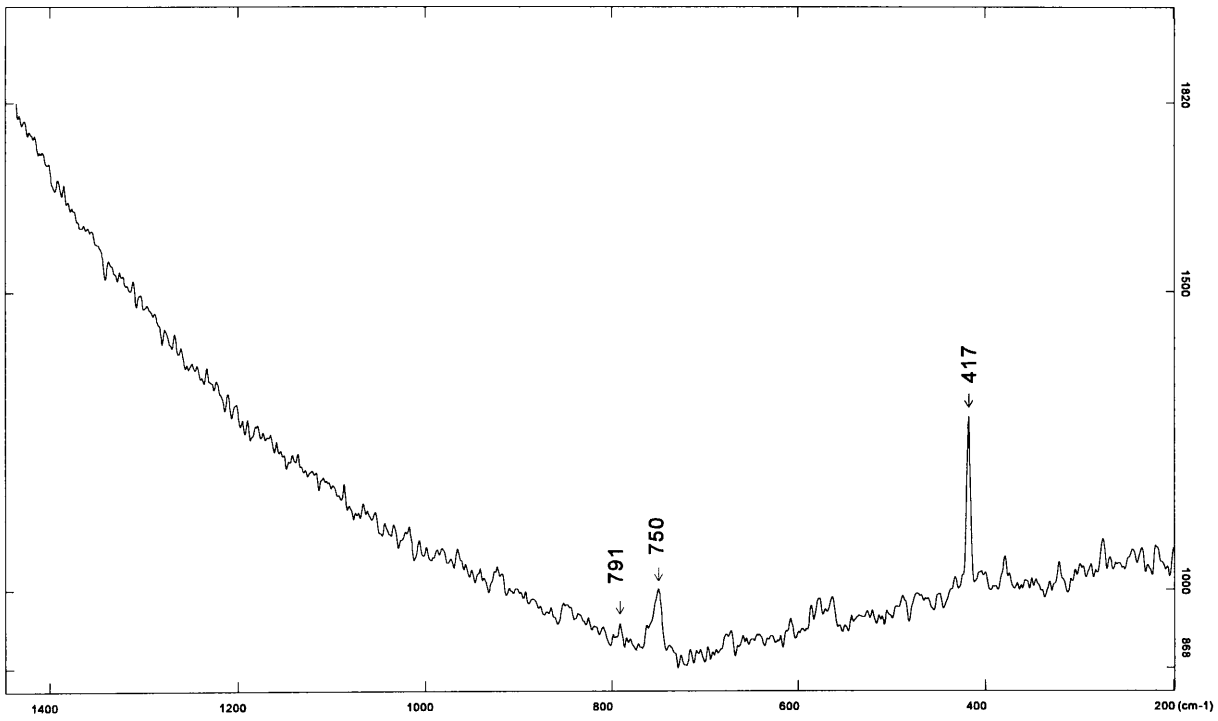

FIGURE 3.21 Raman spectrum of natural α-alumina (ruby) doped with chromium.

1.2.1.2 INFRARED SPECTRA (CHAPTER 3)

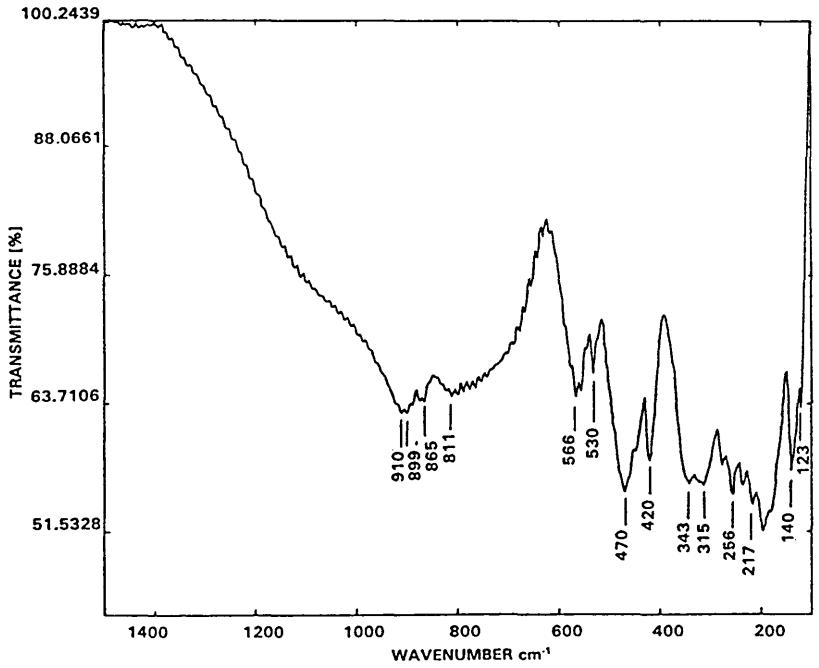

FIGURE 3.22 Infrared spectrum of undoped malayaite ($CaSnSiO_5$) prepared at a temperature of 1500°C without mineraliser.
(Section 3.2.1, CHAPTER 3)

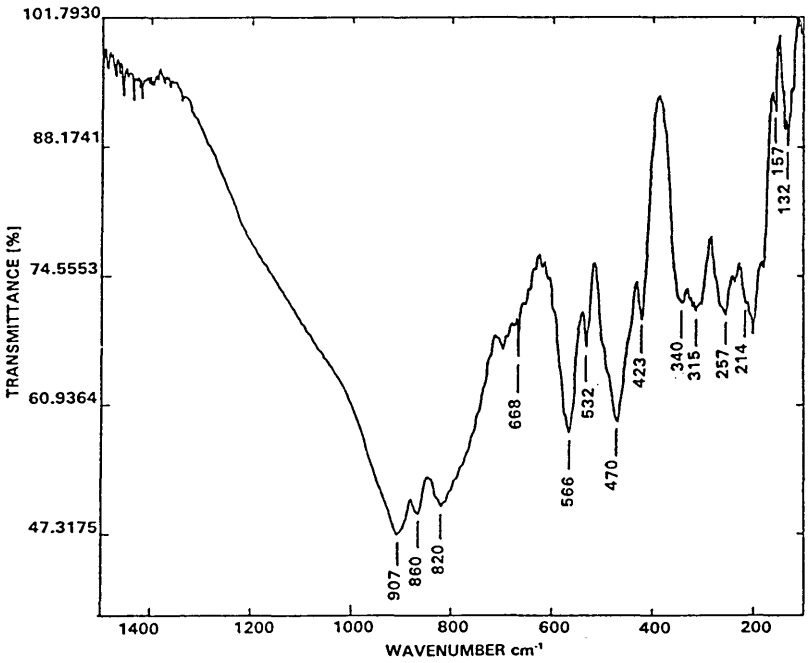

FIGURE 3.23 Infrared spectrum of malayaite ($CaSnSiO_5$) doped with 4 atom% of chromium, prepared at a temperature of 1300°C with mineraliser.
(Reaction number 8, table 3.2)

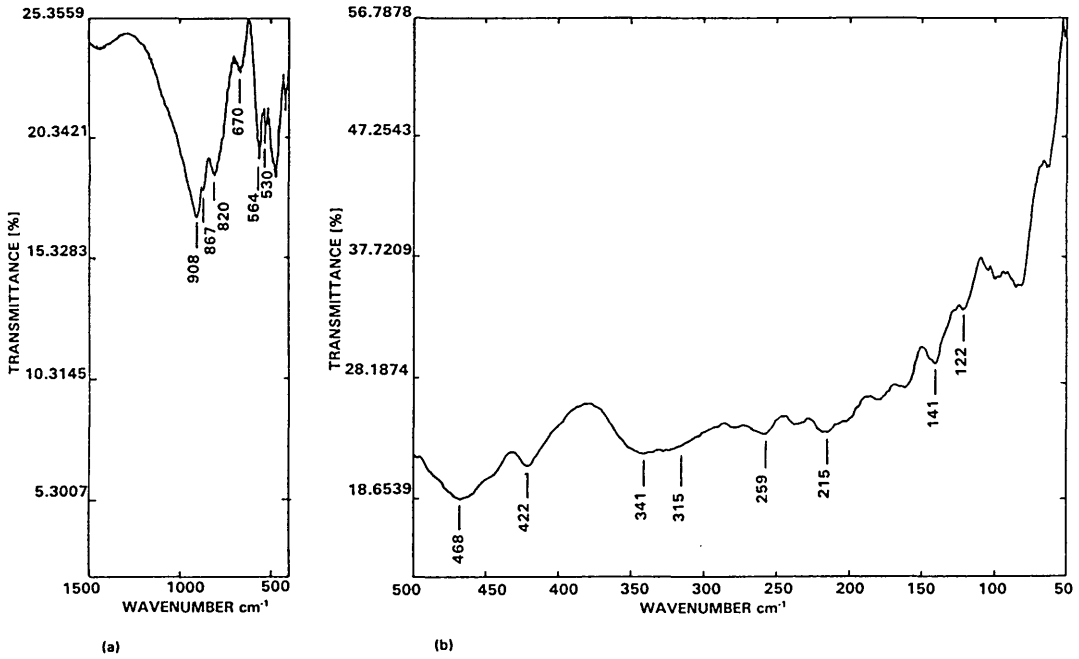

FIGURE 3.24 a&b Mid-infrared spectrum (a), and far-infrared spectrum (b), of malayaite ($CaSnSiO_5$) doped with 2 atom% of cobalt, prepared at a temperature of 1200°C without mineraliser.
(Reaction number 11, table 3.3)

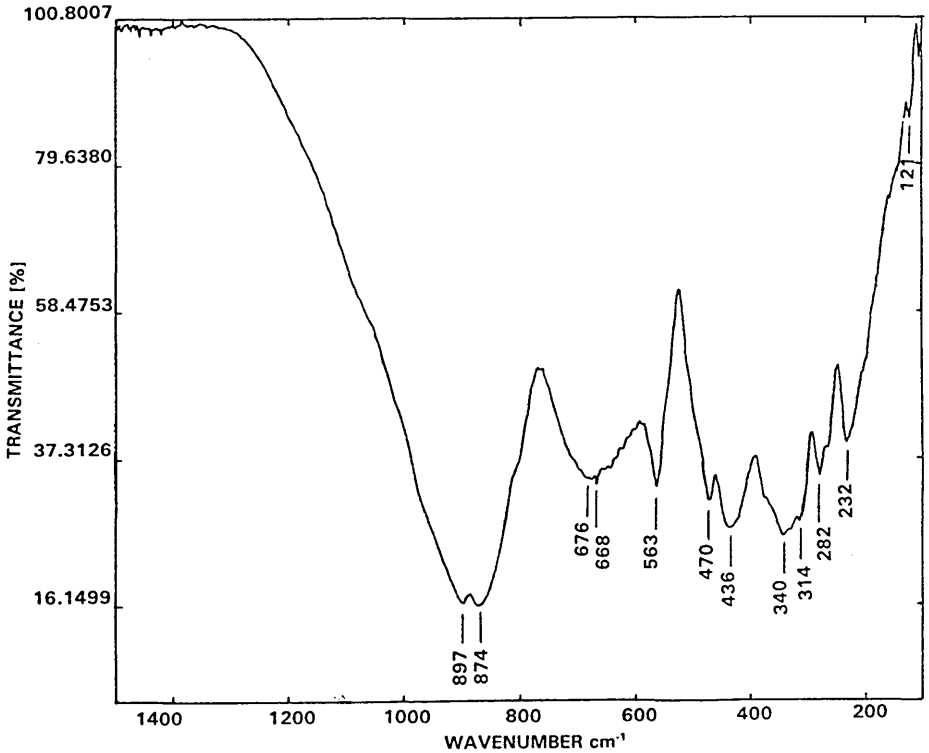

FIGURE 3.25 Infrared spectrum of undoped titanite ($CaTiSiO_5$) prepared at a temperature of 1150°C with mineraliser.
(Reaction number 3, table 3.7)

1.2.2 ELECTRONIC SPECTRA (CHAPTER 3)

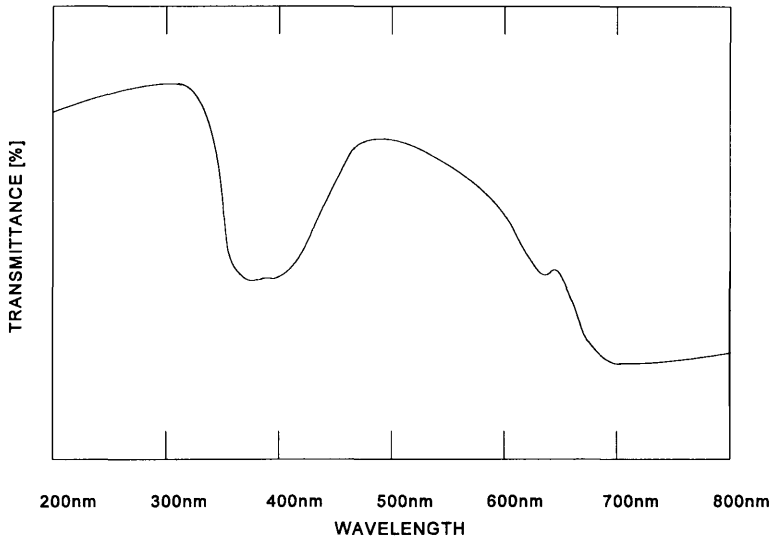

FIGURE 3.26 Diffuse reflectance electronic spectrum of malayaite ($CaSnSiO_5$), doped with 1 atom% of chromium, and prepared at a temperature of 1300°C with mineraliser. (Reaction number 2, table 3.2.)

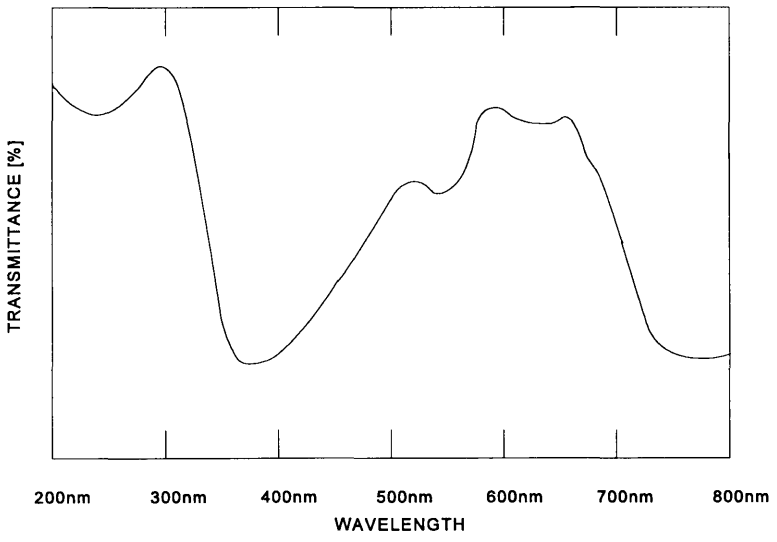

FIGURE 3.27 Diffuse reflectance electronic spectrum of malayaite ($CaSnSiO_5$), doped with 2 atom% of cobalt, and prepared at a temperature of 1300°C without mineraliser. (Reaction number 9, table 3.2.)

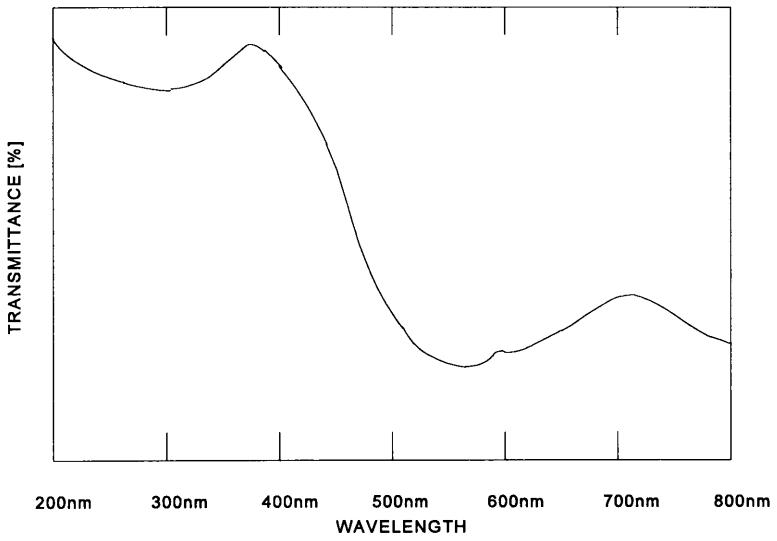

FIGURE 3.28 Diffuse reflectance electronic spectrum of wollastonite ($CaSiO_3$), doped with 2 atom% of chromium, and prepared at a temperature of 1150°C with mineraliser. (Reaction number 5, table 3.8.)

APPENDIX II

Vibrational Spectroscopy

2.1 HISTORY OF RAMAN SPECTROSCOPY

In 1928, when Sir Chandrasekhra Venkata Raman discovered the phenomenon that bears his name, only crude instrumentation was available. Sir Raman used sunlight as the source, a telescope as the collector and his eyes as the detector [41]. That such a feeble phenomenon as the Raman scattering was detected was remarkable. Since then the technique has been developed in leaps and bounds to the point where today it employs sophisticated equipment. What follows is intended to be a brief overview of what is a rather complex technique.

2.2 ORIGIN OF RAMAN AND INFRARED SPECTROSCOPY

IR and Raman spectra are similar in that both are observed as a result of vibrational transitions.

In IR spectra we measure the absorption of infrared light by the sample as a function of frequency. The molecule absorbs $\Delta E = h\upsilon$ from the IR source at each vibrational transition. The intensity of IR absorption is governed by the Beer-Lambert law (equation II-1).

$$I = I_o e^{-\varepsilon cd} \qquad \text{(II-1)}$$

Here, I_o and I denote the intensities of the incident and transmitted beams, respectively, ε is the molecular absorption coefficient, and c and d are the concentration of the sample and the cell length, respectively. (See Figure II-1 below). In IR spectroscopy, it is customary to plot the percentage transmission (T) versus wavenumber (equation II-2).

$$T(\%) = I/I_o \times 100 \qquad \text{(II-2)}$$

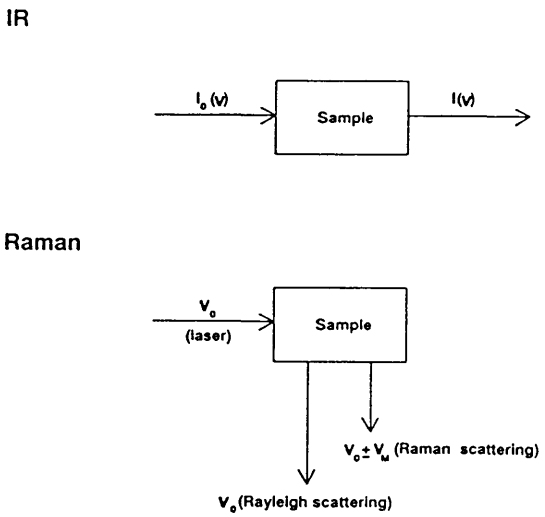

FIGURE II-1 Mechanisms that result in the infrared and Raman spectra of a sample.

It should be noted that $T(\%)$ is not proportional to c. Consequently, for quantitative analysis, the absorbance (A) defined below is used (equation II-3).

$$A = \log I_0/I = \varepsilon cd \qquad \text{(II-3)}$$

The origin of Raman spectra is markedly different to that of IR spectra. In Raman spectroscopy, the sample is irradiated by intense laser beams in the UV-visible region (ν_0), and the scattered light is usually observed in the direction perpendicular to the incident beam (figure II-1 above). The scattered light consists of two types. The first, *Rayleigh scattering*, is strong and has the same frequency as the incident beam (ν_0). The second, *Raman scattering*, is very weak (~10^{-5} of that of the incident beam) and has frequencies $\nu_0 \pm \nu_m$ where ν_m is a vibrational frequency of a molecule. The $\nu_o - \nu_m$ and $\nu_o + \nu_m$ lines are called *Stokes* and *anti-Stokes* lines respectively. Thus, in Raman spectroscopy, we measure the vibrational frequency (ν_m) as a shift from the incident beam frequency (ν_0). In contrast to IR spectra, Raman spectra are

measured in the UV-visible region where the excitation as well as Raman lines appear.

2.3 RAMAN SCATTERING ACCORDING TO CLASSICAL THEORY

According to classical theory, Raman scattering can be explained as follows. The electric field strength (E) of the electromagnetic wave (laser beam) fluctuates with time (t) as shown by equation II-4.

$$E = E_0 \cos 2\pi\nu_0 t \qquad \text{(II-4)}$$

where E_0 is the vibrational amplitude and ν_0 is the frequency of the laser. If a diatomic molecule is irradiated by this light, an electric dipole moment P is induced (equation II-5).

$$P = \alpha E = \alpha E_0 \cos 2\pi\nu_0 t \qquad \text{(II-5)}$$

Here, α is a proportionality constant and is called *polarisability*. If the molecule is vibrating with frequency ν_m, the nuclear displacement q is written

$$q = q_0 \cos 2\pi\nu_m t \qquad \text{(II-6)}$$

where q_0 is the vibrational amplitude. For a small amplitude of vibration, α is a linear function of q. Thus we can write

$$\alpha = \alpha_0 + (\partial\alpha/\partial q)_0 q_0 + \ldots\ldots \qquad \text{(II-7)}$$

Here, α_0 is the polarisability at the equilibrium position, and $(\partial\alpha/\partial q)_0$ is the

rate of change of α with respect to the rate of change in q, evaluated at the equilibrium position.

Combining II-5 with II-6 and II-7, we obtain

$$\begin{aligned} P &= \alpha E_0 \cos 2\pi\nu_0 t \\ &= \alpha_0 E_0 \cos 2\pi\nu_0 t + (\partial\alpha/\partial q)_0 \, q_0 E_0 \cos 2\pi\nu_0 t \cos 2\pi\nu_m t \\ &= \alpha_0 E_0 \cos 2\pi\nu_0 t \\ &\quad + (\partial\alpha/\partial q)_0 \, q_0 E_0 [\cos\{2\pi(\nu_0 + \nu_m)t\} \\ &\quad + \cos\{2\pi(\nu_0 - \nu_m)t\}] \end{aligned} \qquad \text{(II-8)}$$

According to classical theory, the first term represents an oscillating dipole that radiates light of frequency ν_0 (Rayleigh scattering), while the second term corresponds to the Raman scattering frequency $\nu_0 + \nu_m$ (anti-Stokes) and $\nu_0 - \nu_m$ (Stokes). If $(\partial\alpha/\partial q)_0$ is zero, the vibration is not Raman active. Namely, to be Raman active, the rate of change of polarisability (α) with the vibration must not be zero.

Figure II-2 illustrates Raman scattering in terms of a simple diatomic energy level.

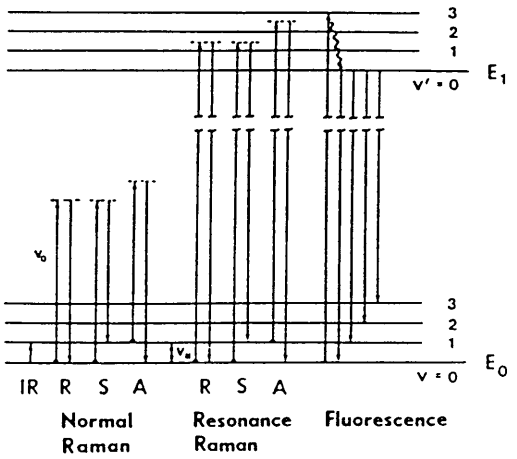

FIGURE II-2 Comparison of energy levels for the normal Raman, resonance Raman, and fluorescence spectra.

In IR spectroscopy, we observe that $v=0 \rightarrow 1$ transition at the electronic ground state. In normal Raman spectroscopy, the exiting line (v_0) is chosen so that its energy is far below the first electronic excited state. The dotted line indicates a "virtual state" to distinguish it from the real exited state. According to the Maxwell-Boltzmann distribution law, the population of molecules at $v=0$ is much greater than that at $v=1$. Thus, the Stokes (S) lines are stronger than the anti-Stokes (A) lines under normal conditions. This is illustrated in figure II-3 below. Since both give the same information, it is customary to measure only the Stokes side of the spectrum.

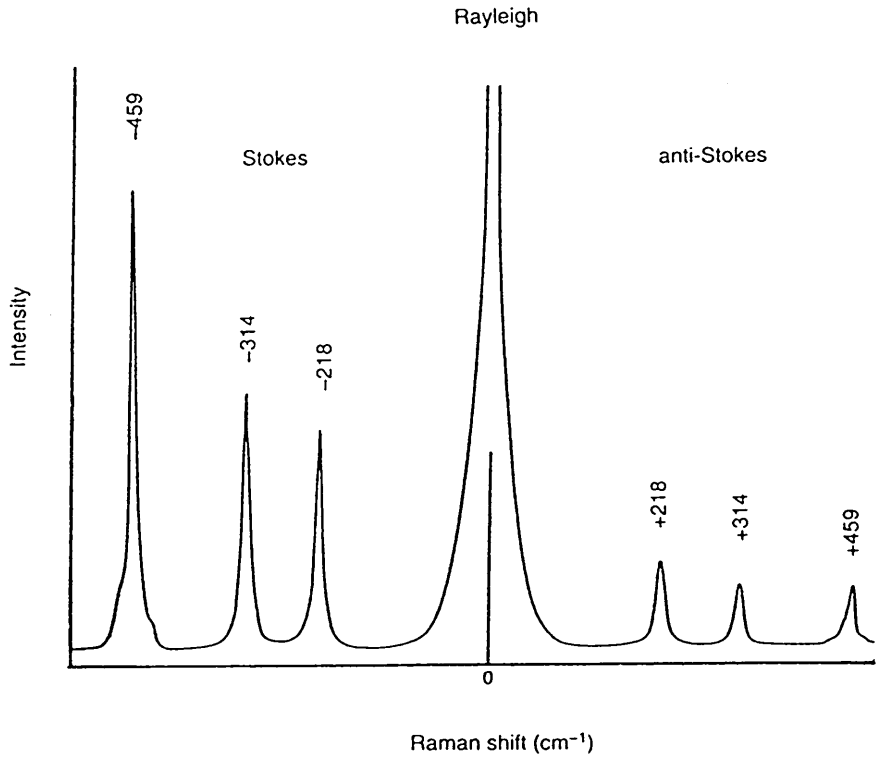

Figure II-4 Raman spectrum of CCl_4 (488.0 nm excitation).

Resonance Raman (RR) scattering occurs when the exiting line is chosen so that its energy intercepts the manifold of an electronic exited state (figure II-2 above). In the liquid and solid states, vibrational levels are broadened to

produce a continuum. In the gaseous state, a continuum exists above a series of discrete levels. Excitation of these continua produces RR spectra that show extremely strong enhancement of Raman bands originating in this particular electronic transition. Resonance Raman is discussed further in 1.5 below. The term "pre-resonance" is used when the exiting line is close in energy to the exited electronic state. Resonance fluorescence (RF) occurs when the molecule is exited to a discreet level of the electronic exited state. This has been observed for gaseous molecules such as I_2 and Br_2. Finally, fluorescence spectra are observed when the exited state molecule decays to the lowest vibrational level via radiationless transitions and then emits radiation, as shown in figure II-2 above. The lifetime of the exited state in RR is very short ($\sim 10^{-14}$s), while those in RF and fluorescence are much longer ($\sim 10^{-8}$ to 10^{-5}s).

2.4 RESONANCE RAMAN SPECTRA

Resonance Raman (RR) scattering occurs when the sample is irradiated with an exciting line whose energy corresponds to that of the electronic transition of a particular chromophoric group in a molecule (figure II-2). Under these conditions, the intensities of Raman bands originating in this chromophore are *selectively enhanced* by a factor of 10^3 to 10^5 . This selectivity is important not only for identifying vibrations of this chromophore in a complex spectrum, but also for locating its electronic transitions in an absorption spectrum.

Suppose that a compound contains two chromophoric groups that exhibit electronic bands at ν_A and ν_B as shown in figure II-4. Then, vibrations of chromophore A are resonance-enhanced when ν_0 is chosen near ν_A , and

those of chromophore B are resonance-enhanced when ν_0 is chosen near ν_B. This is called *resonance Raman (RR) scattering.*

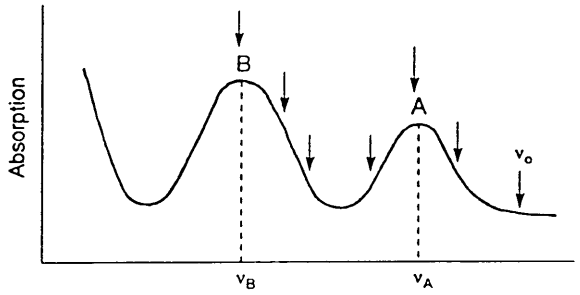

FIGURE II-4 Absorption spectrum of an arbitrary compound containing two chromophoric groups (A and B).

A good example of resonance Raman can be seen in this thesis. It is exhibited by the chromium bands in chromium doped malayaite. A characteristic of resonance Raman is the way in which the bands resonates throughout the spectrum at exactly twice the wavenumber each time. The intensity of the bands decreace with increase in wavenumber. Note, for example figures 3.4 - appendix I. The band at 739 nm is seen to resonate at 1486 nm and at 2223 nm. Without the effects of resonance Raman, these bands may very well not have been seen. Resonance Raman will be instrumental in further studies of the chromium doped malayaite.

2.5 FACTORS DETERMINING VIBRATIONAL FREQUENCIES

The vibrational frequency of a diatomic molecule is given by equation II-9.

$$\nu' = 1/2\pi c \sqrt{K/\mu'} \qquad \text{II-9}$$

where K is the force constant and μ is the reduced mass. This equation shows that ν' is proportional to $\sqrt{K}$ (force constant effect), but inversely

proportional to $\sqrt{\mu'}$ (mass effect). The results of these two effects is best illustrated by a few examples (all examples are in order of decreasing frequency (v')).

Example 1 $H_2 > HD > D_2$

In this case, the downward shift is due to the mass effect since the force constant is not affected by isotopic substitution.

Example 2 $HF > HCl > HBr > HI$

In this case the downward shift is due to the force constant effect (the bond becomes weaker in the same order) since the reduced mass is almost constant.

Example 3 $F_2 > Cl_2 > Br_2 > I_2$

In this case the downward shift is due to a combination of both effects. The molecule becomes heavier and the bond becomes weaker in the same order.

It is important to note, however, that a large force constant does not necessarily mean a stronger bond, since the force constant is the curvature of the potential well near the equilibrium position,

$$K = (d^2V/dq^2)_{q \to 0} \qquad \text{II-10}$$

whereas the bond strength (dissociation energy) is measured by the depth of the potential well (figure II-5). Thus, a large K means a sharp curvature near the bottom of the potential well, and does not directly imply a deep potential well. A roughly parallel relationship is observed between the force constants and the dissociation energy when we plot these quantities for a large number of compounds.

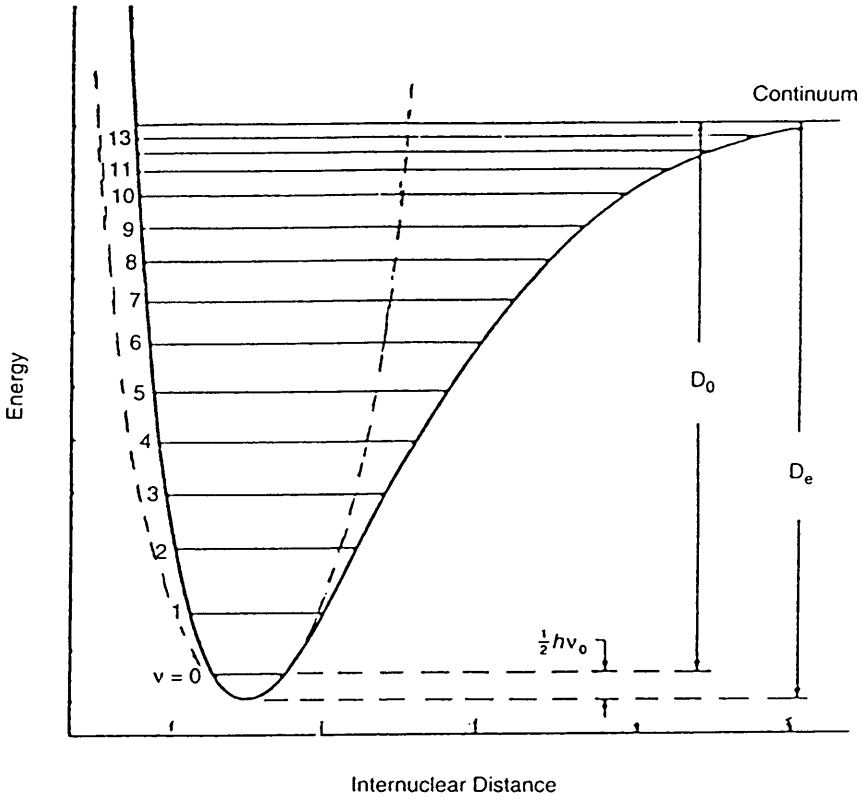

FIGURE II-5 Potential energy curve for a diatomic molecule. Solid line indicates Morse potential that approximates the actual potential. Broken line is a parabolic potential for a harmonic oscillator. D_e and D_0 are the theoretical and spectroscopic dissociation energies respectively.

2.6 SPACE GROUP SYMMETRY

1 *Point Group*

The spatial arrangement of the atoms in a molecule is called its equilibrium configuration or structure. This configuration is invariant under a certain set of geometric operations called a group. The molecule is orientated in a coordinate system. If by carrying out a certain geometric operation on the original configuration, the molecule is transformed into another configuration that is superimposable on the original, the molecule is said to contain a point symmetry element. These elements are used to *define the symmetry of a point*. All point symmetry elements of a molecule are grouped together in a *point group*.

2 *Space Group*

If one takes into account symmetry elements combined with translations, one obtains operations or elements that can be used to *define the symmetry of space*. Here, a translation is defined as the superposition of atoms or molecules from one site onto the same atoms or molecules in another site without the use of a rotation. Just as the *point group* collects all of the *point symmetry elements* , the *space group* collects all of the *space symmetry elements* in a crystal involving translation. For the space group selection rules, it is necessary to work on crystals for which space groups are known from X-ray studies, or where sufficient information is available, to make a choice of structure. (Conversely, the structure may be assumed and the space group selection rules can then serve as a test of this assumption.) In deriving space group selection rules, one must deal with a primitive (or Bravais) unit cell. A primitive unit cell is the smallest unit in a crystal which, by a series of translations, would build up the whole crystal. The spectroscopist is concerned with the primitive unit cell in dealing with lattice vibrations.

3 *Factor Group*

In a crystal , one primitive cell or unit cell can be carried into another primitive cell or unit cell by a translation. The number of translations of the unit cell would then seem to be infinite since a crystal is composed of many such units. If, however, one considers only one translation and consequently only two unit cells, and defines the translation that takes a point in one unit cell to an equivalent point in another unit cell as the identity, one can define a finite group, called a *factor group,* of the space group.

4 *Site Group*

A unit cell of a crystal is composed of points (molecules or ions) located at certain positions in the lattice that are called sites, that is, they can only be located on one of the symmetry elements of the factor group and thus remain invariant under that operation independent of translation. The point has fewer symmetry elements than the parent factor group and belongs to what is called a *site group* which is a sub-group of the factor group. In general, factor groups can have a variety of different sites possible. That is, many sub-groups can be formed from the factor group. Also, a number of distinct sites in the primitive (or Bravais) unit cell with the same site group are possible.

5 *Normal Vibrations in a Crystal*

A crystal can be regarded as a mechanical system of nN particles, where n is the number of particles (atoms) per unit cell and N is the number of primitive cells contained in the crystal. Since N is very large, a crystal has a huge number of vibrations. However, the observed spectrum is relatively simple. This is because only where equivalent atoms in primitive unit cells are moving in phase are they observed in the IR or Raman spectrum.

2.7 RAMAN AND INFRARED SPECTROSCOPY - PROS AND CONS

Although IR spectroscopy and Raman spectroscopy are similar in that both techniques provide information on vibrational frequencies of bonds, there are distinct advantages and disadvantages for each type of spectroscopy. Some of the more prominent advantages and disadvantages are discussed below.

1. As we have already seen, the selection rules of the two spectroscopies are markedly different. Thus, some vibrations are only Raman-active while others are only infrared-active. In general, a vibration is IR-active, Raman active, or active in both; however, totally symmetric vibrations are always Raman-active.

2. Some vibrations are inherently weak in IR spectra and strong in Raman spectra. In general, vibrations are strong in Raman if the bond is covalent, and strong in IR if the bond is ionic. Bending vibrations are generally weaker than stretching vibrations in Raman spectra.

3. Using the resonance Raman effect (RR) it is possible to selectively enhance vibrations of a particular chromophoric group in the molecule.

4. Since the diameter of the laser beam is normally 1-2 mm, only a small sample area is needed to obtain Raman spectra. This is a great advantage over conventional IR spectroscopy when only a small quantity of the sample (such as isotopic chemicals) is available.

5. Raman spectra in hygroscopic and/or air sensitive compounds can be obtained by placing the sample in sealed glass tubing. In IR spectroscopy, this is not possible since glass tubing absorbs IR radiation.

6. In Raman spectroscopy, the region from 4000 to 50 cm^{-1} can be covered by a single recording. In contrast, gratings, beam spitters, and detectors must be changed to cover the same region by IR spectroscopy. This has a marked effect on the amount of time required to record the respective spectra.

While the following factors have little or no role to play in the spectra of solid state materials, they are listed here for completeness sake.

7. Measurements of depolarisation ratios provide reliable information

about the symmetry of a normal vibration in solution. Such information cannot be obtained from IR spectra of solutions where molecules are randomly orientated.

8. Since water is a weak Raman scatterer, Raman spectra of samples in aqueous solution can be obtained without major interference from water vibrations. In contrast, IR spectroscopy suffers from the strong absorption of water.

Some disadvantages of Raman spectroscopy are listed below.

1. A powerful laser source is required to observe weak Raman scattering. This may cause local heating and/or photo decomposition, especially in resonance Raman studies where the laser frequency is deliberately tuned in to the absorption band of the molecule.

2. Some compounds fluoresce when irradiated by the laser beam.

3. It is more difficult to obtain rotational and rotation-vibration spectra with high resolution in Raman than in IR spectroscopy. This is because Raman spectra are observed in the UV-visible region where high resolving power is difficult to obtain.

4. The state of the art Raman system costs much more than a conventional FT-IR spectrophotometer.

Finally, it should be noted that vibrational spectroscopy (both IR and Raman), is unique in that it is applicable to the solid state as well as to the gaseous state and solution. In contrast, X-ray diffraction is applicable only to the crystalline state, whereas NMR spectroscopy is applicable largely to the sample in solution. Vibrational spectroscopy may be applied successfully to both solids and liquids, and of coarse, to gasses as well.

APPENDIX III

Instrumentation

and

Techniques

3.1 SCANNING ELECTRON MICROSCOPY

Instrumentation

All measurements were carried out on a Phillips 500 Scanning Electron Microscope coupled to a Tracor Northern/Noran EDS System.

Comments

This analytical technique was used to determine the elemental composition of the reaction products. It was not found to be the perfect analysis technique for application in this sort of chemistry for a number of reasons.

1. It could only be used to determine elements of around atomic mass 11 (sodium) and higher. A mineraliser used in this study, for example, contained boron which is lighter than sodium and could consequently not be determined by this technique.

2. The accuracy of analysis done in this study was found to be broadly around 5 atom percent up or down. This can be seen from the reproducibility of the analyses. While this is good enough for broad discussion about the host lattice, it is useless for components such as the dopants or mineralisers. One sees, for example, in many of the reaction mixtures analysed in this study that more of a certain element is found in the reaction product than was added as starting material.

3. Its accuracy of determination of a certain element can be effected by the presence of other elements (chemical effects). An example of this can be seen in chapter 2 of this thesis. The determination of the yttrium in the two pyrochlores is reasonably accurate when no dopant (in the form of calcium and vanadium) is present but when the dopants are present, the analysis is inaccurate by as much as 50 atom percent in all cases.

4. Many of these factors are influenced by the fact that ideally,

the sample being analysed should have a smooth surface. This is of course difficult with fine, agglomerated powders, with different particle sizes and shapes.

The positive aspects of this technique are the ease and speed with which they are carried out. The SEM analysis results were useful for getting an idea of the composition of the reaction products with relatively ease (cf. Wet analysis techniques). The above points should be born in mind when gaining inference from the results of the SEM analysis.

3.2 X-RAY POWDER DIFFRACTION

Instrumentation

X-ray powder diffraction data was collected on an automated Siemens D501 diffractometer with a 40 position sample changer. Monochromated $Cu_{K\alpha}$ radiation was employed at 25mA and 30kV, at a scanning speed of 3° 2θ/min (step size = 0.05° 2θ, measuring time = 1 second). Patterns were recorded from 5 to 65° 2θ.

Comments

This technique is very useful in the study of solid state metal oxides and it was most certainly employed very successfully in this study. It gives useful information about the chemical state of the elements in a reaction product. For example, in chapter 3, a mixture of calcium carbonate, tin oxide and silicon oxide were mixed together and calcined. XRD tells us whether or not the reactants have reacted, and if they have, what the reaction products are. We might expect to find $CaSnSiO_5$, $CaSnO_3$, $CaSiO_3$, or some other products, or a mixture of reactants and products. XRD will tell us what the composition of the reaction products are. On the above instrumentation, the product needs to be present in at least 3-5 weight percent to be detected

and so this technique could also not shed much light on the chemical state of the dopants or mineralisers used. Some indirect information on the dopants and mineralisers can be obtained from the effect that the have on other reaction products however.

3.3 INFRARED SPECTROSCOPY

Instrumentation

Infrared spectra were recorded on a Bruker ifs 113v spectrometer. Mid-infrared spectra were recorded with the samples in the form of KBr (potassium bromide) pellets. Far-infrared spectra were recorded with the samples in the form of polyethylene pellets.

Comments

See appendix II - Vibrational spectroscopy.

3.4 RAMAN SPECTROSCOPY

Instrumentation

All Raman spectra were recorded on a Dilor XY Raman Instrument with a microprobe , under a 100× objective, using the 514.5 nm excitation line (from an Ar^+ ion laser (Coherent Innova 90)).

Comments

See appendix II - Vibrational Spectroscopy.

3.5 ELECTRONIC SPECTROSCOPY

Instrumentation

Electronic (diffuse reflectance transmittance) spectra were recorded at room temperature on a Carey 2390 (UV-Vis-NIR) spectrometer from Varian.

REFERENCES

1. W. Noll, R. Holm and L. Born, "Painting of Ancient Ceramics", *Angew. Chem. Int. Ed. Engl.*, **14,** 639, 1975.

2. A. Burgyan and R. E. Eppler, "Classification of Mixed-Metal-Oxide Inorganic Pigments", *Am. Ceram. Soc. Bull.,* **62** [9], 1001-03, 1983.

3. F. Hund, "Inorganic Pigments: Bases for Coloured, Uncoloured, and Transparent Products", *Angew. Chem. Int. Ed. Engl.,* **20,** 723-30, 1981.

4. T. C. Patton, "Pigment Handbook - Vol.2 Applications and Markets", John Wiley & Sons 1973.

5. G. R. Streatfield, "Ceramic Colour", *Br. Ceram. Trans. J.*, **89,** 177-80, 1990.

6. P. A. Lewis, "Pigment Handbook - Vol. 1 Properties and Economics", (second edition), John Wiley & Sons 1987.

7. G. Buxbaum, "Industrial Inorganic Pigments", VCH Verlagsgesellschaft mbH, 1993.

8. A. J. H. Macke and G. Blasse, "Vibrational Spectra of Oxidic Stannates in Relation to Order-Disorder Phenomena", *J. Inorg. Nucl. Chem.,* **38,** 1407-9, 1976.

9. M. T. Vandenborre and E. Husson, "Comparison of the Force Field in Various Pyrochlore Families. I. The $A_2B_2O_7$ Oxides", *J. Solid State Chem.*,**50,** 362-71, 1983.

10. M. T. Vandenborre, E. Husson, J. P. Chatry and D. Michel, "Rare-Earth Titanites and Stannates of Pyrochlore Structure; Vibrational Spectra and Force Fields", *J. Raman Spectroscopy,* **14** [2], 1983.

11. R. W. G. Wyckoff, "Crystal Structures - Volume III" (Second Edition), Interscience Publishers (John Wiley & Sons) 1965.

12. C. G. Whinfrey and A. Tauber, "Rare Earth Stannates, $R_2Sn_2O_7$", *J. Am. Chem. Soc.,* **83,** 755-6, 1961.

13. C. G. Whinfrey, D. W. Eckart and A. Tauber, "Preparation and X-Ray Diffraction Data for Some Rare Earth Stannates", *J. Am. Chem. Soc.,* **82,** 2695-7, 1960.

14. C. P. Grey, C. M. Dobson, A. K. Cheetham and R. J. B. Jakeman, "Studies of Rare-Earth Stannates by ^{119}Sn MAS NMR. The use of Paramagnetic Shift Probes in the Solid State", *J. Am. Chem. Soc.,* **111,** 505-11, 1989.

15. G. R. Facer, C. J. Howard and B. J. Kennedy, "Structure Refinement and Calculated X-Ray Powder Data for the Pyrochlore $Y_2Sn_2O_7$ Derived from Powder Neutron Data", *Powder Diffr.,* **8** [4], 245-8, 1993.

16. K. Fujiyoshi, H. Yokoyama, F. Ren and S. Ishida, "Chemical State of Vanadium in Tin-Based Yellow Pigment", *J. Am. Ceram. Soc.,* **76** [4], 981-96, 1993.

17. C. K. Jørgensen, "Absorption Spectra and Chemical Bonding in Complexes", Pergamon Press Ltd., Oxford 1964.

18. F. D. Hardcastle and I. E. Wachs, "Determination of Vanadium-Oxygen Bond Distances and Bond Orders by Raman Spectroscopy", *J. Phys. Chem.,* **95,** 5031- 41, 1991.

19. S. Takenouchi, "Hydrothermal Synthesis and Consideration of the Genesis of Malayaite", *Mineral. Deposita (Berl.),* **6,** 335-47, 1971.

20. R. A. Eppler, "Lattice Parameters of Tin Sphene", *J. Am. Ceram. Soc.,* **59** [9-10], 445, 1976.

21. D. V. Sanghani, G. R. Abrams and P. J. Smith, "A Structural Investigation of Some Tin-Based Coloured Ceramic Pigments", *Trans. J. Br. Ceram. Soc.,* **80,** 210-214, 1981.

22. J. Carda, P. Escribano, G. Monrós, M. D. Rodrigo and J. Alarcon, "Co-SnO_2-CaO-SiO_2 Based Ceramic Pigments", *Interceram.,* **39**[3], 22-24, 1990.

23. F. A. Cotton, G. Wilkinson and P. L. Gaus, "Basic Inorganic Chemistry" - second edition, John Wiley & Sons, 1987.

24. F. A. Cotton and G. Wilkinson, "Advanced Inorganic Chemistry" - fifth edition, John Wiley & Sons, 1988.

25. J. Alcron, P. Escribano and R. Mª. Marin, "Pigments with Spinel Structure", *Br. Ceram. Trans.* J., **84,** 175-7, 1985.

26. A. Burgyan and R. A. Eppler, "Classification of Mixed-Metal-Oxide Inorganic Pigments", *Am. Ceram. Soc. Bull.,* **62** [9], 1001-3, 1983.

27. R. A. Eppler, "Ceramic Colorants", *Ullmann's Encyclopaedia of Science and Technology,* Vol. A5, 545-56, 1986.

28. R. A. Eppler, "Selecting Ceramic Pigments", *Ceramic Bulletin,* **66** [11], 1600-4, 1987.

29. F. Hund, "Inorganic Pigments: Bases for Coloured, Uncoloured, and Transparent Products", *Angew. Chem. Int. Ed. Engl.,* **20,** 723-30, 1981.

30. D. M. Adams and D. C. Newton, "Tables for Factor Group and Point Group Analysis", Beckman Instruments (UK).

31. J. B. Higgins and P. H. Ribbe, "The Structure of Malayaite, $CaSnOSiO_4$, a Tin Analog of Titanite", *American Minerologist,* **62,** 801-6, 1977.

32. J. A. Speer and G. V. Gibbs, "The Structure of Synthetic Titanite, $CaTiOSiO_5$, and the Domain Textures of Natural Titanite", *American Mineralogist,* **61,** 238-247, 1976.

33. M. Taylor and G. E. Brown, "High-Temperature Structural Study of the $P2_1/a \rightleftharpoons A2/a$ a Phase Transition in Synthetic Titanite, $CaTiSiO_5$", *American Mineralogist,* **61,** 435-47, 1976.

34. E. Salje, C. Schmidt and U. Bismayer, "Structural Phase Transition in Titanite, $CaTiSiO_5$: A Ramanspectroscopic Study", *Phys. Chem. Minerals,* **19,** 502-6, 1993.

35. V. C. Farmer, "The Infrared Spectra of Minerals", Mineralogical Society, 1974.

36. Y. Gohshi and A. Ohtsuka, "The application of Chemical Effects in High Resolution X-Ray Spectrometry", *Spectrochimica Acta,* **28B,** 179-188, 1973.

37. G. Villers, P. Gibart and R. Druilhe, "Magnetic Oxides Crystallising in the Rutile Structure", *J. Applied Physics,* **39**[2], 1968.

38. R. M. Chrenko and D. S. Rodbell, "On the Infrared Spectra of CrO_2", *Physics Letters,* **24A**[4], 211-2, 1967.

39. H. A. Willis and J. H. Van Der Mass, "Laboratory Methods in Vibrational Spectroscopy", John Wiley & Sons, 1987.

40. D. de Waal and A. M. Heyns, "A Reinvestigation of the Decomposition Products of $(NH_4)_2CrO_4$ and $(NH_4)_2Cr_2O_7$", *J. Alloys and Compounds,* **187,** 171-80, 1992.

41. J. R. Ferraro and K. Nakamoto, "Introductory Raman Spectroscopy", Academic Press, Inc., 1994.